

Molecular genetics of myeloid malignancy predisposition:
Insights into pathogenesis and therapeutic translation

Michelle C. Krutein

A dissertation

submitted in partial fulfillment of the
requirements for the degree of

Doctor of Philosophy

University of Washington

2019

Reading Committee:

Marshall Horwitz, Chair

William Mahoney

Carol B. Ware

Program Authorized to Offer Degree:

Pathology

©Copyright 2019

Michelle C. Krutein

University of Washington

Abstract

Molecular genetics of myeloid malignancy predisposition:

Insights into pathogenesis and therapeutic translation

Michelle C. Krutein

Chair of the Supervisory Committee:

Professor Marshall S Horwitz

Department of Pathology

Preleukemic diseases are highly informed by genetic predisposition and require appropriate models for studying pathogenesis and the progression to hematological malignancy. Although rare, familial platelet disorder (FPD) and severe congenital neutropenia (SCN) have few or no therapies available to patients and also possess high rates of leukemic transformation to myeloid malignancy. With these points in mind, my graduate work aimed to elucidate the molecular mechanisms of *ELANE*-associated severe congenital neutropenia, identify new genetic mutations causing preleukemic diseases, and evaluate novel therapies for platelet disorder with predisposition to myeloid malignancy.

Familial platelet disorder with predisposition to acute myelogenous leukemia is an autosomal dominant disorder caused by monoallelic mutation of *RUNX1*, initially resulting in half-normal levels of *RUNX1* protein. Patients develop leukemia only after a protracted prodrome consisting of thrombocytopenia and bleeding diathesis relating to functional platelet granule deficiency, suggesting that early intervention affords an opportunity for preventing malignant transformation. We hypothesize that pharmacological inhibition of *RUNX1* protein degradation may normalize *RUNX1* protein levels and restore platelet numbers and function.

RUNX1 is rapidly degraded through the ubiquitin-proteasome pathway. Moreover, RUNX1 auto-regulates its own expression. A predicted kinetic property of auto-regulatory circuits is that transient perturbations of steady-state levels result in continued maintenance of expression at adjusted levels, even after inhibitors of degradation or inducers of transcription are withdrawn, suggesting that transient inhibition of RUNX1 degradation may have lasting effects. Here we evaluate cell lines, FPD/AML patient derived induced pluripotent stem cells (iPSC), and FPD/AML primary bone marrow cells and show that, in some circumstances, transient expression of exogenous RUNX1 or inhibition of steps leading to RUNX1 ubiquitylation and proteasomal degradation restore RUNX1 levels, thereby advancing megakaryocytic differentiation *in vitro*. Thus, drugs retarding RUNX1 proteolytic degradation may represent a therapeutic avenue for treating bleeding complications and preventing leukemia in FPD/AML.

Heterozygous mutations in *ELANE*, encoding the potent serine protease, neutrophil elastase (NE), cause cyclic neutropenia (CyN) and are the most common cause of severe congenital neutropenia (SCN). Patient presentation is marked by profoundly low neutrophil counts accompanied by predisposition to myelodysplasia (MDS) and acute myeloid leukemia (AML). There is no unified theory of SCN or CyN pathogenesis. However, out of the >100 mutations recorded in SCN and CyN, none of these mutations have been found to encompass the three catalytic residues necessary for NE proteolysis, which may suggest retention of these residues is important for SCN and CyN pathology. To address this question, I developed novel iPSC models of EA-associated severe congenital neutropenia via genome editing strategies using CRISPR-Cas9 targeting with homology directed integration of synthetically designed non-viral vectors. These vectors either harbored an aggressive SCN mutation or a single residue substitution of the catalytic serine of neutrophil elastase. Additional work must be performed to generate iPSC lines possessing both the SCN and catalytic inactivation mutation *in cis* as well as a wild type *ELANE* control iPSC line. All vectors contained a green fluorescent protein (GFP) gene trap whereby mutant NE expression is announced through GFP reporting.

These cell lines allow us the opportunity to investigate how catalytic activity of neutrophil elastase influences neutrophil development and SCN pathology, both questions that are unanswered or under scrutiny in the field. It is also critical to mention that our method of genome editing creates models whereby expression of the mutant protein is detectable through a reporter. This characteristic makes our models superior to other existing iPSC models that have not been able to achieve mutant protein reporting due to direct reprogramming of primary SCN samples. Additionally, these integration vectors can be easily adapted to harbor any desired changes in exon 4 or 5 of *ELANE*. Lastly, although neither homozygous or S202A mutations in *ELANE* have been observed in normal, SCN, or CyN individuals, these novel cell models will provide us with the tools to determine the interaction between NE proteolysis and granulopoiesis in both normal and diseased states.

Congenital neutropenia is a genetically heterogeneous disease whereby our lab has contributed to this growing list of genetic factors found causative of neutropenia. In order to expand the current knowledge of neutrophil development and biology it is critical for us to continue the search for novel genes or mutations that produce a neutropenic phenotype. Genetic screening of neutropenic children in two unrelated families revealed the same T679I variant of unknown significance in the gene *SUZ12*. A critical transcription factor governing stem cell differentiation, *SUZ12* protein normally facilitates epigenetic remodeling through global H3K27me3 yet has not been reported as having a role in neutrophil development specifically. I reprogrammed primary patient samples to *SUZ12*-iPSCs and subsequently subjected them to hematopoietic stem cell (HSC) and neutrophil differentiation which recapitulated phenotypes observed in patients. Epigenetic landscape evaluation of *SUZ12*-iPSCs via western blot and chromatin immunoprecipitation sequencing (ChIPseq) revealed reduced H3K27me3 repressive genome markers, elevated H3K4me3 activation markers, and some differences in *SUZ12* binding. These studies reflect the first report of mutations in epigenetic proteins, more specifically *SUZ12*, as being causative of SCN.

Table of Contents

List of Abbreviations	i
List of Figures	iii
List of Tables	v
Acknowledgements	vi
Chapter 1. Introduction	1
1.1. Hematopoiesis	1
1.2. Cells of the Blood: Myelopoiesis and the myeloid lineage	3
1.3. Preleukemia: cytopenia and myelodysplastic syndromes	5
1.4. Genetics of preleukemic diseases	6
1.4.1. Pancytopenia	7
1.4.2. Thrombocytopenia	8
1.4.3. Anemia	9
1.4.4. Neutropenia	10
1.4.5. Complex presentation	14
1.4.6. Inherited acute myeloid leukemia	14
1.5. Leukemogenesis in inherited bone marrow failure syndromes	15
1.6. Current treatments and therapies for inherited bone marrow failure syndromes	17
1.7. Disease models for studying inherited bone marrow failure syndromes	19
1.8. Tables	21
1.9. References	22
Chapter 2. Inhibition of protein degradation pathways in RUNX1 deficient FPD/AML restores RUNX1 gene expression levels and promotes megakaryopoiesis	32
2.1. Introduction	32
2.2. Methods	33
2.3. Results	39
2.4. Discussion	45
2.5. Figures	49
2.6. Supplementary Tables	56
2.7. Supplementary Figures	58
2.8. References	67
Chapter 3. Additional studies of preleukemic diseases	71
3.1. Determining the role of neutrophil elastase proteolysis in <i>ELANE</i> -associated congenital neutropenia pathogenesis and normal neutrophil development iPSC modeling	71
3.1.1. Introduction	71
3.1.2. Methods	74
3.1.3. Results	76
3.1.4. Discussion	77
3.1.5. Figures	78
3.2. <i>SUZ12</i> : a novel gene implicated in severe congenital neutropenia	83
3.2.1. Introduction	83
3.2.2. Methods	85
3.2.3. Results	86
3.2.4. Discussion	88
3.2.5. Figures	90
3.3. References	95
Chapter 4. Conclusions, broader impacts, and future directions	98
4.1. Closing remarks	98
4.2. References	102

List of Abbreviations

Alphabetical order

AGM: Aorta-gonad-mesonephros
AML: Acute myeloid leukemia
ANKRD26: Ankyrin repeat domain 26 gene
ANKRD26-RT: *ANKRD26*-Related thrombocytopenia
APC: Anaphase promoting complex
BSA: bovine serum albumin
CBC: Complete blood count
CBF β : Core binding factors
CEBP α : CCAAT enhancer binding protein alpha protein
CFU: Colony forming unit
C/EBP ϵ : CCAAT-enhancer-binder protein epsilon protein
ChIPseq: Chromatin immunoprecipitation sequencing
CHOP: Children's Hospital of Philadelphia
CLL: Chronic lymphocytic leukemia
CML: Chronic myeloid leukemia
CMP: Common myeloid progenitor
CMML: Chronic myelomonocytic leukemia
CSF3R: Granulocyte-colony stimulating factor receptor 3 gene
CyN: Cyclic neutropenia
DBA: Diamond-Blackfan anemia
DC: Dyskeratosis congenita
DMEM: Dulbecco's Modified Eagle Medium
DMSO: dimethylsulfoxide
DS: Down's syndrome
EA-SCN: *ELANE*-associated severe congenital neutropenia
ER: Endoplasmic reticulum
FA: Fanconi anemia
FACS: Fluorescent-activated cell sorting
FBS: Fetal bovine serum
FPD/AML: Familial platelet disorder with propensity to myeloid malignancy
G6PC3: Glucose 6 phosphatase catalytic subunit 3 gene
GATA2: GATA binding protein 2 gene
GCSF: Granulocyte-colony stimulating factor
GCSF-R: Granulocyte-colony stimulating factor receptor protein
GF11: growth factor-independent protein 1 gene
GFP: Green fluorescent protein
GMP: Granulocyte/monocyte restricted progenitor
GVHD: Graft versus host disease
IRB: Institutional Review Board
IMDM: Iscove's Modified Dulbecco's Medium
HAX1: HCLS1-associated protein X-1 gene
HSC: Hematopoietic stem cell
IBMFS: Inherited bone marrow failure syndromes
ILC: Innate lymphoid cells
iPSC: Induced pluripotent stem cell
IRES: Internal ribosomal entry site
ISCRM: University of Washington Institute for Stem Cell and Regenerative Medicine
KS: Kostmann syndrome

MDS: Myelodysplastic syndromes
MEP: Megakaryocyte/erythrocyte restricted progenitor
MK: Megakaryocytes
MNC: Peripheral blood mononuclear cells
MPD: Myeloproliferative disorders
MPP: Multipotent progenitor
MSKCC: Memorial Sloan Kettering Cancer Center
NAE: NEDD8 activating enzyme
NE: Neutrophil elastase
NK: Natural killer cells
PBMC: Peripheral blood mononuclear cell
PMSF: Phenylmethylsulfonyl fluoride
PRC2: Polycomb repressive complex 2
PVDF: Polyvinylidene difluoride
qRT-PCR: Real-time quantitative reverse transcription polymerase chain reaction
RBC: Red blood cells
RFP: Red fluorescent protein
ROS: Reactive oxygen species
RUNX1: Runt-related transcription factor 1 gene
RUNX1: Runt-related transcription factor 1 protein
SBDS: Shwachman-Bodian-Diamond syndrome gene
SCN: Severe congenital neutropenia
SCN-iPSC: Severe congenital neutropenia-induced pluripotent stem cells
SCT: Stem cell/bone marrow transplant
SDS: Shwachman-Diamond syndrome
SLPI: Secretory leukocyte protease inhibitor protein
T-ALL: T-cell acute lymphocytic leukemia
TBST: Tris-buffered saline, 0.1% Tween 20
TEM: Transmission electron microscope
TF: Transcription factor
TP53: tumor protein 53 gene
TPM: Transcripts per million
UPR: Unfolded protein response
VUS: Variant of unknown significance
WAS: Wiskott-Aldrich syndrome gene
WASp: Wiskott-Aldrich syndrome protein
WBC: White blood cell
WT: Wild type
WTC: Wild type iPSC cell
YS: Yolk sac

List of Figures

Figure 2.1. Effect of transient expression of exogenous RUNX1 upon endogenous RUNX1 expression in 293T cells.

Figure 2.2. Effect of drugs inhibiting RUNX1 proteolytic degradation on RUNX1 protein and transcript levels in 293T cells transiently transfected with RUNX1-FLAG.

Figure 2.3. Inhibition of endogenous RUNX1 proteolytic degradation in cell lines.

Figure 2.4. Persistence of RUNX1 expression in cell lines following transient inhibition of its proteolytic degradation.

Figure 2.5. Transient inhibition of RUNX1 proteolytic degradation during megakaryocytic differentiation of FPD/AML patient-derived iPSC.

Figure 2.6. Primary FPD/AML mononuclear bone marrow cells treated with inhibitors of RUNX1 proteolytic degradation early during *in vitro* megakaryocyte differentiation.

Figure 2.7. Effect of RUNX1 degradation inhibitor treatment on platelet granule formation during *in vitro* megakaryocyte differentiation of primary FPD/AML mononuclear bone marrow cells.

Supplementary Figure 2.1. Flow cytometry analysis of primary FPD patient bone marrow-derived megakaryocytes.

Supplementary Figure 2.2. Transmission electron microscopy images of primary FPD-1 patient bone marrow-derived megakaryocytes.

Figure 3.1.1. Schematic of *ELANE* locus after non-viral vector integration and strategies of clone characterization.

Figure 3.1.2. Transfection protocol and timeline used to generate *ELANE*-edited iPSCs.

Figure 3.1.3. Characterization of clone G214R-G13-het.

Figure 3.1.4. Characterization of clone G214R-G9-homo.

Figure 3.1.5. Characterization of clone G214R-G6-homo.

Figure 3.1.6. Characterization of clone S202A-S9-het.

Figure 3.1.7. Characterization of clone S202A-S20-homo.

Figure 3.1.8. Characterization of clone S202A-S23-homo.

Figure 3.2.1. Kindred 1 pedigree denoting patient presentations and genotype.

Figure 3.2.2. Patient 16-2 iPSC clone characterization.

Figure 3.2.3. Flow cytometry results of 16-2 iPSC clones C-1, C-2, C-3 to assess surface markers indicative of stem cell identity and differentiation.

Figure 3.2.4. Western blot of 16-2 PRC2 protein components and epigenetic markers.

Figure 3.2.5. ChIPseq of chromosome 12 in undifferentiated 16-2 patient-derived iPSC.

Figure 3.2.6. *In vitro* hematopoietic differentiation of 16-2 iPSC clones.

Figure 3.2.7. Colony forming unit assay of 16-2 iPSCs and control samples.

Figure 3.2.8. Quantitative analysis of cell types present in CFU-G plugs.

List of Tables

Table 1.1. Single-gene disorders encompassing bone marrow failure syndromes, myelodysplastic syndromes, and predisposition to myeloid neoplasms.

Supplementary Table 2.1. FPD patient information and flow cytometry analysis at time of harvest following *in vitro* megakaryocytic differentiation

Supplementary Table 2.2. Summary of drug information and concentrations used for cell studies.

Supplementary Table 2.3. Summary of antibodies used for immunoblotting in cell studies.

Supplementary Table 2.4. Summary of antibodies used for flow cytometry in cell studies.

Acknowledgements

I would like to acknowledge my thesis advisor, Dr. Marshall Horwitz for his experimental guidance, thoughtful edits, financial support, and endless intellectual antidotes. This work would not have been possible without collaborations with Drs. Eirini Papapetrou and Diana Kotini from the Memorial Sloan Kettering Cancer Center, Dr. Sioban Keel from the University of Washington, and the Lutzko Lab at Cincinnati Children's Hospital. Lab members Dr. Matthew Hart, Donovan Anderson and Dr. Timothy Tidwell were paramount in my scientific training, and I am deeply appreciative of all their time and effort.

Special thanks to Steve Berard, Dr. Jean Campbell, Megan Barker, and Dr. Bill Mahoney for all of their support during my graduate career. I am so thankful for these individuals; they are truly the best advisors and colleagues I could ever ask for. I am also grateful to my committee members Carol Ware and Dan Miller for their scientific guidance, oversight, and training.

To my family, Ralf and Cindy Krutein, Lyndsey Kneebone, and the entire Kneebone family; I share this accomplishment with you. Mom and dad, thank you for constantly reminding me of my impact and loving me so fiercely during this endeavor. I love you both to the moon and back and can't thank you enough for everything you two have done and continue to do. Sissy, you are my hero. You have taught me the importance of trying and the freedom in failure, and watching your family grow over these last years has been one of the greatest joys of my life.

Joel Hoyer, your love, support, kindness, patience, and creativity inspired me to take risks and dream big and I am such a better scientist and human because of you. Thank you for everything bubs, I fucking love you.

To my dear friends Andrew Cooper, Analisa Sarno, Kaylee Allen, Jillian Bou, Danielle Regello, Lori Sugitachi, and my entire MBD graduate cohort, I couldn't have done this without you. Dr. Natalie Vandeven, especially, you are my rock, muse, and best friend. I would climb Mount Everest in flip flops for you.

Holy shit, I'm a fucking doctor, go me.

Chapter 1

Introduction

1.1. Hematopoiesis

Hematopoiesis is the process whereby all blood cells are created within the body. Although not completely understood, conventional wisdom suggests hematopoiesis is temporally and spatially divided into two waves throughout human development (1). First to occur is the primitive wave, which produces the body's first blood reservoir. Following gastrulation, the yolk sac (YS) begins to generate blood islands from the extraembryonic mesoderm that contain large, nucleated erythroblasts expressing both embryonic (ϵ) and fetal (γ) hemoglobin (2, 3). These proteins allow specialized erythrocytes to deliver oxygen rapidly to the developing embryo (2). This wave also produces the body's first macrophage and megakaryocyte progenitors, the latter ultimately supplying the embryo with its first, small platelet pool (4). Recent literature shows this initial cell population is unique in that they do not develop from hematopoietic stem cells (HSC)s, which is strictly the case in later stages of hematopoiesis (5, 6). Knock-out studies have concluded that expression of genes *RUNX1*, *HOXA3*, *GATA2* and *NOTCH1* initiates the primitive wave and are critical developmental switches that continue to shepherd both early and late hematopoiesis (7-10).

Definitive hematopoiesis occurs in the aorta-gonad-mesonephros (AGM), where HSCs emerge and give rise to cells of myeloid, lymphoid, and enucleated erythroid lineages (5). A portion of cells subsequently migrate to the fetal liver, where mature HSC populations are established at multiple sites within the body by week 9 of gestation (11, 12). It is then during late gestation when hematopoietic precursors start to seed the bone marrow. Shortly after birth, erythrocytes undergo hemoglobin switching, whereby the embryonic and fetal hemoglobin genes are silenced and adult hemoglobin (β) is exclusively expressed for the remainder of life (13). This hemoglobin transition is optimized for necessary oxygen exchange in adults and is one of the key

examples of developmental divergence between early and late hematopoiesis. The bone marrow is the primary site of HSC activity in adulthood, and ultimately gives rise to all blood cells before they exit into circulation (14). The bone marrow houses one of the few large, adult stem cell populations within the human body. This stable population of HSCs constantly drive hematopoiesis, and although it is not technically considered an organ, these cells have the unique ability to be transplanted where they quickly replenish the recipient's blood supply and can continue to do so for the remainder of their life.

Attempts to model human hematopoiesis *in vitro* have proved complex as fetal HSCs are in low abundance and present at various stages of maturation and proliferation, with no or limited capacity for transplantation (15). Cord blood harvested from babies immediately after birth can be effectively transplanted so these samples are rarely used for *in vitro* studies (16). Adult HSCs are commonly used to model hematopoiesis because they are very abundant and have the ability to undergo *in vitro* differentiation into various cell types. However, cell culture conditions for HSC maintenance is rarely successful as the cells have limited capacity to expand or self-renew *in vitro*. Additionally, heterogeneity in differentiation can obstruct our ability to confidently define developmental niches and lineage mapping, therefore preventing their use in transplantation (5). Induced pluripotent stem cells (iPSC)s can also be subjected to *in vitro* hematopoietic differentiation. This can provide us with immense knowledge in the case of modeling genetic diseases, however, it is important to note that the cells generated resemble a developmental route more closely related to fetal instead of adult hematopoiesis (17). This molecular observation during iPSC differentiation *in vitro* indicates current iPSC-derived cells are incapable of surviving and thriving post-transplantation. New iPSC studies have utilized the power of transient expression of master regulators of hematopoiesis, including leukemia driver mutations such as the chromosomal translocation-generated *MLL-AF4*, to influence maturation capacity. These samples were found to successfully engraft in mice, although the long-term risk of leukemic transformation was, perhaps not surprisingly, significantly increased (18).

On the whole, we have made great strides in the field of developmental hematology, yet these gains currently reveal more basic science discoveries that although insightful, do not necessarily translate towards clinical application for the aforementioned reasons.

1.2. Cells of the Blood: Myelopoiesis and the myeloid lineage

There are over a dozen different types of specialized blood cells circulating within our bodies, all of which perform specific functions such as: oxygen delivery, maintaining immunity, wound mitigation via clotting, waste removal and more (12). The developmental 'tree of hematopoiesis' has evolved with research over the years to represent the pathways of blood cell maturation, commitment, and function. Starting with an HSC acting as a seed, the tree first branches off into two groups: lymphoid and myeloid by way of an intermediate, short lived multipotent progenitor (MPP).

Lymphoid cells account for B and T cells as well as all their many subtypes to govern our adaptive immune system. Cells in this lineage slowly learn to facilitate targeted responses to specific pathogens and in turn form long term memory against them to prepare the body for future exposure. There are additional lymphoid cells defined as innate lymphoid cells (ILC)s, an example being natural killer cells (NK)s that interestingly bridge innate and adaptive immunity by assembling quickly and impartially to attack pathogens, yet utilizing the same molecular tactics as T cells (19). Dendritic cells are another example of a unique cell type in that it can arise from both lymphoid and myeloid origins (20). The lymphoid lineage of cells is critical to human health, but not the focus of this dissertation. For more information on this order of cells, refer to (21-25).

The myeloid lineage claims the other first line of HSC commitment. Myelopoiesis is the broad term used to describe development of the myeloid compartment, representing a broad class of granulocytes, as well as monocytes, red blood cells (RBC)s, megakaryocytes (MK)s and in turn platelets, including all the progenitors and precursors that precede them. Still, within the confines of the bone marrow, an HSC first transitions to a common myeloid progenitor (CMP), an oligopotent progenitor capable of producing all various types of myeloid cells (26). The CMP then

undergoes further commitment where it can branch into one of two directions; a granulocyte/monocyte restricted progenitor (GMP) or a megakaryocyte/erythrocyte restricted progenitor (MEP) (27). This process is achieved by strictly regulated gene expression profiles, which will be discussed later in this chapter.

As indicated in the name, the GMP has the capability to differentiate into a monocyte or a granulocyte, a broad term to describe a subset of cells such as a mast cell, neutrophil, eosinophil or basophil. All of these cells each have their own set of precursors that ultimately represent the stages of granulopoiesis. Granulopoiesis takes place exclusively within the bone marrow until cells reach the final stages of maturation and are released into circulation. Granulocytes are so named because they possess granules, compartments of enzymes and other agents to assist in their cellular functions (28). It is also important to note that all of the cells generated from GMPs are involved in the other arm of our immune system, innate immunity (29). As opposed to the lymphoid lineage that rules our adaptive immunity, cells involved in innate immunity constantly survey our bodies for pathogens and when activated can launch non-specific, rapid responses to curb infection (29). The term white blood cell (WBC) is a general designation to describe all the cells within both arms of immunity.

Neutrophils, specifically, account for the majority of the WBCs in circulation. They employ multiple tactics to combat infection, one being phagocytosis, or the consumption of extracellular material, which is then trafficked to granules to facilitate decomposition. There are four different classes of neutrophil granules whose contents can also be released into the extracellular space to launch large scale immune response in a process called degranulation (30). Degranulation can also occur at sites of injury or inflammation in the absence of infection, whereby potent, unspecific granule proteins can degrade healthy tissue, most commonly observed in cases of chronic pulmonary diseases (31). Monocytes and their mature counterparts, macrophages, as well as mast and dendritic cells also have the ability to phagocytize, however these cells are far less abundant in circulation. Neutrophils also have the capability to unleash a suite of cytokines and

chemokines to recruit additional immune cells to the site of activation (32). Although this attribute is shared among other cell types, it further highlights the critical role neutrophils play in our innate immunity.

On the other side of immediate CMP differentiation, the MEP bears a smaller branch of the developmental tree, representing erythrocytes, or RBCs, as well as megakaryocytes (27). The latter eventually sheds its cellular components encapsulated in portions of membrane to yield thrombocytes, otherwise known as platelets. Red blood cells are the most abundant cell in our blood. As described earlier, the primary function of RBCs is to facilitate oxygen delivery and carbon dioxide clearance at all sites within the body, governed by the protein hemoglobin.

Megakaryocytes have many unique properties, one example being they are one of the few terminally differentiated blood cells that permanently reside in the bone marrow (33). Megakaryocytes also undergo endomitosis, whereby they achieve all the steps of mitosis however fail to complete anaphase or cytokinesis, leaving them polyploid, with up to 128 copies of each chromosome per cell (34). Although rare (~0.01% of blood cells), MKs are the largest cell of the blood (~50-100 μ M) and in turn give rise to the smallest blood cells, thrombocytes or platelets (2-3 μ M) (35). These platelets are released at the tips of proplatelets, long MK processes that extend to sinusoidal blood vessels where they are then transported across into circulation (36). Each megakaryocyte has the ability to produce 10^4 platelets into circulation with a lifespan of 7-10 days (37, 38). Platelet formation is the primary function of MKs, as these cell fragments are critical for maintaining hemostasis or thrombosis, which is the process of blood clot formation (39).

Blood as a whole plays a paramount role in maintaining homeostasis. A myriad of cell types within the blood and bone marrow work together to deliver oxygen and nutrients to all tissues, defend against invading pathogens, and prevent blood loss through clotting (6, 40, 41). However, this complex system can be easily be disrupted in the case of hematological diseases, those of which can ultimately have fatal consequences.

1.3. Preleukemia: cytopenia and myelodysplastic syndromes

The term 'preleukemia' was first described by Block in 1953 as a hematopoietic disorder presenting with a block in myeloid cell development paired with chronic cytopenia, or an insufficient amount of a certain mature cell type (42). Normally, blood cell progenitors within the marrow adhere to an ordered pathway of maturation where few progenitors yield many mature cells. However, in the case of preleukemic disorders this route is molecularly corrupted due to genetic mutations that prevent cells from reaching their mature, functional form. This leads to an overrepresentation of progenitors within the marrow combined with a lack of mature, functional cells within circulation (43). For the purpose of this thesis I will be focusing specifically on congenital preleukemic disorders although many of these can also be found sporadically in the population, or via somatic, acquired mutations.

In the time since 1953, congenital preleukemic disorders have evolved to be known as inherited bone marrow failure syndromes (IBMFS) those of which can progress to myelodysplastic syndrome (MDS) (43). These syndromes possess a clonal population of cells harboring a genetic mutation that predisposes them to acquire additional mutations or epigenetic changes which can progress to overt leukemia or other malignances (44). There are multiple categories of IBMFS and MDS that are graded based off of morphologic characteristics, proliferative status, and cytogenetic presentation of the bone marrow cells (45). Acute myeloid leukemia (AML) is the most common type of cancer to be associated with IBMFS and MDS and is known to have both high morbidity and mortality (46, 47). The typical pathway of disease progression begins with IBMFS-related cytopenia, which can advance to MDS at any time or rate, thus priming the individual for leukemic transformation to AML or rarely other forms of leukemia or solid cancers (44). Although not all preleukemic individuals develop cancer during their lifetime, the ominous pathway to malignancy is laid out at the genetic level and can have devastating effects upon families unfortunate enough to inherit germline mutations predisposing to bone marrow failure.

1.4. Genetics of preleukemic diseases

Preleukemic diseases can arise from somatic or germline mutations within genes involved in blood cell development (48). Pediatric cases of preleukemic disorders are most often attributed to germline mutations. Adults often present with somatic mutations acquired over their lifetime, while *de novo* mutations can be found in both populations. Mutational and cytogenetic analysis of these individuals is key, because knowing the affected gene can influence their risk of disease progression and guide treatment approaches (49).

As stated, IBMFSs/preleukemia, represents a genetically heterogeneous group of disorders. There are many single-gene loci that when mutated, cause a spectrum of hematological pathology while predisposing the individual to an increased risk of MDS and/or AML for their lifetime (Table 1.1). Substitutions, insertions, and deletions have been found in the following genes: FA complementation group genes, *DKC1*, *RUNX1*, *ANKRD26*, RPS genes, *HAX1*, *SBDS*, *ELANE*, *CSF3R*, *WAS*, *GFI1*, *GP63*, *GATA2* and others have all been implicated as causative of distinct IBMFSs, each with their own uniquely associated clinical features, predisposing to MDS/AML (43, 46, 48, 50, 51). For clarity this review will be organized by the associated primary cytopenia.

1.4.1. Pancytopenia

Dyskeratosis congenita (DC) is an IBMFS characterized by the mucocutaneous triad: nail dystrophy, mucosal leukoplakia and lacy skin pigmentation (52). Although DC can manifest in multiple systems (neurological, gastrointestinal, skeletal and others) bone marrow failure is the main cause of mortality in these individuals. Pancytopenia occurs in the majority of patients early on, with >90% of patients experiencing total bone marrow failure or multiple peripheral cytopenias by the age of 40 (53). Affected individuals also have a 40% risk of malignant transformation to MDS, AML or solid tumors by the age of 50 (54).

Inheritance can be autosomal dominant or recessive as well as X-linked, depending on the gene mutated. Many genes have been identified in DC: *DKC1*, *TERT*, *TERC*, *TINF2*, *TTEL1*, *NOP10*, *NHP2*, *WRAP53*, *CTC1*, and *PARN* (46). A telomere biology disorder, DC-associated

genes are involved in maintaining telomere length and stability, therefore when mutated, cells generated possess extremely short telomeres (55). Diagnosis of DC is not always straightforward as some patients do not present with symptoms until late childhood or early adulthood due to the fact that the disorder exhibits genetic anticipation through intergenerational shortening of telomeres (48).

Fanconi anemia (FA) is another rare predisposition syndrome to bone marrow failure and malignancy caused by homozygous or compound heterozygous mutations in one of the 19 genes within FA complementation groups (*FANCA-FANCP*) (56). These groups normally mediate the repair of stalled DNA replication forks and homologous recombination, thus in the case of FA genetic alterations result in chromosomal fragility (51). Following autosomal recessive or X-linked inheritance, FA typically presents with congenital anomalies and pancytopenia leading to complete bone marrow failure within the first decade of life (43). A truly multi-system disease, FA can rapidly progress to MDS, AML or solid tumors due to increased chromosomal breakage. This is clearly reflected in that the projected median survival age for FA, which is only 23 years (48). Interestingly, heterozygous carriers of many of the FA genes, such as *BRCA1*, are themselves predisposed to adult onset cancers.

1.4.2. Thrombocytopenia

Familial platelet disorder with propensity to myeloid malignancy (FPD/AML) is an autosomal dominant, hereditary disorder caused by germline, heterozygous mutations in the transcription factor (TF) runt-related transcription factor 1 (*RUNX1*). The majority of cases harbor loss of function mutations, resulting in haploinsufficiency, or half-normal levels of RUNX1 protein (57). Hypomorphic alleles with reduced activity or dominant-negative alleles have also been reported in FPD/AML (58). Known as one of the “master regulators” of hematopoiesis, RUNX1 normally binds to its core binding partner CBF β to form a complex that can bind to DNA regulatory domains of genes involved in blood development (59, 60). Similar to other TFs, wild type (WT) RUNX1 protein can also autoactivate its own expression to create a stable feedback loop to

maintain downstream gene profiles (61). Both of these processes can be severely disrupted in FPD/AML.

FPD/AML patients often present with mild to moderate thrombocytopenia, abnormal megakaryocytes, and platelet granule defects, ultimately resulting in bleeding/bruising (62, 63). Importantly, FPD/AML is one of several autosomal dominantly inherited disorders predisposing to MDS/AML and less commonly T-cell acute lymphocytic leukemia (T-ALL), chronic lymphocytic leukemia (CLL), and chronic myelomonocytic leukemia (CMML) (63, 64). Heritable *RUNX1* mutations collectively account for a high proportion of all leukemia, regardless of family history (65).

ANKRD26-Related thrombocytopenia (*ANKRD26*-RT) also known as thrombocytopenia 2, this disorder is caused by single nucleotide substitutions and small deletions within the promoter and/or 5' untranslated region of ankyrin repeat domain 26 gene (*ANKRD26*) (66). Although the molecular implications of these mutations are not yet fully known, theories suggest that the mutated promoter of *ANKRD26* escapes normal downregulation by *RUNX1*, which is believed to be necessary for megakaryocyte development and proplatelet formation (67). Patients present with moderate thrombocytopenia resulting in mild bleeding and are greatly predisposed to undergo leukemic transformation to MDS, AML or chronic myeloid leukemia (CML) (68). Initially thought to be very rare, this autosomal dominant disorder has recently been reported in 11 additional families in Italy making it a more prominent form of inherited thrombocytopenia predisposing to malignancy than first believed (69).

1.4.3. Anemia

Diamond-Blackfan anemia (DBA) is an IBMFS presenting with congenital anomalies and red cell hypoplasia or failure, with an increased incidence of developing cancer (70, 71). Diagnosis typically occurs within the first year of life due to pronounced anemia. An autosomal dominant inherited disorder of ribosome biogenesis, a suite of genes have been implicated in DBA: *RPS19*, *RPS17*, *RPS24*, *RPL35A*, *RPL5*, *RPL11*, *RPS7*, *RPS26*, and *RPS10* (72, 73). Longitudinal

studies have concluded that DBA patients have an elevated risk of MDS, AML, colon cancer, osteosarcoma and HPV-related cancer (70) whereby 20% of individuals progress to MDS/AML during their lifetime (51). Interestingly, an equivalent proportion of DBA patients undergo spontaneous remission, the reason for which is unknown (74).

1.4.4. Neutropenia

Kostmann syndrome (KS) is an IBMFS within the umbrella of severe congenital neutropenia (SCN) caused by homozygous, germline mutations in the gene HCLS1-associated protein X-1 (*HAX1*). Encoding a protein with the same name, HAX1 is known to function in signal transduction and cytoskeletal control, but most importantly it plays a role maintaining inner mitochondrial membrane potential and preventing apoptosis specifically in myeloid cells (75). Early in life KS patients present with profound neutropenia with granulocytic maturation arrest which can be paired with neurological symptoms, depending on the mutation (76, 77). Kostmann syndrome accounts for approximately 7% of SCN cases (78). Leukemic transformation to AML in KS has been observed in 20-40% of patients (75).

Shwachman-Diamond syndrome (SDS) also falls within the SCN group and is associated with non-hematological pathologies such as pancreatic insufficiency and skeletal abnormalities (79). This syndrome accounts for roughly 14% of total congenital neutropenia cases reported (78). Homozygous, or compound heterozygous mutations in Shwachman-Bodian-Diamond syndrome gene (*SBDS*) cause SDS due to faulty ribosome assembly. Hematological presentations include neutropenia, with a smaller percentage of SDS patients experiencing thrombocytopenia or anemia (80). Approximately one third of SDS cases undergo leukemic transformation to MDS or AML (81, 82).

ELANE-associated congenital neutropenia accounts for the majority of inherited neutropenia cases cataloged (>50%) (83). There are two types of *ELANE*-associated neutropenia with widely different presentations, severe (EA-SCN) and cyclic neutropenia (CyN). Interestingly enough, both forms are inherited via autosomal dominance or *de novo* heterozygous mutations in the gene

ELANE and in some cases, the same mutation was reported in both EA-SCN and CyN presenting individuals (84, 85). *ELANE* produces the protein neutrophil elastase (NE), a potent granule enzyme involved in degradation of bacteria and necrotic tissues at sites of inflammation, which frequently retains some level of catalytic activity, even when mutated (86). Unlike other forms of IBMFSs characterized by haploinsufficiency of the mutated protein, all disease model studies to date show that mutant NE is expressed, or theoretically expressed. This is because *ELANE* mutations are mostly single residue substitutions, in-frame transitions, or nonsense mutations restricted to the final exon, whereby the mutant transcript would escape nonsense mediated decay. EA-SCN patients present with profound, life-long neutropenia, monocytosis, and a block in neutrophil maturation at the promyelocyte stage (87). On the other hand, in the case of CyN, neutrophil counts dramatically oscillate between normal to nearly zero on a 21-day cycle with monocytes cycling reciprocally (88). Other than presentation, the primary difference distinguishing EA-SCN from CyN is that EA-SCN has a high rate of leukemic transformation to MDS/AML while CyN patients generally do not progress to MDS/AML.

There are three well-supported hypotheses for mutant NE pathogenesis, one being the mislocalization hypothesis which states that mutations in NE ultimately disrupt its ability to traffic to granules, causing proteolytic damage at unintended destinations (89-92). The misfolding hypothesis is also accepted as a mechanism of disease for some mutations, whereby upon expression, NE mutations cause the nascent protein to misfold, initiating the endoplasmic reticulum (ER) stress response, with consequent activation of the unfolded protein response (UPR) (93). It is thought that these events eventually force mutant NE-producing cells to apoptose, explaining the evident block in maturation coincidentally with *ELANE* expression at the promyelocyte stage. Cell models and patient neutrophils have shown markers of ER stress by way of BiP/GRP78 expression, and XBP1 mRNA splicing (90, 91, 94-96). The most recent hypothesis for neutrophil elastase pathogenesis stems from our lab's discovery of multiple SCN patients with various mutations at or near the translational start site of *ELANE* (97-99). Upon

thorough investigation it was found that Kozak ribosome binding site and translational start site mutations produce three genetically intact short polypeptides by way of an internal ribosomal entry site (IRES) nested within genomic *ELANE*. These short peptides bypassed ER homing and mislocalized to the nucleus. Interestingly one of the three peptides was found to retain minimal catalytic activity (90). It is important to note that in times of protein misfolding and ER stress, the pathway of IRES-mediated translation is preferentially chosen over normal 5' cap-dependent translation (100). Therein lies the mistranslation hypothesis, stating that *ELANE* start site mutations and others known to induce ER stress/UPR will utilize internal start sites to produce short, catalytically active, pathogenic polypeptides facilitating disease. This further supports the notion that the three proposed mechanisms of disease are not mutually exclusive, rather more likely complementary or additive.

Severe congenital neutropenia is genetically heterogenous with a small proportion (<5% total cases) attributed to mutations in the genes *CSF3R*, *WAS*, *GFI1*, *GP6C3* and others.

There are two classes of granulocyte-colony stimulating factor receptor 3 (*CSF3R*) mutations that have been found as causative of SCN (101). The protein product, granulocyte-colony stimulating factor receptor (GCSF-R) plays a huge role in granulopoiesis, more specifically acting as a main driver of neutrophil development when activated by the presence of granulocyte-colony stimulating factor (GCSF) (27). Hyper-responsive mutations in *CSF3R* due to C-terminal truncations cause GCSF-R to enhance granulocytic proliferation at the expense of maturation (102). Patients present with modest neutropenia and a block in neutrophil development within the bone marrow, and have a strong predisposition to MDS and AML transformation (103). Hypo-responsive mutations in GCSF-R act oppositely in that developing cells are unable to process normal and therapeutic doses of GCSF due to disruptions in the extracellular domain and therefore fail to mature (104). It should be emphasized, however, that most *CSF3R* mutations that occur in association with SCN are of somatic, rather than germline origin, and may represent a first step along transformation to MDS or AML.

An extremely rare form of X-linked SCN is due to a mutation in Wiskott-Aldrich syndrome gene (*WAS*) resulting in gain of function activity for the expressed protein Wiskott-Aldrich syndrome protein (*WASp*) (105), whereas *WAS* mutations are more typically associated with thrombocytopenia, one of the primary features of Wiskott-Aldrich syndrome. Constitutively active *WASp* results in unregulated actin polymerization causing defects in mitosis and cytokinesis which in turn target myeloid progenitors to decrease turnover and increase cell death (106, 107). In conjunction with neutropenia, patients experience lymphopenia and altered neutrophil phagocytic activity (106, 108, 109). Similar to *ELANE* and *CSF3R* associated SCN, there have been reported cases of *WAS*-related SCN cases progressing to MDS and AML (105).

Roughly 1-2% of individuals affected with SCN harbor heterozygous mutations in growth factor-independent protein 1 (*GFI1*) (110). Normally this oncoprotein acts to transcriptionally repress specific gene targets to further shepherd myeloid and neutrophil maturation, which in the case of SCN is completely inactivated. Evidence suggests the molecular implication of this loss in activity causes in an upregulation of *ELANE* over baseline causing overexpression of NE resulting in ER stress leading to UPR (110). Other studies have showed that the loss of functional *GFI1* increases expression of the critical transcription factor CCAAT-enhancer-binder protein epsilon (*C/EBP ϵ*) to promote lineage switching towards monocytes (111). These patients present with neutropenia with maturation arrest, monocytosis, primitive myeloid cells in circulation, and lymphopenia (87). Although *GFI1* is a known oncoprotein there have been so few reports of *GFI1* mutations in SCN the risk of MDS or AML progression is currently unknown.

Approximately 2% of SCN cases are caused by biallelic, missense mutations in the gene glucose 6 phosphatase catalytic subunit 3 (*G6PC3*) (112). Patients present with severe neutropenia showing an arrest in myeloid maturation, intermittent thrombocytopenia as well as extra-hematological pathologies such as cardiac and/or urogenital malformations, hearing loss or delayed growth (108). The wild type protein is typically localized to the ER. However, when mutated, rapidly induces ER stress, UPR and increased susceptibility to apoptosis. Due to the

low frequency of *G6PC3* associated SCN, the threat of leukemic transformation is not determined (50).

1.4.5. Complex presentation: GATA2 deficiency

GATA2 deficiency syndrome is another example of how germline haploinsufficiency of a master transcription regulator can influence hematopoiesis. Heterozygous loss of function mutations or deletions in the gene GATA binding protein 2 (*GATA2*) or its promoter region is the most common germline predisposition to MDS/AML in children (113, 114). Patients can present different constellations of symptoms, such as mild neutropenia (115), Emberger syndrome indicated by lymphedema and monosomy 7, or MonoMAC syndrome revealed by monocytopenia, eosinophilia, deficient NK and B cells as well as increased incidence of opportunistic infections (113). Importantly, leukemic transformation to MDS, AML or CMML occurs in 70% of individuals by the age of 29 (116).

As mentioned previously, WT *GATA2* is critical for basal hematopoiesis, normally regulating other genes involved in HSC maintenance and myeloid development such as *GFI1* and *RUNX1* (117, 118). This is further supported by observations of deregulated proliferation and differentiation of HSCs the bone marrow in affected individuals (119). When unmutated, *GATA2* protein directly binds to *RUNX1* as well as other TFs (*SCL*, *LYL1*, *LMO2*, *FLI-1*, and *ERG*), which forms a complex to bind to promoters of genes associated with HSC proliferation, quiescence and differentiation (120). With these points in mind it is therefore understandable why individuals with *GATA2* deficiency syndrome experience such a complex presentation spanning multiple avenues of blood cell formation.

1.4.6. Inherited acute myeloid leukemia

Familial AML syndrome with heterozygous mutations in CCAAT enhancer binding protein alpha (*CEBP α*) is a rare, autosomal dominant inherited form of preleukemia with near complete penetrance (121, 122). Transformation to AML from a stable MDS-like state typically occurs once

somatic, biallelic mutations arise in the wild type allele of *CEBP α* at a median age of 24.5 years (122). As another master regulator of hematopoiesis, *CEBP α* acts upon MPPs to favor myeloid commitment at the expense of lymphoid differentiation, and then later pushes progenitor populations toward the granulocytic lineage by inducing expression of *CSF3R* resulting in malignancy (123-125).

1.5. Leukemogenesis in inherited bone marrow failure syndromes

As implied in the name and the previously discussed material, inherited preleukemic disorders can undergo leukemic transformation to MDS, hematological or nonhematological malignancies anytime during affected patient's lifetime. This threat is most often dependent on the individual's preexisting mutations which can potentiate or select for additional, specific genetic abnormalities to arise.

In the case of malignant transformation in FA, patients can progress to hematological or solid tumors with a high prevalence. Although not completely understood, the most common driver mutation in FA is acquisition of mutations in *BRCA2* which is found in 97% of solid tumors and 80% of AML cells from FA patients (126, 127), noting that homozygous germline mutations in *BRCA2* are a rare cause of FA. Both FA and DC cells show increased chromosomal instability, rearrangements, gaps and breaks that may promote leukemogenesis (128, 129).

Leukemic transformation of FPD rarely results from a two-hit mechanism involving acquisition of mutations in the wild type *RUNX1* allele (130-133). More often, cooperating mutations in other genes associated with sporadic (non-inherited) forms of MDS and leukemia are found, such as *DNMT3A* and in some populations *CDC25C* and *CBL* (130, 134, 135). Thrombocytopenia 2 has a very low risk of developing cancer and due to the rarity of the disease driver mutations have not yet been identified. Additional studies into mechanisms of leukemogenesis in Diamond Blackfan anemia are needed to resolve the pathways of cancer predisposition and progression as well.

Severe congenital neutropenia caused by mutations in *ELANE*, *CSF3R*, and *WAS* have a particularly high rate of leukemic transformation to MDS and in turn AML (136). Over 70% of *ELANE*-associated SCN patients that developed MDS/AML were found to harbor heterozygous mutations in *CSF3R* (101, 137, 138). The most common class of mutations are nonsense mutations resulting in carboxyl truncation and loss of the receptor portions responsible for transducing maturation signals and inhibiting proliferative cues, which in turn drive strong proliferative and survival signals (103, 139). These mutations have also been detected in secondary malignancies from SCN attributed to *WAS* mutations and curiously, hyporesponsive *CSF3R* SCN (140, 141). Mutations in GSCF-R do not occur in some other forms of inherited neutropenia, such as SDS (142). Studies also found that *RUNX1* mutations occur in roughly 65% of transformed SCN patients, most commonly occurring in the clones already possessing *CSF3R* mutations where both mutations are believed to promote leukemogenesis (143). Kostmann syndrome also follows similar mechanisms of leukemic transformation at similar rates (140). Although rare, mutations in *RAS*, *SUZ12*, *EP300*, and *ASXL1* have been reported in SCN cases post leukemic transformation (143, 144). As stated before, SCN attributed to mutations in *GFI1*, *G6PC3* and *ELANE* in cases of CyN are not known to progress to MDS, leukemia, or solid cancers. However, due to few reports and complex presentation in the instance of CyN, additional genetic screenings are always encouraged in patient care.

Acquired driver mutations in *NRAS*, *RUNX1*, *STAG2*, *IDH2*, *TP53* and *SETDB1* have all been recorded in cases of secondary AML from *GATA2* deficiency (145). Interestingly, *ASXL1* mutations have also been identified exclusively in *GATA2* deficient females (146, 147). In the case of SDS, acquisition of tumor protein 53 (*TP53*) mutations provide HSCs with an enormous selective advantage for expansion and in turn initiates leukemogenesis (148). Somatic *TP53* mutations, which are found in roughly 50% of all cancers, account for 5% of primary leukemia, and is commonly associated with poor prognosis (149).

Chromosomal abnormalities have also been detected in many IBMFSs that advance to malignancy. Clonal expansion of monosomy 7 has been detected in FA, SDS, GATA2 deficiency, and SCN-associated malignancies (140, 147, 150). Loss of 20q has also been observed in many cases of SDS that develop cancer (151, 152). Data are insufficient to conclude that monosomy 20q alone is causative of MDS, but regardless this chromosomal abnormality is frequently observed in MDS, AML and myeloproliferative disorders (MPD) (153, 154). Acquisition of trisomy 8 and 13 have also been recorded in transformed SCN (143). There is also considerable evidence that acquired trisomy 21 promotes leukemogenesis in SCN and FPD (133). It is important to note that individuals born with trisomy 21 resulting in Down's syndrome (DS) have a higher incidence of ALL in early life with the risk for leukemia transitioning to AML later in childhood, when compared to the general population (155). Although it is still unknown why germline and acquired trisomy 21 has a particular high rate of hematological malignancy it is worth noting that the *RUNX1* gene resides on chromosome 21.

The field has made large strides in understanding the mechanisms of IBMFS progression to myeloid malignancy in the past decades. However, there is still work to be done to not only improve the basic understanding of disease pathogenesis but also how to mitigate the risk of leukemic transformation. In order to achieve this, we must think outside the pill box to discover alternative approaches to treat these diseases.

1.6. Current treatments and therapies for inherited bone marrow failure syndromes

Treatment options vary for IBMFSs depending on presentation, severity, and causative mutation. The most reliable cure for IBMFSs, MDS, and all leukemias remains a stem cell/bone marrow transplant (SCT) following bone marrow ablation; however, the risks associated with this procedure for any patient remains significant (156).

In cases of FA prior to transformation, androgens have been shown to improve blood counts and reduce the need for transfusions in 60-70% of patients (157). However, if leukemia develops, these patients have poor survival outcomes (43). Unfortunately, there are no therapies

available to manage DC or other telomere diseases, and similar to FA, patients have a high rate of post-SCT complications (54). Moreover, there are no current treatment options in place for rescuing *RUNX1* haploinsufficiency in FPD causing thrombocytopenia outside of necessary platelet transfusions (158). Some cases of *ANKRD29*-related thrombocytopenia have improved under corticosteroid treatment as well as regular platelet transfusions (159). Further support for corticosteroid administration was gained when 80% of non-transformed DBA patients were found to undergo spontaneous remission as a result of treatment (160). Alternatively, regular RBC transfusions paired with intermittent iron chelation was found to rescue anemia to an extent in DBA (161). Deficiency of *GATA2* is similarly limited in therapeutic options outside of SCT, however when SCT is performed these patients typically have a good prognosis (119).

Historically, profound neutropenia would result in childhood death due to infections (162). First used in 1987, and now considered the frontline therapy for acquired and congenital neutropenia patients (other than those harboring *GFI1* and hyporesponsive *CSF3R*), is recombinant G-CSF, administered subcutaneously or through intravenous injection (163). As previously described, G-CSF is one of the main regulators of granulopoiesis, this cytokine is able to influence the survival, proliferation, and differentiation of all cells within the neutrophil lineage. Upon G-CSF release or administration, receptors on myeloid progenitors induce myriad signal transduction pathways, such as Ras/Raf/MAPK, PI3-Kineas, and JAK/STAT cascades resulting in increased neutrophil production and their rapid release into circulation which often restores neutrophil numbers to normal (164). Although standard, recombinant G-CSF therapy for neutropenic individuals is not without complications. It has been reported that G-CSF mobilized neutrophils are functionally less capable, with abnormal granule formation (165). Furthermore, there is still argument within the field that EA-SCN patients who require high doses of G-CSF have a higher rate of leukemic transformation compared to KS patients with the same *CSF3R* mutations (101, 142, 166). Interestingly however, recent studies have shown that acquisition of

mutations in *CSF3R* may protect myeloid precursor cells from apoptosis induced by mutant NE (167).

Overall, avenues for IBMFS therapy are very limited and because of that physicians focus on symptoms they can treat directly. Exemplified in the case of SDS, the use of pancreatic enzymes and fat-soluble vitamins have historically helped patients with non-hematological pathology, which can be applied to other complex presentations of IBMFSs (43). It is also important to manage the threat of infection for any IBMFS as affected patients are always struggling to maintain sufficient hematopoiesis. Therefore bacterial, viral, or fungal infections can prove fatal when not closely monitored. Complete blood counts (CBC) and annual bone marrow aspirations with cytogenetic panels are critical to screen for clonal evolution towards leukemic transformation (46). Considering there is a clear void in treatment options available to individuals affected with IBMFSs, the field must work to present novel therapeutic approaches and importantly, continue to develop new models for studying disease pathogenesis.

1.7. Disease models for studying inherited bone marrow failure syndromes

There have been substantial advancements in personalized medicine in the last decade. Humanized animal models recapitulating aspects of hematological diseases have improved our understanding of how these heritable mutations can have systemic effects on health. With the power of iPSC reprogramming, we have been able to develop disease-specific cell lines for many IBMFSs (reviewed in (168)). High-throughput drug screenings of new agents have progressed towards clinical trials to challenge pathogenic mechanisms like reactive oxygen species (ROS), cytokines, and drivers of graft versus host disease (GVHD) (43). The age of genome editing and gene therapy is now upon us, allowing scientists to successfully expand the boundaries of translational medicine. These gains have provided us with insights into the disease mechanisms of IBMFSs and revealed potential therapeutic avenues for exploration, certain aspects of which will be presented in this thesis.

This thesis addresses two IBMFSs in particular: familial platelet disorder with predisposition to myeloid malignancy and *ELANE*-associated severe congenital neutropenia. Chapter 2 focuses on FPD, whereby we show that brief inhibition of RUNX1 protein degradation pathways may prove as a valid technique to combat RUNX1 haploinsufficiency. By utilizing multiple cancer cell lines, FPD-iPSCs, and primary FPD bone marrow samples we find that temporary proteasome or cyclin dependent kinase inhibition can rescue features of megakaryocyte malfunction. This approach could potentially reach outside the realm of FPD to other diseases associated with haploinsufficiency of auto-activating transcription factors, such as GATA2 deficiency.

Chapter 3 will describe the extensive work I have completed to assess the importance of neutrophil elastase catalysis in *ELANE*-associated neutropenia. Considering that the residues involved in NE proteolysis have never found to be affected in SCN or CyN, paired with the exciting work evaluating G-CSF and NE inhibitor treatment of SCN iPSCs (91), we used techniques of genome editing in iPSCs to test the role of NE catalysis in SCN. With this strategy we have generated novel iPSC lines to study how NE catalysis governs neutrophil development overall, as well as SCN pathogenesis. Lastly, collaborations with colleagues from Memorial Sloan Kettering Cancer Center yielded evidence to suggest that a variant of unknown significance in the gene *SUZ12* (T679I) is causative of congenital neutropenia. By using proband blood-derived iPSCs we were able to produce phenotypes found in the patient upon myeloid differentiation and determine differences in epigenetic landscape compared to WT iPSCs. This is the first instance, to our knowledge, indicating that mutations in proteins directly involved in chromatin remodeling can result in congenital neutropenia.

1.8. Tables

Table 1.1 Single-gene disorders encompassing bone marrow failure syndromes, myelodysplastic syndromes, and predisposition to myeloid neoplasms.

Primary cytopenia	Syndrome	Gene	Inheritance	Associated hematological phenotypes	Home malignancy	Risk of MDS/AML
Pancytopenia	Fanconi anemia	FA complementation groups	AR, X-linked	progressive bone marrow, pancytopenia, thrombocytopenia, aplastic anemia	MDS/AML/solid tumors	40-50%
	Dyskeratosis congenita	DKC1, TERC, TERT, others	AD, AR, X-linked	macrocytosis, thrombocytopenia, aplastic anemia	MDS/AML/solid tumors	30-40%
Thrombocytopenia	Familial platelet disorder with propensity to myeloid malignancies	RUNX1	AD	Mild-moderate thrombocytopenia, megakaryocyte abnormalities	MDS/AML/T-cell ALL	20-60%
	ANKRD26-related thrombocytopenia	ANKRD26-RT	AD	moderate thrombocytopenia	MDS/AML/CML	1-3-5%
Anemia	Diamond-Blackfan anemia	FPS genes	AD	anemia, macrocytosis, elevated RBC adenosine deaminase	MDS/AML/ALL/other cancers	1-20%
	Kostmann syndrome	HAX1	AR	neutropenia, increase apoptosis of myeloid cells	MDS/AML	20-40%
	Shwachman-Diamond syndrome	SBDS	AR, compound heterozygous	mild neutropenia, low serum enzymes, dysgranulopoiesis	MDS/AML/ALL	20-30%
	Neutropenia	Severe congenital neutropenia	ELANE	AD	neutropenia, arrest of neutrophil development, monocytosis	MDS/AML
CSF3R			AD	maturation arrest of granulocytes, unresponsive to therapy, increased apoptosis of neutrophils	MDS/AML	16%
WAS			X-linked	lymphopenia, monocytopenia, low NK levels	MDS/AML	unknown
G6PC3			AD	monocytosis, defective myeloid differentiation, lymphopenia	unknown	unknown
ELANE			AD	cycling neutropenia with reciprocal monocytosis	unknown	unknown
Complex presentation	GATA2 Deficiency	GATA2	AD	severe viral infections, neutropenia, monocytopenia, esodinothilia, low NK and B cell levels	MDS/AML/CML	50%
Familial AML	Familial AML with mutated CEBPA	CEBPA	AD	AML	AML	100%

1.9. References

1. Costa G, Kouskoff V, Lacaud G. Origin of blood cells and HSC production in the embryo. *Trends Immunol.* 2012;33(5):215-23.
2. Palis J. Ontogeny of erythropoiesis. *Curr Opin Hematol.* 2008;15(3):155-61.
3. Ferkowicz MJ, Yoder MC. Blood island formation: longstanding observations and modern interpretations. *Exp Hematol.* 2005;33(9):1041-7.
4. Tober J, Koniski A, McGrath KE, Vemishetti R, Emerson R, de Mesy-Bentley KK, et al. The megakaryocyte lineage originates from hemangioblast precursors and is an integral component both of primitive and of definitive hematopoiesis. *Blood.* 2007;109(4):1433-41.
5. Kumar A, D'Souza SS, Thakur AS. Understanding the Journey of Human Hematopoietic Stem Cell Development. *Stem Cells Int.* 2019;2019:2141475.
6. Dzierzak E, Bigas A. Blood Development: Hematopoietic Stem Cell Dependence and Independence. *Cell Stem Cell.* 2018;22(5):639-51.
7. Swiers G, de Bruijn M, Speck NA. Hematopoietic stem cell emergence in the conceptus and the role of Runx1. *Int J Dev Biol.* 2010;54(6-7):1151-63.
8. Iacovino M, Chong D, Szatmari I, Hartweck L, Rux D, Caprioli A, et al. HoxA3 is an apical regulator of haemogenic endothelium. *Nat Cell Biol.* 2011;13(1):72-8.
9. Ling KW, Ottersbach K, van Hamburg JP, Oziemlak A, Tsai FY, Orkin SH, et al. GATA-2 plays two functionally distinct roles during the ontogeny of hematopoietic stem cells. *J Exp Med.* 2004;200(7):871-82.
10. Hadland BK, Huppert SS, Kanungo J, Xue Y, Jiang R, Gridley T, et al. A requirement for Notch1 distinguishes 2 phases of definitive hematopoiesis during development. *Blood.* 2004;104(10):3097-105.
11. Muench MO, Kapidzic M, Gormley M, Gutierrez AG, Ponder KL, Fomin ME, et al. The human chorion contains definitive hematopoietic stem cells from the fifteenth week of gestation. *Development.* 2017;144(8):1399-411.
12. Jagannathan-Bogdan M, Zon LI. Hematopoiesis. *Development.* 2013;140(12):2463-7.
13. Sankaran VG, Orkin SH. The switch from fetal to adult hemoglobin. *Cold Spring Harb Perspect Med.* 2013;3(1):a011643.
14. Medvinsky A, Rybtsov S, Taoudi S. Embryonic origin of the adult hematopoietic system: advances and questions. *Development.* 2011;138(6):1017-31.
15. Batsivari A, Rybtsov S, Souilhol C, Binagui-Casas A, Hills D, Zhao S, et al. Understanding Hematopoietic Stem Cell Development through Functional Correlation of Their Proliferative Status with the Intra-aortic Cluster Architecture. *Stem Cell Reports.* 2017;8(6):1549-62.
16. Ballen K. Umbilical Cord Blood Transplantation: Challenges and Future Directions. *Stem Cells Transl Med.* 2017;6(5):1312-5.
17. Chou BK, Ye Z, Cheng L. Generation and homing of iPSC-derived hematopoietic cells in vivo. *Mol Ther.* 2013;21(7):1292-3.
18. Tan YT, Ye L, Xie F, Beyer AI, Muench MO, Wang J, et al. Respecifying human iPSC-derived blood cells into highly engraftable hematopoietic stem and progenitor cells with a single factor. *Proc Natl Acad Sci U S A.* 2018;115(9):2180-5.
19. Eberl G, Colonna M, Di Santo JP, McKenzie AN. Innate lymphoid cells. Innate lymphoid cells: a new paradigm in immunology. *Science.* 2015;348(6237):aaa6566.

20. Manz MG, Traver D, Miyamoto T, Weissman IL, Akashi K. Dendritic cell potentials of early lymphoid and myeloid progenitors. *Blood*. 2001;97(11):3333-41.
21. Blom B, Spits H. Development of human lymphoid cells. *Annu Rev Immunol*. 2006;24:287-320.
22. Bonilla FA, Oettgen HC. Adaptive immunity. *J Allergy Clin Immunol*. 2010;125(2 Suppl 2):S33-40.
23. Crotty S. A brief history of T cell help to B cells. *Nat Rev Immunol*. 2015;15(3):185-9.
24. Hoffman W, Lakkis FG, Chalasani G. B Cells, Antibodies, and More. *Clin J Am Soc Nephrol*. 2016;11(1):137-54.
25. Koch U, Radtke F. Mechanisms of T cell development and transformation. *Annu Rev Cell Dev Biol*. 2011;27:539-62.
26. Akashi K, Traver D, Miyamoto T, Weissman IL. A clonogenic common myeloid progenitor that gives rise to all myeloid lineages. *Nature*. 2000;404(6774):193-7.
27. Weiskopf K, Schnorr PJ, Pang WW, Chao MP, Chhabra A, Seita J, et al. Myeloid Cell Origins, Differentiation, and Clinical Implications. *Microbiol Spectr*. 2016;4(5).
28. Geering B, Stoeckle C, Conus S, Simon HU. Living and dying for inflammation: neutrophils, eosinophils, basophils. *Trends Immunol*. 2013;34(8):398-409.
29. Bruce Alberts AJ, Julian Lewis, Martin Raff, Keith Roberts, and Peter Walter. *Innate Immunity. Molecular Biology of the Cell*. 4th ed. New York: Garland Science; 2002.
30. Rosales C. Neutrophil: A Cell with Many Roles in Inflammation or Several Cell Types? *Front Physiol*. 2018;9:113.
31. Grommes J, Soehnlein O. Contribution of neutrophils to acute lung injury. *Mol Med*. 2011;17(3-4):293-307.
32. Rosales C, Uribe-Querol E. Phagocytosis: A Fundamental Process in Immunity. *Biomed Res Int*. 2017;2017:9042851.
33. Pease DC. An electron microscopic study of red bone marrow. *Blood*. 1956;11(6):501-26.
34. Lordier L, Jalil A, Aurade F, Larbret F, Larghero J, Debili N, et al. Megakaryocyte endomitosis is a failure of late cytokinesis related to defects in the contractile ring and Rho/Rock signaling. *Blood*. 2008;112(8):3164-74.
35. Frojmovic MM, Milton JG. Human platelet size, shape, and related functions in health and disease. *Physiol Rev*. 1982;62(1):185-261.
36. Richardson JL, Shivdasani RA, Boers C, Hartwig JH, Italiano JE, Jr. Mechanisms of organelle transport and capture along proplatelets during platelet production. *Blood*. 2005;106(13):4066-75.
37. Long MW. Megakaryocyte differentiation events. *Semin Hematol*. 1998;35(3):192-9.
38. Harker LA, Finch CA. Thrombokinetics in man. *J Clin Invest*. 1969;48(6):963-74.
39. Holinstat M. Normal platelet function. *Cancer Metastasis Rev*. 2017;36(2):195-8.
40. Doulatov S, Notta F, Laurenti E, Dick JE. Hematopoiesis: a human perspective. *Cell Stem Cell*. 2012;10(2):120-36.
41. Morrison SJ, Scadden DT. The bone marrow niche for haematopoietic stem cells. *Nature*. 2014;505(7483):327-34.
42. Block M, Jacobson LO, Bethard WF. Preleukemic acute human leukemia. *J Am Med Assoc*. 1953;152(11):1018-28.

43. Savage SA, Dufour C. Classical inherited bone marrow failure syndromes with high risk for myelodysplastic syndrome and acute myelogenous leukemia. *Semin Hematol.* 2017;54(2):105-14.
44. Shlush LI, Minden MD. Preleukemia: the normal side of cancer. *Curr Opin Hematol.* 2015;22(2):77-84.
45. Albitar M, Manshouri T, Shen Y, Liu D, Beran M, Kantarjian HM, et al. Myelodysplastic syndrome is not merely "preleukemia". *Blood.* 2002;100(3):791-8.
46. Rafei H, DiNardo CD. Hereditary myeloid malignancies. *Best Pract Res Clin Haematol.* 2019;32(2):163-76.
47. Ma X. Epidemiology of myelodysplastic syndromes. *Am J Med.* 2012;125(7 Suppl):S2-5.
48. Alter BP. Diagnosis, genetics, and management of inherited bone marrow failure syndromes. *Hematology Am Soc Hematol Educ Program.* 2007:29-39.
49. Cargo CA, Rowbotham N, Evans PA, Barrans SL, Bowen DT, Crouch S, et al. Targeted sequencing identifies patients with preclinical MDS at high risk of disease progression. *Blood.* 2015;126(21):2362-5.
50. Touw IP. Game of clones: the genomic evolution of severe congenital neutropenia. *Hematology Am Soc Hematol Educ Program.* 2015;2015:1-7.
51. Babushok DV, Bessler M. Genetic predisposition syndromes: when should they be considered in the work-up of MDS? *Best Pract Res Clin Haematol.* 2015;28(1):55-68.
52. Walne AJ, Dokal I. Advances in the understanding of dyskeratosis congenita. *Br J Haematol.* 2009;145(2):164-72.
53. Dokal I. Dyskeratosis congenita in all its forms. *British Journal of Haematology.* 2000;110(4):768-79.
54. Alter BP, Giri N, Savage SA, Rosenberg PS. Cancer in dyskeratosis congenita. *Blood.* 2009;113(26):6549-57.
55. Dokal I, Vulliamy T. Inherited bone marrow failure syndromes. *Haematologica.* 2010;95(8):1236-40.
56. Bogliolo M, Surrallés J. Fanconi anemia: a model disease for studies on human genetics and advanced therapeutics. *Curr Opin Genet Dev.* 2015;33:32-40.
57. Harada H, Harada Y, Niimi H, Kyo T, Kimura A, Inaba T. High incidence of somatic mutations in the AML1/RUNX1 gene in myelodysplastic syndrome and low blast percentage myeloid leukemia with myelodysplasia. *Blood.* 2004;103(6):2316-24.
58. Matheny CJ, Speck ME, Cushing PR, Zhou Y, Corpora T, Regan M, et al. Disease mutations in RUNX1 and RUNX2 create nonfunctional, dominant-negative, or hypomorphic alleles. *EMBO J.* 2007;26(4):1163-75.
59. Ichikawa M, Asai T, Chiba S, Kurokawa M, Ogawa S. Runx1/AML-1 Ranks as a Master Regulator of Adult Hematopoiesis. *Cell Cycle.* 2014;3(6):720-2.
60. Tober J, Maijenburg MW, Speck NA. Taking the Leap: Runx1 in the Formation of Blood from Endothelium. *Curr Top Dev Biol.* 2016;118:113-62.
61. Martinez M, Hinojosa M, Trombly D, Morin V, Stein J, Stein G, et al. Transcriptional Auto-Regulation of RUNX1 P1 Promoter. *PloS one.* 2016;11(2):e0149119.
62. Downton SB, Beardsley D, Jamison D, Blattner S, Li FP. Studies of a familial platelet disorder. *Blood.* 1985;65(3):557-63.

63. Latger-Cannard V, Philippe C, Bouquet A, Baccini V, Alessi MC, Ankri A, et al. Haematological spectrum and genotype-phenotype correlations in nine unrelated families with RUNX1 mutations from the French network on inherited platelet disorders. *Orphanet J Rare Dis.* 2016;11:49.
64. Hayashi Y, Harada Y, Huang G, Harada H. Myeloid neoplasms with germ line RUNX1 mutation. *Int J Hematol.* 2017;106(2):183-8.
65. DiNardo CD, Bannon SA, Routbort M, Franklin A, Mork M, Armanios M, et al. Evaluation of Patients and Families With Concern for Predispositions to Hematologic Malignancies Within the Hereditary Hematologic Malignancy Clinic (HHMC). *Clin Lymphoma Myeloma Leuk.* 2016;16(7):417-28 e2.
66. Pippucci T, Savoia A, Perrotta S, Pujol-Moix N, Noris P, Castegnaro G, et al. Mutations in the 5' UTR of ANKRD26, the ankirin repeat domain 26 gene, cause an autosomal-dominant form of inherited thrombocytopenia, THC2. *Am J Hum Genet.* 2011;88(1):115-20.
67. Bluteau D, Balduini A, Balayn N, Currao M, Nurden P, Deswarte C, et al. Thrombocytopenia-associated mutations in the ANKRD26 regulatory region induce MAPK hyperactivation. *J Clin Invest.* 2014;124(2):580-91.
68. Noris P, Favier R, Alessi MC, Geddis AE, Kunishima S, Heller PG, et al. ANKRD26-related thrombocytopenia and myeloid malignancies. *Blood.* 2013;122(11):1987-9.
69. Noris P, Perrotta S, Seri M, Pecci A, Gnan C, Loffredo G, et al. Mutations in ANKRD26 are responsible for a frequent form of inherited thrombocytopenia: analysis of 78 patients from 21 families. *Blood.* 2011;117(24):6673-80.
70. Vlachos A, Rosenberg PS, Atsidaftos E, Alter BP, Lipton JM. Incidence of neoplasia in Diamond Blackfan anemia: a report from the Diamond Blackfan Anemia Registry. *Blood.* 2012;119(16):3815-9.
71. Lipton JM, Ellis SR. Diamond-Blackfan anemia: diagnosis, treatment, and molecular pathogenesis. *Hematol Oncol Clin North Am.* 2009;23(2):261-82.
72. Gazda HT, Grabowska A, Merida-Long LB, Latawiec E, Schneider HE, Lipton JM, et al. Ribosomal protein S24 gene is mutated in Diamond-Blackfan anemia. *Am J Hum Genet.* 2006;79(6):1110-8.
73. Draptchinskaia N, Gustavsson P, Andersson B, Pettersson M, Willig TN, Dianzani I, et al. The gene encoding ribosomal protein S19 is mutated in Diamond-Blackfan anaemia. *Nat Genet.* 1999;21(2):169-75.
74. Vlachos A, Muir E. How I treat Diamond-Blackfan anemia. *Blood.* 2010;116(19):3715-23.
75. Klein C, Grudzien M, Appaswamy G, Germeshausen M, Sandrock I, Schaffer AA, et al. HAX1 deficiency causes autosomal recessive severe congenital neutropenia (Kostmann disease). *Nat Genet.* 2007;39(1):86-92.
76. Germeshausen M, Grudzien M, Zeidler C, Abdollahpour H, Yetgin S, Rezaei N, et al. Novel HAX1 mutations in patients with severe congenital neutropenia reveal isoform-dependent genotype-phenotype associations. *Blood.* 2008;111(10):4954-7.
77. Matsubara K, Imai K, Okada S, Miki M, Ishikawa N, Tsumura M, et al. Severe developmental delay and epilepsy in a Japanese patient with severe congenital neutropenia due to HAX1 deficiency. *Haematologica.* 2007;92(12):e123-5.
78. Skokowa J, Dale DC, Touw IP, Zeidler C, Welte K. Severe congenital neutropenias. *Nat Rev Dis Primers.* 2017;3:17032.

79. Boocock GR, Morrison JA, Popovic M, Richards N, Ellis L, Durie PR, et al. Mutations in SBDS are associated with Shwachman-Diamond syndrome. *Nat Genet.* 2003;33(1):97-101.
80. Woloszynek JR, Rothbaum RJ, Rawls AS, Minx PJ, Wilson RK, Mason PJ, et al. Mutations of the SBDS gene are present in most patients with Shwachman-Diamond syndrome. *Blood.* 2004;104(12):3588-90.
81. Woods WG, Roloff JS, Lukens JN, Krivit W. The occurrence of leukemia in patients with the Shwachman syndrome. *The Journal of Pediatrics.* 1981;99(3):425-8.
82. Dror Y, Freedman MH. Shwachman-Diamond syndrome marrow cells show abnormally increased apoptosis mediated through the Fas pathway. *Blood.* 2001;97(10):3011-6.
83. Ancliff PJ, Gale RE, Liesner R, Hann IM, Linch DC. Mutations in the ELA2 gene encoding neutrophil elastase are present in most patients with sporadic severe congenital neutropenia but only in some patients with the familial form of the disease. *Blood.* 2001;98(9):2645-50.
84. Dale DC, Person RE, Bolyard AA, Aprikyan AG, Bos C, Bonilla MA, et al. Mutations in the gene encoding neutrophil elastase in congenital and cyclic neutropenia. *Blood.* 2000;96(7):2317-22.
85. Horwitz M, Benson KF, Person RE, Aprikyan AG, Dale DC. Mutations in ELA2, encoding neutrophil elastase, define a 21-day biological clock in cyclic haematopoiesis. *Nat Genet.* 1999;23(4):433-6.
86. Li FQ, Horwitz M. Characterization of mutant neutrophil elastase in severe congenital neutropenia. *J Biol Chem.* 2001;276(17):14230-41.
87. Berliner N. Lessons from congenital neutropenia: 50 years of progress in understanding myelopoiesis. *Blood.* 2008;111(12):5427-32.
88. Guerry Dt, Dale DC, Omine M, Perry S, Wolff SM. Periodic hematopoiesis in human cyclic neutropenia. *J Clin Invest.* 1973;52(12):3220-30.
89. Salipante SJ, Rojas ME, Korkmaz B, Duan Z, Wechsler J, Benson KF, et al. Contributions to neutropenia from PFAAP5 (N4BP2L2), a novel protein mediating transcriptional repressor cooperation between Gfi1 and neutrophil elastase. *Mol Cell Biol.* 2009;29(16):4394-405.
90. Tidwell T, Wechsler J, Nayak RC, Trump L, Salipante SJ, Cheng JC, et al. Neutropenia-associated ELANE mutations disrupting translation initiation produce novel neutrophil elastase isoforms. *Blood.* 2014;123(4):562-9.
91. Nayak RC, Trump LR, Aronow BJ, Myers K, Mehta P, Kalfa T, et al. Pathogenesis of ELANE-mutant severe neutropenia revealed by induced pluripotent stem cells. *J Clin Invest.* 2015;125(8):3103-16.
92. Massullo P, Druhan LJ, Bunnell BA, Hunter MG, Robinson JM, Marsh CB, et al. Aberrant subcellular targeting of the G185R neutrophil elastase mutant associated with severe congenital neutropenia induces premature apoptosis of differentiating promyelocytes. *Blood.* 2005;105(9):3397-404.
93. Thusberg J, Vihinen M. Bioinformatic analysis of protein structure-function relationships: case study of leukocyte elastase (ELA2) missense mutations. *Hum Mutat.* 2006;27(12):1230-43.
94. Grenda DS, Murakami M, Ghatak J, Xia J, Boxer LA, Dale D, et al. Mutations of the ELA2 gene found in patients with severe congenital neutropenia induce the unfolded protein response and cellular apoptosis. *Blood.* 2007;110(13):4179-87.
95. Xia J, Link DC. Severe congenital neutropenia and the unfolded protein response. *Curr Opin Hematol.* 2008;15(1):1-7.

96. Kollner I, Sodeik B, Schreek S, Heyn H, von Neuhoff N, Germeshausen M, et al. Mutations in neutrophil elastase causing congenital neutropenia lead to cytoplasmic protein accumulation and induction of the unfolded protein response. *Blood*. 2006;108(2):493-500.
97. Bellanne-Chantelot C, Clauin S, Leblanc T, Cassinat B, Rodrigues-Lima F, Beauvils S, et al. Mutations in the ELA2 gene correlate with more severe expression of neutropenia: a study of 81 patients from the French Neutropenia Register. *Blood*. 2004;103(11):4119-25.
98. Germeshausen M, Deerberg S, Peter Y, Reimer C, Kratz CP, Ballmaier M. The spectrum of ELANE mutations and their implications in severe congenital and cyclic neutropenia. *Hum Mutat*. 2013;34(6):905-14.
99. Setty BA, Yeager ND, Bajwa RP. Heterozygous M1V variant of ELA-2 gene mutation associated with G-CSF refractory severe congenital neutropenia. *Pediatr Blood Cancer*. 2011;57(3):514-5.
100. Fernandez J, Yaman I, Sarnow P, Snider MD, Hatzoglou M. Regulation of internal ribosomal entry site-mediated translation by phosphorylation of the translation initiation factor eIF2alpha. *J Biol Chem*. 2002;277(21):19198-205.
101. Germeshausen M, Ballmaier M, Welte K. Incidence of CSF3R mutations in severe congenital neutropenia and relevance for leukemogenesis: Results of a long-term survey. *Blood*. 2007;109(1):93-9.
102. Ward AC, van Aesch YM, Schelen AM, Touw IP. Defective internalization and sustained activation of truncated granulocyte colony-stimulating factor receptor found in severe congenital neutropenia/acute myeloid leukemia. *Blood*. 1999;93(2):447-58.
103. Touw IP, Bontenbal M. Granulocyte colony-stimulating factor: key (f)actor or innocent bystander in the development of secondary myeloid malignancy? *J Natl Cancer Inst*. 2007;99(3):183-6.
104. Ward AC, van Aesch YM, Gits J, Schelen AM, de Koning JP, van Leeuwen D, et al. Novel point mutation in the extracellular domain of the granulocyte colony-stimulating factor (G-CSF) receptor in a case of severe congenital neutropenia hyporesponsive to G-CSF treatment. *J Exp Med*. 1999;190(4):497-507.
105. Devriendt K, Kim AS, Mathijs G, Frints SG, Schwartz M, Van Den Oord JJ, et al. Constitutively activating mutation in WASP causes X-linked severe congenital neutropenia. *Nat Genet*. 2001;27(3):313-7.
106. Ancliff PJ, Blundell MP, Cory GO, Calle Y, Worth A, Kempinski H, et al. Two novel activating mutations in the Wiskott-Aldrich syndrome protein result in congenital neutropenia. *Blood*. 2006;108(7):2182-9.
107. Moulding DA, Blundell MP, Spiller DG, White MR, Cory GO, Calle Y, et al. Unregulated actin polymerization by WASp causes defects of mitosis and cytokinesis in X-linked neutropenia. *J Exp Med*. 2007;204(9):2213-24.
108. Xia J, Bolyard AA, Rodger E, Stein S, Aprikyan AA, Dale DC, et al. Prevalence of mutations in ELANE, GF11, HAX1, SBDS, WAS and G6PC3 in patients with severe congenital neutropenia. *Br J Haematol*. 2009;147(4):535-42.
109. Beel K, Cotter MM, Blatny J, Bond J, Lucas G, Green F, et al. A large kindred with X-linked neutropenia with an I294T mutation of the Wiskott-Aldrich syndrome gene. *Br J Haematol*. 2009;144(1):120-6.

110. Person RE, Li FQ, Duan Z, Benson KF, Wechsler J, Papadaki HA, et al. Mutations in proto-oncogene GFI1 cause human neutropenia and target ELA2. *Nat Genet.* 2003;34(3):308-12.
111. Zhuang D, Qiu Y, Kogan SC, Dong F. Increased CCAAT enhancer-binding protein epsilon (C/EBPepsilon) expression and premature apoptosis in myeloid cells expressing Gfi-1 N382S mutant associated with severe congenital neutropenia. *J Biol Chem.* 2006;281(16):10745-51.
112. Boztug K, Appaswamy G, Ashikov A, Schaffer AA, Salzer U, Diestelhorst J, et al. A syndrome with congenital neutropenia and mutations in G6PC3. *N Engl J Med.* 2009;360(1):32-43.
113. Collin M, Dickinson R, Bigley V. Haematopoietic and immune defects associated with GATA2 mutation. *Br J Haematol.* 2015;169(2):173-87.
114. Wlodarski MW, Hirabayashi S, Pastor V, Stary J, Hasle H, Masetti R, et al. Prevalence, clinical characteristics, and prognosis of GATA2-related myelodysplastic syndromes in children and adolescents. *Blood.* 2016;127(11):1387-97; quiz 518.
115. Pasquet M, Bellanne-Chantelot C, Tavitian S, Prade N, Beaupain B, Larochelle O, et al. High frequency of GATA2 mutations in patients with mild chronic neutropenia evolving to MonoMac syndrome, myelodysplasia, and acute myeloid leukemia. *Blood.* 2013;121(5):822-9.
116. Spinner MA, Sanchez LA, Hsu AP, Shaw PA, Zerbe CS, Calvo KR, et al. GATA2 deficiency: a protean disorder of hematopoiesis, lymphatics, and immunity. *Blood.* 2014;123(6):809-21.
117. Vassen L, Fiolka K, Mahlmann S, Moroy T. Direct transcriptional repression of the genes encoding the zinc-finger proteins Gfi1b and Gfi1 by Gfi1b. *Nucleic Acids Res.* 2005;33(3):987-98.
118. Moroy T, Vassen L, Wilkes B, Khandanpour C. From cytopenia to leukemia: the role of Gfi1 and Gfi1b in blood formation. *Blood.* 2015;126(24):2561-9.
119. Hsu AP, McReynolds LJ, Holland SM. GATA2 deficiency. *Curr Opin Allergy Clin Immunol.* 2015;15(1):104-9.
120. Wilson NK, Foster SD, Wang X, Knezevic K, Schutte J, Kaimakis P, et al. Combinatorial transcriptional control in blood stem/progenitor cells: genome-wide analysis of ten major transcriptional regulators. *Cell Stem Cell.* 2010;7(4):532-44.
121. Sellick GS, Spendlove HE, Catovsky D, Pritchard-Jones K, Houlston RS. Further evidence that germline CEBPA mutations cause dominant inheritance of acute myeloid leukaemia. *Leukemia.* 2005;19(7):1276-8.
122. Smith ML, Cavenagh JD, Lister TA, Fitzgibbon J. Mutation of CEBPA in familial acute myeloid leukemia. *N Engl J Med.* 2004;351(23):2403-7.
123. Ross SE, Radomska HS, Wu B, Zhang P, Winnay JN, Bajnok L, et al. Phosphorylation of C/EBPalpha inhibits granulopoiesis. *Mol Cell Biol.* 2004;24(2):675-86.
124. Zhang DE, Zhang P, Wang ND, Hetherington CJ, Darlington GJ, Tenen DG. Absence of granulocyte colony-stimulating factor signaling and neutrophil development in CCAAT enhancer binding protein alpha-deficient mice. *Proc Natl Acad Sci U S A.* 1997;94(2):569-74.
125. Zhang P, Iwama A, Datta MW, Darlington GJ, Link DC, Tenen DG. Upregulation of interleukin 6 and granulocyte colony-stimulating factor receptors by transcription factor CCAAT enhancer binding protein alpha (C/EBP alpha) is critical for granulopoiesis. *J Exp Med.* 1998;188(6):1173-84.

126. Rosenberg PS, Greene MH, Alter BP. Cancer incidence in persons with Fanconi anemia. *Blood*. 2003;101(3):822-6.
127. Alter BP. Fanconi anemia and the development of leukemia. *Best Pract Res Clin Haematol*. 2014;27(3-4):214-21.
128. Dokal I, Luzzatto L. Dyskeratosis congenita is a chromosomal instability disorder. *Leuk Lymphoma*. 1994;15(1-2):1-7.
129. Solder B, Weiss M, Jager A, Belohradsky BH. Dyskeratosis congenita: multisystemic disorder with special consideration of immunologic aspects. A review of the literature. *Clin Pediatr (Phila)*. 1998;37(9):521-30.
130. Churpek JE, Pyrtel K, Kanchi KL, Shao J, Koboldt D, Miller CA, et al. Genomic analysis of germ line and somatic variants in familial myelodysplasia/acute myeloid leukemia. *Blood*. 2015;126(22):2484-90.
131. Song WJ, Sullivan MG, Legare RD, Hutchings S, Tan X, Kufrin D, et al. Haploinsufficiency of CBFA2 causes familial thrombocytopenia with propensity to develop acute myelogenous leukaemia. *Nat Genet*. 1999;23(2):166-75.
132. Owen CJ, Toze CL, Koochin A, Forrest DL, Smith CA, Stevens JM, et al. Five new pedigrees with inherited RUNX1 mutations causing familial platelet disorder with propensity to myeloid malignancy. *Blood*. 2008;112(12):4639-45.
133. Preudhomme C, Renneville A, Bourdon V, Philippe N, Roche-Lestienne C, Boissel N, et al. High frequency of RUNX1 biallelic alteration in acute myeloid leukemia secondary to familial platelet disorder. *Blood*. 2009;113(22):5583-7.
134. Yoshimi A, Toya T, Kawazu M, Ueno T, Tsukamoto A, Iizuka H, et al. Recurrent CDC25C mutations drive malignant transformation in FPD/AML. *Nat Commun*. 2014;5:4770.
135. Shiba N, Hasegawa D, Park MJ, Murata C, Sato-Otsubo A, Ogawa C, et al. CBL mutation in chronic myelomonocytic leukemia secondary to familial platelet disorder with propensity to develop acute myeloid leukemia (FPD/AML). *Blood*. 2012;119(11):2612-4.
136. Rosenberg PS, Zeidler C, Bolyard AA, Alter BP, Bonilla MA, Boxer LA, et al. Stable long-term risk of leukaemia in patients with severe congenital neutropenia maintained on G-CSF therapy. *Br J Haematol*. 2010;150(2):196-9.
137. Dong F, Brynes RK, Tidow N, Welte K, Lowenberg B, Touw IP. Mutations in the gene for the granulocyte colony-stimulating-factor receptor in patients with acute myeloid leukemia preceded by severe congenital neutropenia. *N Engl J Med*. 1995;333(8):487-93.
138. Tidow N, Pilz C, Teichmann B, Muller-Brechlin A, Germeshausen M, Kasper B, et al. Clinical relevance of point mutations in the cytoplasmic domain of the granulocyte colony-stimulating factor receptor gene in patients with severe congenital neutropenia. *Blood*. 1997;89(7):2369-75.
139. Liu F, Kunter G, Krem MM, Eades WC, Cain JA, Tomasson MH, et al. Csf3r mutations in mice confer a strong clonal HSC advantage via activation of Stat5. *J Clin Invest*. 2008;118(3):946-55.
140. Vandenberghe P, Beel K. Severe congenital neutropenia, a genetically heterogeneous disease group with an increased risk of AML/MDS. *Pediatr Rep*. 2011;3 Suppl 2:e9.
141. Ward AC, Gits J, Majeed F, Aprikyan AA, Lewis RS, O'Sullivan LA, et al. Functional interaction between mutations in the granulocyte colony-stimulating factor receptor in severe congenital neutropenia. *Br J Haematol*. 2008;142(4):653-6.

142. Klimiankou M, Uenalan M, Kandabarau S, Nustede R, Steiert I, Mellor-Heineke S, et al. Ultra-Sensitive CSF3R Deep Sequencing in Patients With Severe Congenital Neutropenia. *Front Immunol.* 2019;10:116.
143. Skokowa J, Steinemann D, Katsman-Kuipers JE, Zeidler C, Klimenkova O, Klimiankou M, et al. Cooperativity of RUNX1 and CSF3R mutations in severe congenital neutropenia: a unique pathway in myeloid leukemogenesis. *Blood.* 2014;123(14):2229-37.
144. Link DC, Kunter G, Kasai Y, Zhao Y, Miner T, McLellan MD, et al. Distinct patterns of mutations occurring in de novo AML versus AML arising in the setting of severe congenital neutropenia. *Blood.* 2007;110(5):1648-55.
145. Koeffler HP, Leong G. Preleukemia: one name, many meanings. *Leukemia.* 2017;31(3):534-42.
146. Wang X, Muramatsu H, Okuno Y, Sakaguchi H, Yoshida K, Kawashima N, et al. GATA2 and secondary mutations in familial myelodysplastic syndromes and pediatric myeloid malignancies. *Haematologica.* 2015;100(10):e398-401.
147. West RR, Hsu AP, Holland SM, Cuellar-Rodriguez J, Hickstein DD. Acquired ASXL1 mutations are common in patients with inherited GATA2 mutations and correlate with myeloid transformation. *Haematologica.* 2014;99(2):276-81.
148. Xia J, Miller CA, Baty J, Ramesh A, Jotte MRM, Fulton RS, et al. Somatic mutations and clonal hematopoiesis in congenital neutropenia. *Blood.* 2018;131(4):408-16.
149. Olivier M, Hollstein M, Hainaut P. TP53 mutations in human cancers: origins, consequences, and clinical use. *Cold Spring Harb Perspect Biol.* 2010;2(1):a001008.
150. Sloand EM, Yong AS, Ramkissoon S, Solomou E, Bruno TC, Kim S, et al. Granulocyte colony-stimulating factor preferentially stimulates proliferation of monosomy 7 cells bearing the isoform IV receptor. *Proc Natl Acad Sci U S A.* 2006;103(39):14483-8.
151. Dror Y, Durie P, Ginzberg H, Herman R, Banerjee A, Champagne M, et al. Clonal evolution in marrows of patients with Shwachman-Diamond syndrome. *Experimental Hematology.* 2002;30(7):659-69.
152. Smith A, Shaw PJ, Webster B, Lammi A, Gaskin K, Diaz S, et al. Intermittent 20q- and consistent i(7q) in a patient with Shwachman-Diamond syndrome. *Pediatr Hematol Oncol.* 2002;19(7):525-8.
153. Kurtin PJ, Dewald GW, Shields DJ, Hanson CA. Hematologic disorders associated with deletions of chromosome 20q: a clinicopathologic study of 107 patients. *Am J Clin Pathol.* 1996;106(5):680-8.
154. Brezinova J, Zemanova Z, Ransdorfova S, Sindelarova L, Siskova M, Neuwirtova R, et al. Prognostic significance of del(20q) in patients with hematological malignancies. *Cancer Genet Cytogenet.* 2005;160(2):188-92.
155. Strati P, Daver N, Ravandi F, Pemmaraju N, Pierce S, Garcia-Manero G, et al. Biological and clinical features of trisomy 21 in adult patients with acute myeloid leukemia. *Clin Lymphoma Myeloma Leuk.* 2013;13 Suppl 2:S276-81.
156. Alter BP. Inherited bone marrow failure syndromes: considerations pre- and posttransplant. *Blood.* 2017;130(21):2257-64.
157. Paustian L, Chao MM, Hanenberg H, Schindler D, Neitzel H, Kratz CP, et al. Androgen therapy in Fanconi anemia: A retrospective analysis of 30 years in Germany. *Pediatr Hematol Oncol.* 2016;33(1):5-12.

158. Duarte BKL, Yamaguti-Hayakawa GG, Medina SS, Siqueira LH, Snetsinger B, Costa FF, et al. Longitudinal sequencing of RUNX1 familial platelet disorder: new insights into genetic mechanisms of transformation to myeloid malignancies. *Br J Haematol*. 2019.
159. Boutroux H, Petit A, Auvrignon A, Lapillonne H, Ballerini P, Favier R, et al. Childhood diagnosis of genetic thrombocytopenia with mutation in the ankyrine repeat domain 26 gene. *Eur J Pediatr*. 2015;174(10):1399-403.
160. Peffault de Latour R, Peters C, Gibson B, Strahm B, Lankester A, de Heredia CD, et al. Recommendations on hematopoietic stem cell transplantation for inherited bone marrow failure syndromes. *Bone Marrow Transplant*. 2015;50(9):1168-72.
161. Roggero S, Quarello P, Vinciguerra T, Longo F, Piga A, Ramenghi U. Severe iron overload in Blackfan-Diamond anemia: a case-control study. *Am J Hematol*. 2009;84(11):729-32.
162. Rosenberg PS, Alter BP, Bolyard AA, Bonilla MA, Boxer LA, Cham B, et al. The incidence of leukemia and mortality from sepsis in patients with severe congenital neutropenia receiving long-term G-CSF therapy. *Blood*. 2006;107(12):4628-35.
163. Bonilla MA, Gillio AP, Rugeiro M, Kernan NA, Brochstein JA, Abboud M, et al. Effects of recombinant human granulocyte colony-stimulating factor on neutropenia in patients with congenital agranulocytosis. *N Engl J Med*. 1989;320(24):1574-80.
164. Roberts AW. G-CSF: a key regulator of neutrophil production, but that's not all! *Growth Factors*. 2005;23(1):33-41.
165. Donini M, Fontana S, Savoldi G, Vermi W, Tassone L, Gentili F, et al. G-CSF treatment of severe congenital neutropenia reverses neutropenia but does not correct the underlying functional deficiency of the neutrophil in defending against microorganisms. *Blood*. 2007;109(11):4716-23.
166. Ye Y, Carlsson G, Wondimu B, Fahlen A, Karlsson-Sjoberg J, Andersson M, et al. Mutations in the ELANE gene are associated with development of periodontitis in patients with severe congenital neutropenia. *J Clin Immunol*. 2011;31(6):936-45.
167. Qiu Y, Zhang Y, Hu N, Dong F. A Truncated Granulocyte Colony-stimulating Factor Receptor (G-CSFR) Inhibits Apoptosis Induced by Neutrophil Elastase G185R Mutant: IMPLICATION FOR UNDERSTANDING CSF3R GENE MUTATIONS IN SEVERE CONGENITAL NEUTROPENIA. *J Biol Chem*. 2017;292(8):3496-505.
168. Elbadry MI, Espinoza JL, Nakao S. Disease modeling of bone marrow failure syndromes using iPSC-derived hematopoietic stem progenitor cells. *Exp Hematol*. 2019;71:32-42.

Chapter 2

Inhibition of protein degradation pathways in RUNX1 deficient FPD/AML restores RUNX1 gene expression levels and promotes megakaryopoiesis

2.1. Introduction

FPD/AML (1) consists of functional platelet granule defects producing bleeding, moderately low platelet counts, and predisposition to MDS/AML and, less commonly, T-ALL, CLL, and CMML (2). FPD/AML is caused by heterozygous, germline mutations in the transcription factor RUNX1. RUNX1 is one of three runt homology DNA-binding domain family members heterodimerizing with a non-DNA binding partner (CBF β), collectively referred to as core binding factors (3), in which translocations and other acquired mutations frequently arise with hematologic malignancies (4). FPD/AML germline *RUNX1* mutations most often create non-functional alleles but can also include hypomorphic alleles with reduced activity or dominant-negative alleles (2, 5-7).

At conception, patients with FPD/AML possess one wild type allele, producing normal protein, albeit at half-normal net levels. It is unclear if RUNX1 behaves as a tumor suppressor gene, requiring acquisition of a “second-hit” mutation inactivating the residual wild type allele in order for malignancy to occur. Among FPD/AML patients, mutations of the wild type *RUNX1* allele are not found (6-8) or, when detected, are seen in some, but not all, patients (9). Malignant progression in FPD/AML may instead be somehow facilitated, at least initially, by *RUNX1* haploinsufficiency and depend upon acquisition of cooperating mutations in other genes frequently mutated in sporadic leukemia, including those involved with DNA methylation, such as *DNMT3A* (6), as well as cytogenetic abnormalities.

RUNX1's half-life is approximately 30-60 minutes, with rapid turnover via the ubiquitin-proteasome degradation pathway (10). In addition to ubiquitylation, RUNX1 is phosphorylated, acetylated, methylated, and sumoylated (11, 12), though phosphorylation appears to primarily govern its nuclear matrix association, transcriptional activity, and—importantly for the strategy

proposed here—serves as the principal gateway for regulating its stability via ubiquitin-dependent proteasomal degradation.

RUNX1 additionally auto-regulates its own expression by binding to and activating expression from its own promoter (13). For an auto-activating transcription factor, small changes prolonging half-life are expected to exponentially elevate its overall abundance, and, once a temporary perturbation affecting half-life ceases, steady state levels become independent of the rate of synthesis or degradation and remain persistently elevated (14). For example, transient inhibition of cellular proteases degrading the skeletal muscle transcription factor MyoD, which similarly auto-activates its own expression, causes MyoD concentration to rise dramatically and remain elevated even after withdrawal of inhibitors (14).

We therefore hypothesize that drugs retarding RUNX1's proteolytic degradation, even transiently, may help to restore steady state levels of RUNX1 in FPD/AML and normalize platelet production. To test this hypothesis we have attempted to “jump start” RUNX1 expression by transient over-expression of exogenous RUNX1 and have also evaluated the effects of small molecule inhibitors of the ubiquitin-proteasome degradation pathway on RUNX1 and correspondingly megakaryocyte differentiation in several different cultured cell lines, patient-derived iPSC, and primary patient bone marrow samples. We find that, in some cases, inhibition of kinases regulating ubiquitylation or direct inhibition of the proteasome can increase RUNX1 levels and advance megakaryocyte differentiation, thereby suggesting potential new therapeutic opportunities for treating bleeding complications and preventing leukemia in FPD/AML.

2.2. Methods

Cell lines: The female human embryonic kidney cell line, 293T (15), was cultured in Dulbecco's Modified Eagle Medium (DMEM) and passaged every 3-4 days or at ~90% confluency. The male human megakaryoblastic leukemia cell line, MEG-01 (16), was cultured semi-adherently at $2-4 \times 10^5$ cells/mL in RPMI-1640 medium and scraped for passaging every 5 days. The female human multipotential leukemia cell line, K562 (17), was cultured between

2×10^5 - 10^6 cells/mL in Iscove's Modified Dulbecco's Medium (IMDM) and passaged every 3-4 days. All media were supplemented with 10% Fetal Bovine Serum (FBS). Cells were cultured in humidified incubators at 37°C in 5% CO₂ and propagated for no more than 20 passages after thaw. Reagents were purchased from Gibco/Thermo Fisher Scientific.

FPD/AML patient-derived iPSC: Sendai virus reprogramming-mediated iPSC (18) were generated from peripheral blood mononuclear cells (MNC) of a non-leukemic adult male FPD/AML patient, heterozygous for a germline *RUNX1* splicing mutation (NM_00100189 c.533-1G>T) (7) and were the generous gift of Drs. Deborah French, Paul Gadue, and Mortimer Poncz at the Children's Hospital of Philadelphia (CHOP). They were cultured as described (19). Studies were approved by the CHOP Institutional Review Board (IRB), protocol 7042-134. Hematopoietic differentiation was performed as described (20); specifically, day 8 embryoid bodies were plated in ultra-low attachment 6-well plates and cultured for 2 days in differentiation media containing vehicle or drugs. Cells were then harvested at day 10 for flow cytometry and colony forming unit assays. Culture occurred in humidified incubators at 37°C in 5% CO₂.

Primary patient samples: Bone marrow was aspirated from three non-leukemic female siblings with FPD/AML at ages 11-, 16- and 20-years, each sharing a heterozygous germline *RUNX1* nonsense mutation (NM_001754 c.1242C>A, p.Y414X) (21). MNC were isolated within six hours of harvest using Corning Lymphocyte Separation Medium and aliquots frozen in 10% DMSO, 90% FBS at -80°C overnight before transfer to liquid nitrogen. Studies were approved by the University of Washington IRB, protocol 52640. Culture occurred in humidified incubators at 37°C in 5% CO₂.

Drug treatments: Roscovitine, flavopiridol hydrochloride, terameprocol, P276-00, R547, SCH 727965, bortezomib, carfilzomib, ixazomib, oprozomib, and pevonedistat, were dissolved in DMSO and stored at -80°C until use (Supplementary Table 2.2). For each cell line, LC₅₀ was measured by determining viability with the CellTiter 96 (Promega) reagent. Additional DMSO was added, if needed, to normalize DMSO concentration to 0.25% across treatment conditions.

2.5×10^6 cells were exposed to continuous treatment for 24 hours at which point cells were either harvested for RNA/protein or pelleted and re-plated in drug-free media for further culture. At the indicated time points, cells were washed with PBS, pelleted, and lysed for RNA using RNeasy Plus Mini Kits (Qiagen) and/or protein lysate using RIPA buffer containing complete protease inhibitor (Roche), 1 mM Na_3VO_4 , and 1 mM phenylmethylsulfonyl fluoride (PMSF).

RUNX1 expression constructs: Human RUNX1 variant 1 cDNA (NM_001754.3) with carboxyl terminal FLAG epitope tag in pcDNA3.1 vector (pcDNA3.1-RUNX1-FLAG) was purchased from Genscript (CloneID OHu26363). In our RNAseq experiment on RUNX1 transfected K562 cells, we introduced synonymous nucleotide changes into *RUNX1*, allowing us to distinguish between endogenous and exogenous transcripts. The following primers, with nucleotide substitutions underlined, were used to insert the indicated synonymous nucleotide changes into the RUNX1 plasmid (pcDNA3.1-RUNX1^{c.24G>A/p.E8E,27A>T/p.S9S}-FLAG) forward primer: 5'-[Phos]CTTCGTACCCACAGTGCTTC-3' and reverse primer: 5'-[Phos]GAAAAGATTCAAATATGCTG-3'.

DNA transfection: 2×10^6 293T cells were transfected with 4 μg pcDNA3.1-RUNX1-FLAG plasmid using 12 μL Lipofectamine 2000 (Thermo Fisher) per 10 cm plate. One day later, cells were passaged and pooled, and the 24 hour post-transfection timepoint was collected; remaining cells were seeded onto 10 cm plates at equal densities for later timepoints. 4×10^6 K562 cells were electroporated with 4 μg of pcDNA3.1-RUNX1^{c.24G>A/p.E8e, 27A>T/p.S9S}-FLAG expression plasmid in 400 μL cuvettes filled with Opti-MEM (Gibco) using a BioRad Gene Pulser Xcell (square wave, 210 V, 2 \times pulse, 0.15 ms).

Real-Time Quantitative Reverse Transcription PCR (qRT-PCR): Superscript IV reverse transcriptase (Thermo Fisher) was used to generate cDNA and qRT-PCR was performed using the Thermo Fisher StepOnePlus Real-Time PCR System with TaqMan probes RUNX1 (Hs01021970_m1) or beta-actin (Applied Biosystems, 4333762F). Relative quantification of gene

expression was calculated by applying the $2^{-\Delta\Delta CT}$ method using *ACTB* or *GAPDH* as endogenous controls (indicated in figure legends).

RNA-seq: RNA extracted from four individual drug-treatments of K562 cells were pooled then divided to create two samples per treatment condition for RNA-seq, in order to reduce experimental “noise” during analysis. K562 cells transfected with either pcDNA3.1 empty vector or pcDNA3.1-RUNX1^{c.24G>A/p.E8e, 27A>T/p.S9S}-FLAG RNA were similarly each performed in replicate and then combined. mRNA libraries were prepared from total RNA (~1 µg per sample) using the Illumina TruSeq Stranded mRNA Library Prep kit and then sequenced on an Illumina NextSeq 500 instrument (1×75 bp read) at the University of Washington Center for Precision Diagnostics. Reads were aligned against GRCh38 using the HISAT2 aligner (Johns Hopkins Center for Computational Biology). Reads mapped to exons defined by GRCh38.88 were counted, and transcripts per million (TPM) values for each gene were calculated using StringTie software (Johns Hopkins Center for Computational Biology).

Immunoblotting: Total protein concentrations were determined by BCA assay (Pierce). Samples were diluted in Laemmli sample buffer and heated at 90°C for 10 min prior to being loaded into a Mini-PROTEAN TGX 4-10% Tris-Glycine SDS precast gel (Bio-Rad). Protein was then transferred to polyvinylidene difluoride (PVDF) membrane (Bio-Rad) and blocked for 30 min at room temperature and washed with TBST. All primary antibodies were diluted in 1% nonfat dry milk or BSA in Tris-buffered saline, 0.1% Tween 20 (TBST) and were incubated overnight at 4°C. Blots were incubated in secondary antibody for 1 hour at room temperature, also in 1% nonfat dry milk or BSA. Antibody sources and concentrations are listed in Supplementary Table 2.3. Blots were developed using Immobilon Western Chemiluminescent HRP Substrate (EMD Millipore), SuperSignal West Pico, or Femto chemiluminescent substrate (Thermo-Fisher) on Kodak BioMax XAR film or using the ChemiDoc MP Imaging System (BioRAD).

iPSC colony forming unit (CFU) assay: Megakaryocyte CFU assay of FPD/AML patient-derived iPSC utilized MegaCult-C complete kit with cytokines (STEMCELL Technologies).

Megakaryocyte progenitors were harvested on day 11-12 of *in vitro* differentiation and analyzed via flow cytometry for CD41a positivity. We then plated 10,000 unsorted, hematopoietic stem and progenitor cells (HSPC) per dish with MegaCult media in duplicate. Dishes were then incubated at 37°C for 12 days before scoring according to the manufacturer's protocol. The number of colonies was normalized to the percentage of CD41a+ cells measured at the day of plating.

Primary cell megakaryocyte differentiation: On day 0, FPD/AML MNCs were thawed in a 37°C water bath, washed with PBS, and quantified on a hemocytometer. Cells were seeded for differentiation at concentrations of $0.2-1 \times 10^6$ cells per 12-well plate, depending on yield during quantification. Megakaryocyte differentiation was achieved using StemSpan SFEM II basal media containing StemSpan Megakaryocyte Expansion Supplement (STEMCELL Technologies). Cells were seeded for differentiation with bortezomib, terameprocol or DMSO vehicle added to the media for the first 24 hours of differentiation. After 24 hours of treatment (day 1), cells were removed from the dish and centrifuged at $200 \times g$ for 5 min at room temperature. Pellets were then resuspended in freshly added drug or vehicle containing differentiation media and transferred back to their corresponding well with incubation for an additional 24 hours. On day 2, after 48 hours of drug exposure, cells were removed, washed with PBS, and transferred to normal differentiation media (without drugs) for the remainder of the experiment. Complete media changes were performed on days 4 and 7, and on day 10 wells were supplemented with an additional 1 mL of fresh differentiation media. Megakaryocyte formation was characterized on day 14 via flow cytometry, Cytospin, electron microscopy, or RNA isolation. Relative megakaryocyte yields were calculated by comparing seed-matched drug and vehicle conditions.

Flow cytometric analysis: Megakaryocytes formed from FPD/AML patient-derived iPSCs were stained with CD41a and CD45 antibodies (BD PharMingen) and assayed with a BD LSRFortessa cell analyzer, as described (20). Primary MNC-derived megakaryocytes were characterized via flow cytometry for surface markers CD41a, CD42b, and CD61 (BD Biosciences) using a BD FACSCanto II flow cytometer. Antibody sources and concentrations are listed in

Supplementary Table 2.4. On day 14 of *in vitro* megakaryocyte differentiation, cells were washed with 0.1% FBS/PBS (FACS buffer) and subsequently incubated for 30 min on ice in the dark with the indicated antibody diluted in the same buffer. Stained cells were washed twice with FACS buffer by centrifugation at 200×g for 4 min at 4°C. Following wash steps, cells were resuspended in 100 µL buffer and transferred into 500 µL fresh FACS buffer for analysis. Sample preparation was performed in 96-well, v-bottom, low-binding plates. Data was processed using FlowJo software, version 10.

Cytospin: On day 14 of *in vitro* megakaryocyte differentiation using MNCs from patient “FPD-2”, 10⁴ cells from the total cell population were centrifuged at 200×g for 4 min and resuspended in 100 µL PBS. Cell suspension was then transferred to a single chamber Cytospin funnel (ThermoFisher), secured onto a coated glass slide and centrifuged at 1,000 RPM for 5 minutes using a ThermoFisher Shandon CytoSpin 4. Slides were then air-dried for 2-3 min, fixed in 100% methanol for 3 min, and air-dried again. After fixation, slides were stored in the dark, until processed by Wright-Giemsa (Sigma) staining.

Electron microscopy: At day 14 of *in vitro* differentiation for patient “FPD-1”, ~10⁶ cells were prepared for electron microscopy. Equal volume of Karnovsky fixative was first added to each well and incubated at 37°C for 10 min. The plate was then centrifuged at 1,400 RPM for 5 min at room temperature. The majority of the media/Karnovsky fixative mixture was gently removed from the well and remaining cells were fixed with pure Karnovsky fixative for 1 hour at room temperature. Cells were then scraped from the well using a sterile spatula, transferred to a 1.5 ml microcentrifuge tube and stored at 4°C until further processing by the Fred Hutchinson Cancer Research Center Imaging Core (Seattle). Images were captured with a JEOL 120 kV JEM-1400 Transmission Electron Microscope (TEM).

Megakaryocyte granule quantification: TEM cell images were scored manually by counting the number of dense and alpha granules per cell, based on standardized morphological classification (22). Dense granules were identified as small (~0.25 µm) dark gray or black, circular

puncta located within in a vesicle space. Alpha granules were scored as larger (~0.75 μ m) gray vesicles, presenting with a defined border and sandy-appearing internal composition. Unidentifiable granules or granule-like components were not scored. Cells were then binned in quartiles. Cells with no obvious granules were scored as “-”, 1-10 granules/cell as “+”, 10-20 granules/cell as “++”, and >20 granules/cell as “+++”. A chi-square test of independence was then performed for each granule type to determine if there was a difference in their abundance when comparing treatment with either bortezomib or terameprocol to vehicle treatment.

2.3. Results

Transient expression of exogenous RUNX1 results in sustained increase of endogenous RUNX1 transcript and protein in 293T cells, consistent with RUNX1 auto-activation.

Given RUNX1's reported ability to auto-activate its own expression (13), we reasoned that transient expression of exogenous RUNX1 might result in prolonged elevation of endogenous RUNX1 mRNA and protein levels (14). As a test of this prediction, we employed the human embryonic kidney cell line, 293T, because it exhibits minimal levels of endogenous RUNX1 expression (23), potentially permitting changes in RUNX1 expression to become more apparent. To distinguish exogenously transfected RUNX1 from endogenous RUNX1, we fused a FLAG epitope tag to the carboxyl terminus of RUNX1 (RUNX1-FLAG). RUNX1 protein is marginally detectable in 293T cells, as measured by western blot with antibodies against RUNX1 (Fig 2.1A, top panel, left-most lane). However, levels of total RUNX1 protein initially peak at days 3-4 following transient transfection of a vector expressing RUNX1-FLAG and then maintain uniform levels throughout the remainder of the 10-day time course (Fig 2.1A, top and bottom panels). In contrast, levels of transiently expressed RUNX1-FLAG disappear (as detected by antibodies to the FLAG epitope tag, Fig 2.1A middle panel) while levels of internal control beta-actin remain constant over the time-course (Fig 2.1A, bottom panel). Semi-quantitative RT-PCR employing primers specific to sequences encoding the FLAG epitope confirm diminution of the transiently

transfected RUNX1-FLAG transcript (Fig 2.1B), while measurement of total *RUNX1* transcript by TaqMan qRT-PCR for *RUNX1* mRNA (Fig 2.1C) mirrors RUNX1 protein levels apparent on western blot. We conclude that transiently-expressed, exogenous RUNX1-FLAG transcriptionally activates expression from the endogenous *RUNX1* locus. RUNX1-FLAG expression vectors possess a constitutive promoter lacking RUNX1 binding sites and are therefore unable to maintain an auto-activation circuit for transfected RUNX1-FLAG. As transiently-expressed RUNX1-FLAG dissipates over time, however, newly increased quantities of endogenous RUNX1 protein subsequently maintain elevated expression via auto-activation of RUNX1-responsive promoter elements at *RUNX1*'s genomic locus.

Small molecule inhibitors of RUNX1 proteolytic degradation elevate levels of exogenously transfected RUNX1 protein and endogenous *RUNX1* transcript.

Because FPD/AML typically results from haploinsufficiency of RUNX1, we wished to determine if retarding degradation of RUNX1 protein could stably elevate its steady-state levels. Phosphorylation of RUNX1 serves as the principal gateway for regulating its stability via ubiquitin-dependent proteasomal degradation. RUNX1 is phosphorylated by cyclin dependent kinases Cdk1, Cdk2, and/or Cdk6 (24-26), which subsequently renders it vulnerable to degradation mediated by the Cdc20-containing anaphase promoting complex (APC) during the G2/M phase of the cell cycle (25, 26), as well as, to a lesser extent, the Skp, Cullin, F-box (SCF)-Skp2 complex during S phase (25). Appropriate Cdk inhibitors in clinical trials for cancer that we tested in these experiments include flavopiridol (Cdk1, Cdk2, and Cdk6), P276-00 (Cdk1, Cdk2, and Cdk6), roscovitine (Cdk1 and Cdk2), R547 (Cdk1 and Cdk2), SCH 727965 (Cdk1 and Cdk2), and terameprocol (Cdk1) (27). The APC and SCF E3 ligase complexes include cullin-RING ubiquitin ligases Cul1 and ANAPC2, respectively, which are dependent on the NEDDylation system, an enzymatic cascade initiating with NEDD8 activating enzyme (NAE). NAE can be inhibited with pevonedistat (MLN4924), which is now in clinical trials for AML and MDS (28). To inhibit the final step in the RUNX1 degradation pathway, we evaluated the 26S proteasome inhibitor, bortezomib,

as well as second-generation inhibitors carfilzomib, ixazomib, and orally administered oprozomib (29), all of which are FDA-approved. The RUNX1 degradation pathway is summarized in Fig 2.2A. As before, we initiated these experiments using 293T cells transiently transfected with RUNX1-FLAG, followed by treatment with inhibitors. Western blot revealed marked increases in transfected RUNX1-FLAG protein, especially with proteasome inhibitors and, to a lesser extent, Cdk inhibitors (Fig 2.2B). Consistent with auto-activation of the endogenous *RUNX1* locus by exogenously transfected RUNX1-FLAG, TaqMan qRT-PCR revealed commensurately elevated *RUNX1* transcript (Fig 2.2C). We conclude that retarding RUNX1 degradation elevates RUNX1 protein, which, in turn elevates *RUNX1* transcript levels.

Inhibiting proteolytic degradation of endogenous RUNX1 in cell lines elevates both RUNX1 protein and transcript levels.

We proceeded to determine how small molecule inhibitors of RUNX1 degradation might influence endogenous levels of RUNX1 protein and transcript in RUNX1-expressing human cell lines. Cdk and, especially, proteasome inhibitors increased levels of RUNX1 protein in non-transfected 293T cells (Fig 2.3A), which, as noted, ordinarily express minimally detectable levels of RUNX1. We next evaluated K562 (Fig 2.3B) and MEG-01 (Fig 2.3C) cells, which are both derived from patients with chronic myelogenous leukemia in blast crisis and have characteristics of granulocytes or megakaryoblasts, respectively. In contrast to 293T cells, exposure to some Cdk inhibitors, such as terameprocol treatment of K562 cells, more potently elevated RUNX1 protein expression, whereas proteasome inhibitors had less of an effect or, in the case of MEG-01 cells, actually reduced levels of RUNX1 protein (with the exception of oprozomib, which elevated RUNX1 expression in MEG-01 cells). Consistent with RUNX1 auto-activating its own expression, changes in *RUNX1* mRNA levels across the cell lines (Fig 2.3D) generally correlated with drug-induced changes in RUNX1 protein levels. Interestingly, however, K652 cells exposed to flavopiridol and roscovatine demonstrated 3- and 2.6-fold increases of *RUNX1* transcript, respectively, yet neither drug appeared to increase total RUNX1 protein levels. It is possible that

drug specific alterations in protein state, such as phosphorylation, could result in unchanged total RUNX1 protein levels but higher levels of transcriptionally active forms of RUNX1. It is also possible that these drugs elevated levels of other transcription factors, besides RUNX1, that we did not evaluate and that are responsible for regulating RUNX1 transcription. The neddylation inhibitor, pevonedistat, either decreased or had no effect on RUNX1 protein and transcript levels, depending on cell line (Fig 2.2B and 2.3).

Transient inhibition of RUNX1 proteolytic degradation exhibits variable effects on prolonging elevated levels of RUNX1 expression in different cell lines.

Due to the autoregulatory capacity of RUNX1, we determined if elevated RUNX1 expression levels persisted following transient inhibition of degradation pathways. We focused on a subset of drugs that elevated RUNX1 levels when they were present in cell growth media, as determined from the initial larger panel. We treated cells for 24-hours, withdrew the drug and continued to grow cells in drug-free media, and then extracted aliquots 24-, 48-, and 72-hours later, in order to measure RUNX1 protein and transcript levels. For 293T cells, we evaluated proteasome inhibitors. All three tested drugs (carfilzomib, ixazomib, and bortezomib), resulted in sustained elevation in RUNX1 protein (Fig 2.4A) and transcript levels (Fig 2.4B), relative to vehicle-treated controls, particularly at 24-hours after their removal but continuing for up to 72 hours later. Because these three proteasome inhibitors generally performed similarly (at least in 293T cells), we selected bortezomib as representative of this class of compounds for further studies with K562 and MEG-01 cells. We additionally evaluated the Cdk1 inhibitor, terameprocol, in K562 and MEG-01 cells, given its efficacy in elevating RUNX1 expression levels upon initial screening. Bortezomib treatment impaired the viability of K562 cells over the time course of this experiment, even after adjusting dosages downward, such that there was an insufficient quantity of cells with which to perform western blots. From the small quantity of K562 cells that did survive following bortezomib treatment, RUNX1 transcript levels were diminished compared to vehicle-treated controls (Fig 2.4D). In terameprocol-treated K562 cells, RUNX1 protein (Fig 2.4C) and

transcript (Fig 2.4D) elevation are apparent 24-hours following drug removal, but effects wane to the point at which they became counterproductive by 48- and 72-hours after drug removal. MEG-01 cells demonstrated increased RUNX1 transcript levels 24-hours following treatment with bortezomib, yet, similar to what we observed in the presence of drug treatment above (Fig 2.3C and 2.3D), this was not reflected in the corresponding western blot (Fig 2.4D and 2.4E), which indicated reduced levels of RUNX1 protein. Transient terameprocol treatment in MEG-01 cells also did not yield noticeably sustained changes in RUNX1 protein; however, mRNA expression decreased at the 48-hour timepoint then subsequently increased above baseline at 72-hours post drug removal (Fig 2.4E and 2.4F). We conclude that, for the case of 293T cells, persistent expression of RUNX1 protein and transcript following withdrawal of drug reinforces the observation shown above in Fig 2.1, indicating that temporary over-expression of RUNX1 in 293T cells (in that case, as a result of transient transfection rather than drug treatment) leads to persistently elevated RUNX1 expression via an autoregulatory feedback loop. However, drug treatment responses appear cell line-dependent and may unsurprisingly have additional effects on cells, beyond just inhibiting degradation of RUNX1.

Transient inhibition of RUNX1 proteolytic degradation during differentiation of FPD/AML patient-derived iPSC improves megakaryocyte output.

FPD/AML patient-derived induced pluripotent stem cells (iPSC) display aberrant megakaryocytic differentiation *in vitro*, including reduced megakaryocytic colony formation and ultrastructural defects in granules (30). We therefore determined if treatment of patient-derived iPSC with drugs inhibiting RUNX1 degradation could normalize differentiation. iPSC were generated from a FPD/AML patient heterozygous for a germline *RUNX1* mutation in the splice acceptor site of exon 4 (NM_00100189 c.533-1G>T), which enforces the use of a cryptic splice acceptor in exon 4 with a resultant frameshift causing a stop codon (7). The iPSC were differentiated into embryoid bodies and then directed toward CD34+ hematopoietic stem and progenitor cell differentiation in the presence of drugs inhibiting RUNX1 proteolytic degradation

(Fig 2.5A). After drug treatment, they were further differentiated into megakaryocytes. Flow cytometric analysis of the pan-megakaryocyte surface marker CD41a (31) revealed a 1.2- and 1.7-fold increase of iPSC-derived megakaryocytes when treated for 2 days with bortezomib or terameprocol, respectively (Fig 2.5B and 2.5C). Colony forming unit (CFU) assays were additionally performed to determine the clonogenic capacity of these megakaryocyte progenitors after treatment. The colonies were scored 14 days after plating in semisolid media and showed that bortezomib treatment produced both more and larger colonies compared to vehicle-treated FPD-iPSCs (Fig 2.5 D). Terameprocol had modest effects on colony number.

Treatment with inhibitors of RUNX1 proteolytic degradation in early stages of *in vitro* differentiation affects megakaryocytic maturation in primary mononuclear cells derived from bone marrow of FPD/AML subjects.

We determined if inhibition of RUNX1 proteolytic degradation influenced *in vitro* megakaryocytic differentiation of FPD/AML patient bone marrow cells. Primary mononuclear cells were isolated from bone marrow collected from three sisters with FPD/AML (none of whom were leukemic) sharing a heterozygous germline *RUNX1* exon 9 nonsense mutation (NM_001754 c.1242C>A, p.Y414X) (21). Cells were treated early in the course of *in vitro* megakaryocytic differentiation with either bortezomib or terameprocol restricted to the first 48 hours of differentiation (Fig 2.6A). Cells were harvested at the conclusion of the differentiation protocol 12 days later and assayed for expression of pan-megakaryocyte surface markers (31) CD41a and CD61, which are integrin binding partners, as well as CD42b, a marker indicative of advanced megakaryocyte maturation, via flow cytometry (Fig 2.6B and Supplementary Fig 2.1). Cells from each of the tested patients responded slightly differently to each drug treatment, and although no one patient or treatment met the threshold of significance there were trends shared across all patients (Fig 2.6C, summarized in Supplementary Table 2.1). When averaging across all patients, bortezomib exposure did not alter the frequency of megakaryocytes overall, defined as CD41a+/CD61+ double positive cells, compared to vehicle-treated controls (1.08 ± 0.29 fold

change relative to vehicle); however, we observed a slight increase of immature (CD41a+/CD42b-) megakaryocytes at the expense of mature megakaryocytes (1.16 ± 0.18 and 0.77 ± 0.09 , respectively) (results summarized in Supplementary Table 1). In contrast, exposure to terameprocol revealed an increase in total megakaryocytes compared to vehicle-treated controls (1.14 ± 0.16), along with a specific increase of mature (1.16 ± 0.23) but not immature (1.04 ± 0.12) megakaryocyte populations. The appearance of cells corroborated these findings (Fig 2.6D). Terameprocol-treated cells exhibited features consistent with proplatelet formation, such as cell surface blebbing (32), which was not detected in bortezomib- or vehicle-treated cells.

Inhibitors of RUNX1 degradation increase formation of dense granules in primary FPD/AML mononuclear bone marrow cells.

Considering that deficient proplatelet formation, especially involving dense granules (33), is a defining pathology of FPD/AML, we employed transmission electron microscopy (TEM) to more closely evaluate maturational changes in megakaryocyte morphology that may be associated with drug treatment (Fig S2.2). Using the protocol shown in Fig 2.6A, vehicle-treated megakaryocytes displays some vacuoles, as well as alpha granules with decreased content, compared to bortezomib or terameprocol-treated samples (Fig 2.7A). We found that cells treated with either drug had a significantly greater abundance of dense granules (Fig 2.7B). The effect was more significant with bortezomib ($P = 0.0025$) than it was for terameprocol ($P = 0.022$). In contrast, alpha granule abundance was not significantly different following treatment with either drug (Fig 2.7C). These observations are in line with those made using FPD/AML patient-derived iPSC and that were shown to be reversed following genome-editing correction of the causative germline RUNX1 (30). These results prove especially exciting as we can infer cellular functionality from the quantity of granules present in megakaryocytes produced after only brief treatment early in the course of differentiation.

2.4. Discussion:

Inhibition of protein degradation is a successful strategy for treatment of some cancers (27, 34). However, use of protease inhibition therapy targeting haploinsufficiency of autoactivating transcription factors has not been previously attempted. Here we show that transient expression of exogenous RUNX1, as well as brief inhibition of global protein degradation, can have long term effects on endogenous RUNX1 steady state levels and consequently rescue arrested megakaryocyte development in Familial Platelet Disorder, which is associated with RUNX1 haploinsufficiency.

We show that sustained RUNX1 expression in 293T-HEK cells following transient expression can result from successfully jump-starting the residual wild type protein's autofeedback loop (13), which we substantiated with our cell line studies. Transfection experiments using these cells have indicated that exogenous RUNX1 protein can act upon the endogenous RUNX1 locus to boost levels above baseline even for as long as seven days after exogenous transcript is no longer detectable. This provides confirmation that RUNX1 expression is capable of self-regulated modulation.

The pathways of RUNX1 protein degradation have been previously described (12, 24-26), and we have exploited them by testing our extensive panel of cyclin dependent kinase, neddylation, and proteasome inhibitors in multiple cell systems. Although treatment of K562 and MEG-01 cells varies in terms of RUNX1 protein and mRNA responsiveness, we must note that these lines are not haploinsufficient, as in the case of FPD. In fact, K562 cells are classified as hypotriploid, harboring a complex translocation involving chromosomes 12 and 21 whereby the RUNX1 locus is rearranged (35, 36). MEG-01 cells are characterized as hyperdiploid with a chromosome 21 duplication (16). Keeping these points in mind, we found that bortezomib and terameprocol represent two strong drug candidates as they are known to impede different avenues of RUNX1 degradation in multiple cell lines we tested.

Bortezomib is already FDA-approved for treating relapsed/refractory multiple myeloma as well as mantle cell lymphoma (29, 37). A reversible 26S proteasome inhibitor, with a half-life of

approximately 40 hours and full clearance after 72 hours (38), bortezomib is an appealing option to briefly modulate wild type RUNX1 degradation in FPD patients. It should be noted that multiple myeloma patients treated with bortezomib can experience thrombocytopenia; however this therapy has also been successful in treating both idiopathic and immune-mediated thrombocytopenic purpura (39, 40).

Terameprocol has an interesting history in that it was consumed medicinally by Native Americans for kidney and gallbladder stones and has been tested in a number of clinical trials for various cancers (41-44). It acts by way of inhibiting Sp1 promoter-driven gene expression, such as CDK1 (Cdc2) and Survivin, which is commonly over-expressed in cancer cells (45, 46). These interactions make terameprocol an attractive approach for FPD in that treatment could both impede wild type RUNX1 degradation and target sensitive cancer cell subpopulations known to promote leukemic transformation to AML (46, 47). Notably, terameprocol also reversibly arrests cell cycling at the G2 stage (48). Interestingly, RUNX1 production is found to fluctuate throughout the cell cycle (49). Previous studies determined that RUNX1 levels are 2-4 fold higher in S and G2/M cells; concurrently, RUNX1-DNA binding activity is also regulated (49). For these reasons we believe terameprocol treatment serves as a valid strategy for FPD and FPD/AML patients.

Our differentiation experiments in FPD-iPSCs and primary cells provide evidence that brief treatment with bortezomib or terameprocol can have lasting effecting upon the quantity and quality of megakaryocytes generated during *in vitro* differentiation. The ultrastructural changes observed by electron microscopy of primary FPD bone marrow-derived megakaryocytes treated with bortezomib or terameprocol is especially exciting. Platelet function tests are optimized for whole blood and high platelet counts, which is unobtainable through *in vitro* differentiation. We can use the frequency of granules to infer platelet functional capacity. FPD patients are known to produce fewer platelet dense granules compared to normal individuals (50-52). We show that the platelet granule defect is at least partly rescued upon bortezomib or terameprocol treatment. With these findings, paired with trends showing increases in mature megakaryocyte output, we propose that

brief exposure to inhibitors of protein degradation is a valid strategy for normalizing megakaryocyte development in individuals with RUNX1 mutations.

It is also important to note that the differences in treatment response between the FPD-iPSC and primary FPD samples adds to the case for bringing personalized medicine to bear in the treatment of FPD. The model cell systems we tested possess different RUNX1 mutations and consequently differ in genetic backgrounds. There is no current therapy available for FPD patients while there is a plethora of CDK and proteasome inhibitors used in clinical settings for hematological cancers. Genetic tests to screen for RUNX1 mutations is still vital to create a treatment plan as there is a proportion of patients who possess dominant-negative acting mutations in RUNX1, for which our proposed therapy would be less likely to be beneficial. However, for the remainder of patients it may even be conceivably possible to treat a patient's hematopoietic stem cells *ex vivo* with drugs inhibiting RUNX1 degradation or by transiently expressing RUNX1, followed by reinfusion into the patient. This strategy of restoring RUNX1 levels to jump-start megakaryocytic development profiles could also relieve pressure on developing cells to acquire additional mutations in order to overcome differentiation arrest, which is a hallmark of leukemic transformation.

Notably, there are a number of other diseases that could benefit from a similar strategy. For example, GATA2 deficiency syndrome (6), sporadic leukemias driven by transcription factor haploinsufficiency—such as PAX5 mutations (53), or even non-hematological diseases such as frontotemporal dementia when caused by haploinsufficient germline mutations in the progranulin gene (9) could be additional avenues for therapeutic exploration.

2.5. Figures

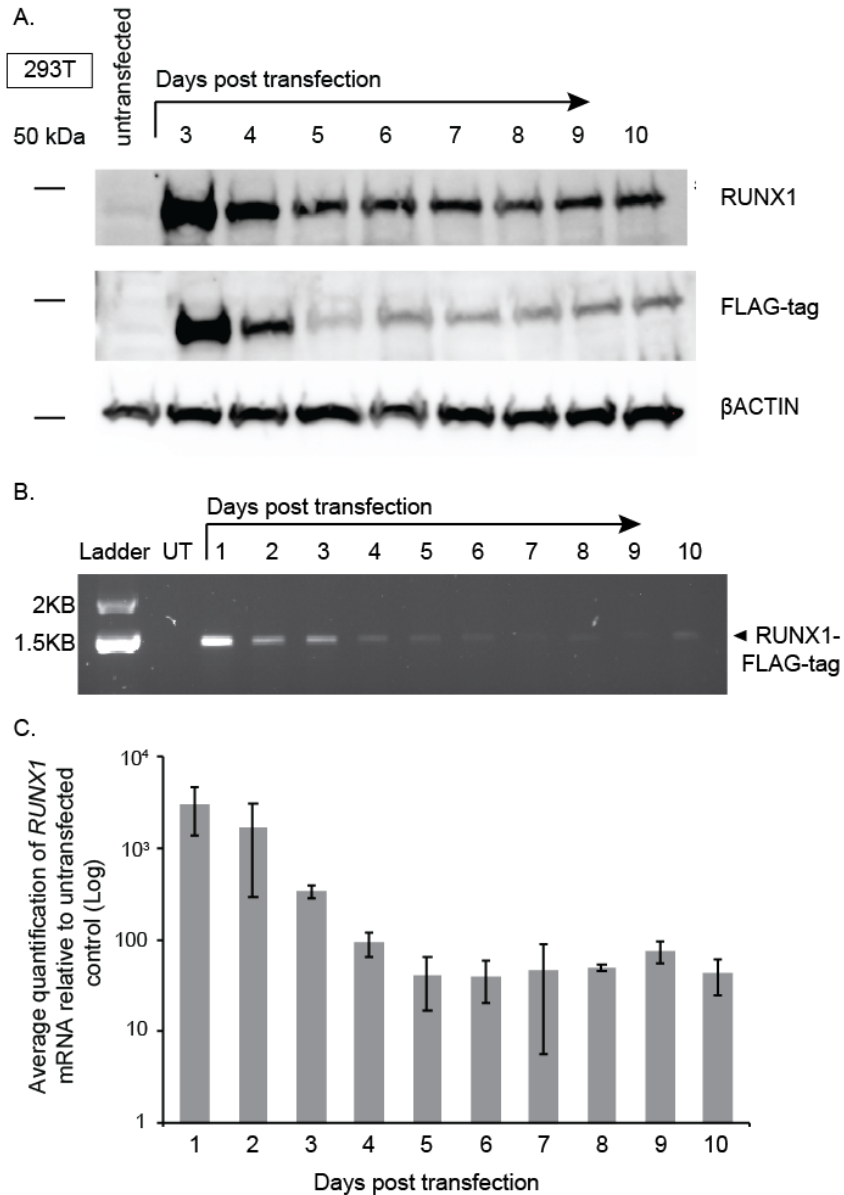


Figure 2.1. Effect of transient expression of exogenous RUNX1 upon endogenous RUNX1 expression in 293T cells. A. Western blot of total RUNX1 protein in 293T cells transiently transfected with FLAG epitope-tagged RUNX1 expression vector (RUNX1-FLAG), over a 10-day time course. Immunostaining performed with antibodies directed against RUNX1, FLAG tag, and beta-actin control. B. Agarose gel electrophoresis showing semi-quantitative qRT-PCR measurement of RUNX1-FLAG transcript, corresponding to transfection performed in part A. UT, untransfected. C. Average fold-change of RUNX1 transcript in 293T cells transiently transfected with RUNX1-FLAG plasmid, relative to untransfected control, as measured by TaqMan qRT-PCR. Confidence intervals represent standard deviation of 3 repetitions.

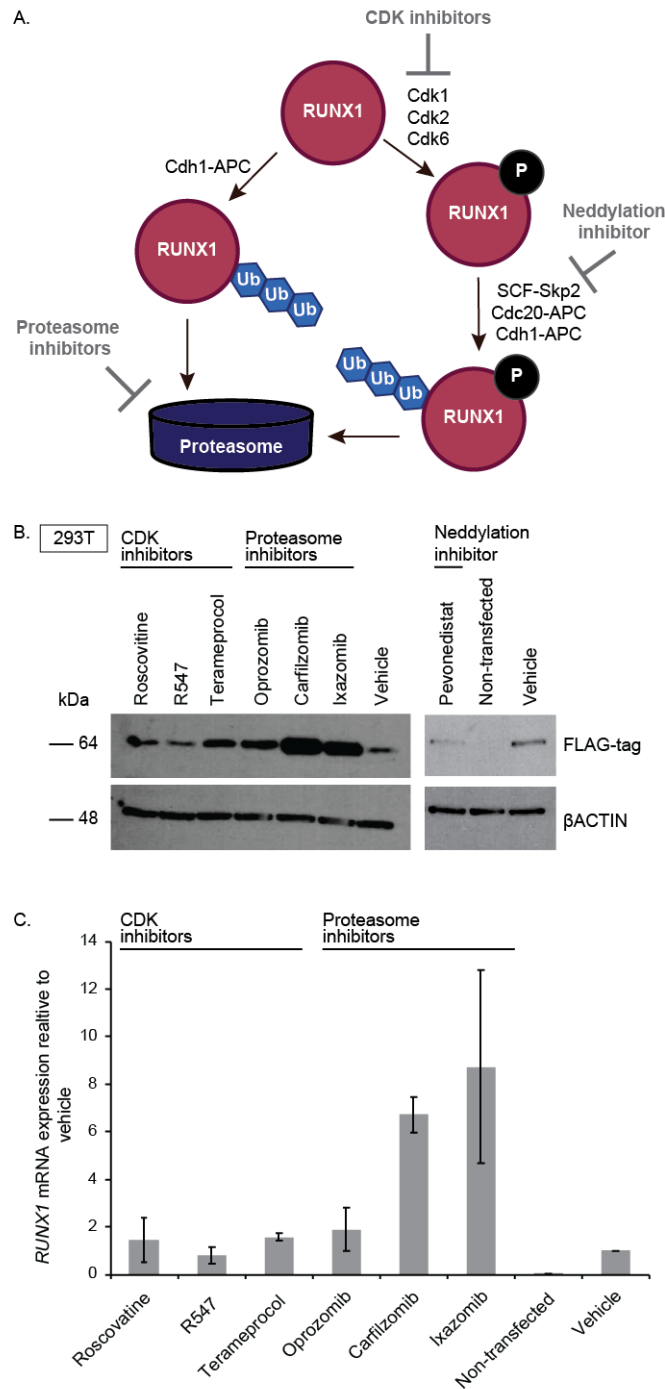


Figure 2.2. Effect of drugs inhibiting RUNX1 proteolytic degradation on RUNX1 protein and transcript levels in 293T cells transiently transfected with RUNX1-FLAG. A. Schematic of RUNX1 protein degradation pathway, showing steps at which inhibitors act. B. Western blot exhibiting elevated levels of exogenous RUNX1-FLAG protein expression in transiently transfected 293T cells following 24-hours of drug treatment vs. vehicle (DMSO) treatment. C. TaqMan qRT-PCR revealing commensurately elevated levels of RUNX1 transcript in drug-treated 293T cells transiently transfected with RUNX1-FLAG. Confidence intervals represent standard deviation of 2 repetitions.

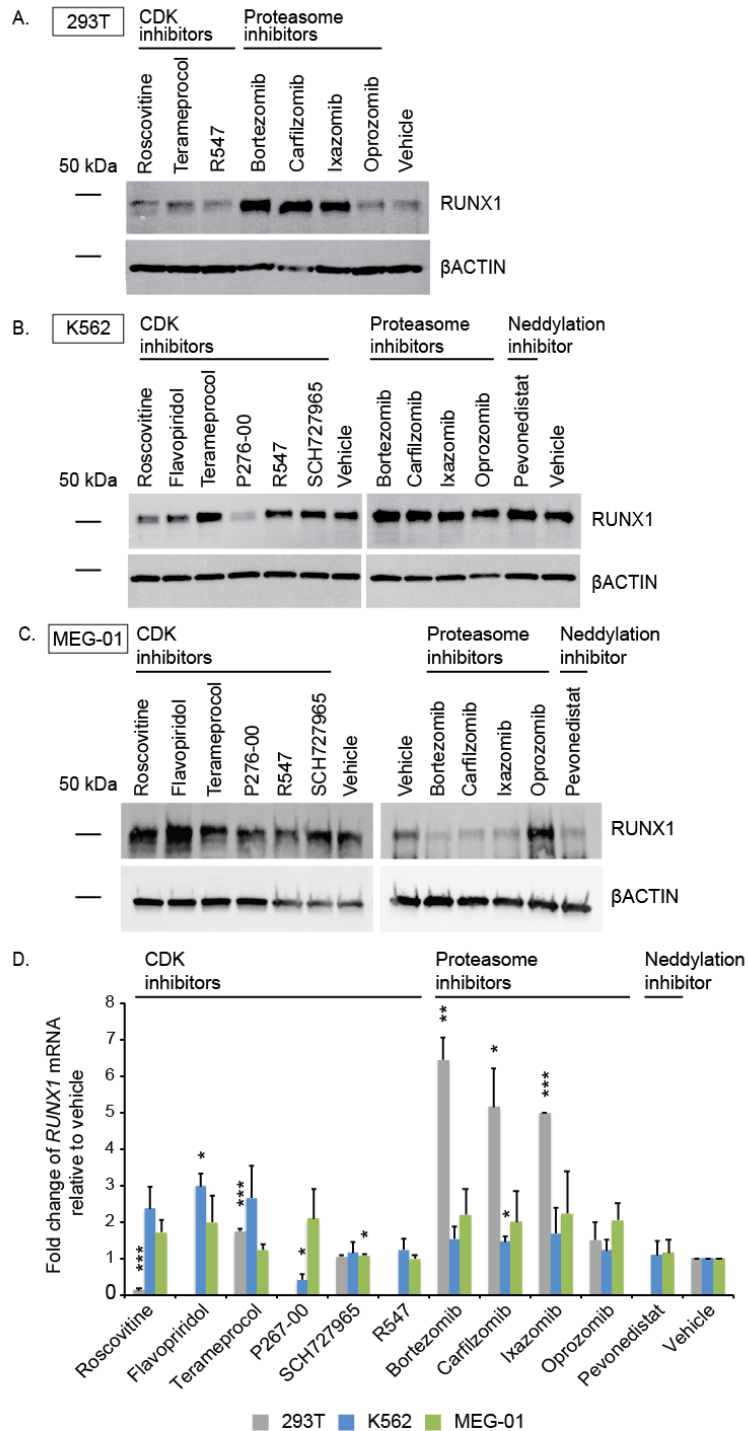


Figure 2.3. Inhibition of endogenous RUNX1 proteolytic degradation in cell lines. Non-transfected 293T (A), K562 (B), and MEG-01 (C) cell lines were treated with indicated drugs or vehicle (DMSO) for 24 hours. Immediately afterward, protein lysates were then subject to western blot detection of endogenous RUNX1 compared to beta-actin control. D. Average fold-change of endogenous *RUNX1* mRNA expression relative to vehicle (DMSO) treatment. Confidence intervals represent standard deviation of 2-3 repetitions. P values: * $p < 0.05$, ** $p < 0.01$, *** $p < 0.001$ in 2-tailed Student's *t*-test assuming unequal variance.

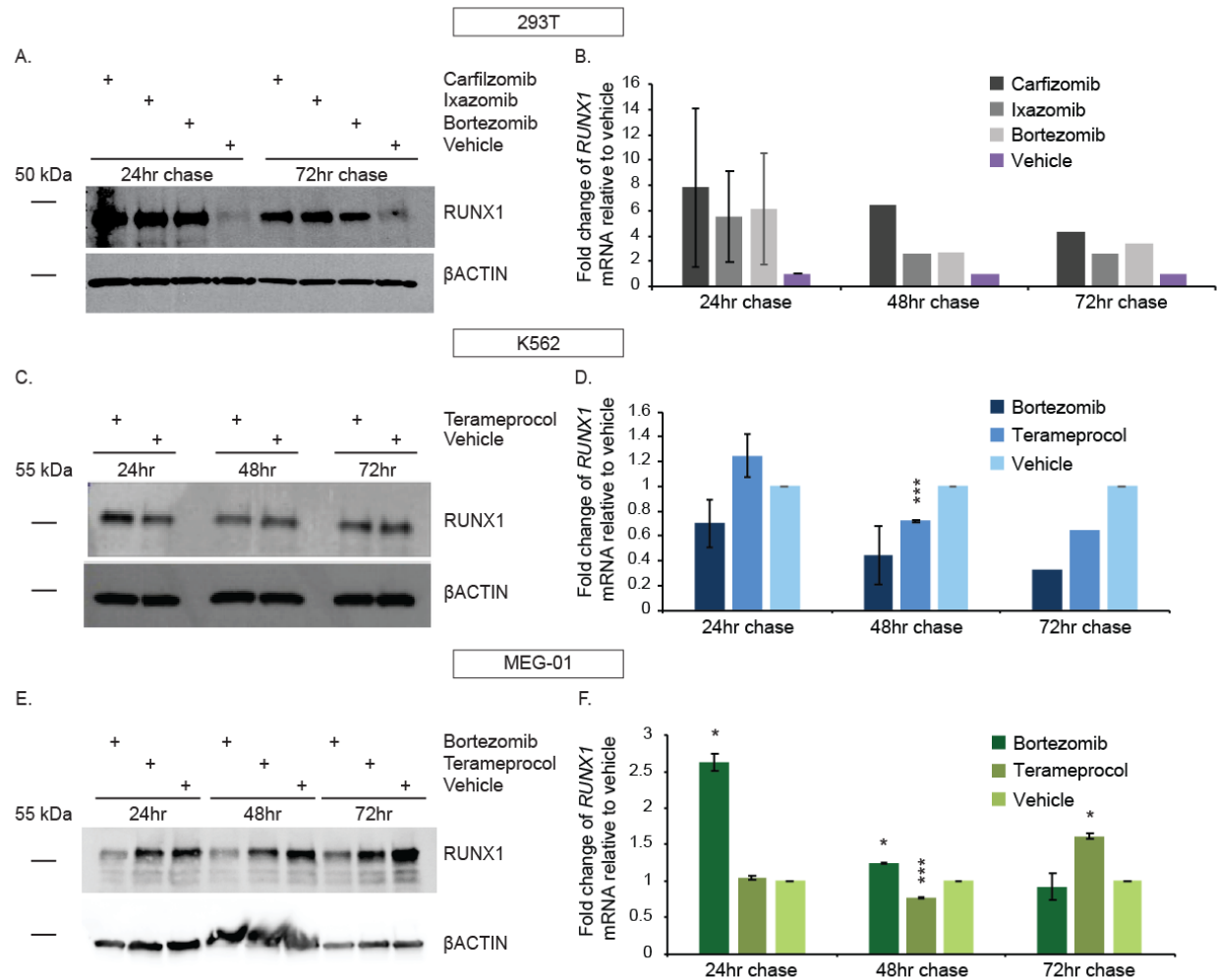


Figure 2.4. Persistence of RUNX1 expression in cell lines following transient inhibition of its proteolytic degradation. Non-transfected 293T (A-B), K562 (C-D), and MEG-01 (E-F) cell lines were treated with indicated drugs or vehicle (DMSO) for 24 hours. At 24-, 48-, and 72-hours following the conclusion of drug treatment, protein lysates from aliquots were then subject to western blot detection of endogenous RUNX1 compared to beta-actin control (A, C, E). At the corresponding timepoints, TaqMan qRT-PCR was used to measure average fold-change of endogenous *RUNX1* mRNA expression relative to vehicle (DMSO) treatment (B, D, F). Confidence intervals represent standard deviation of 1-3 repetitions. P values: * <0.05 , ** <0.01 , *** <0.001 in 2-tailed Student's t test assuming unequal variance.

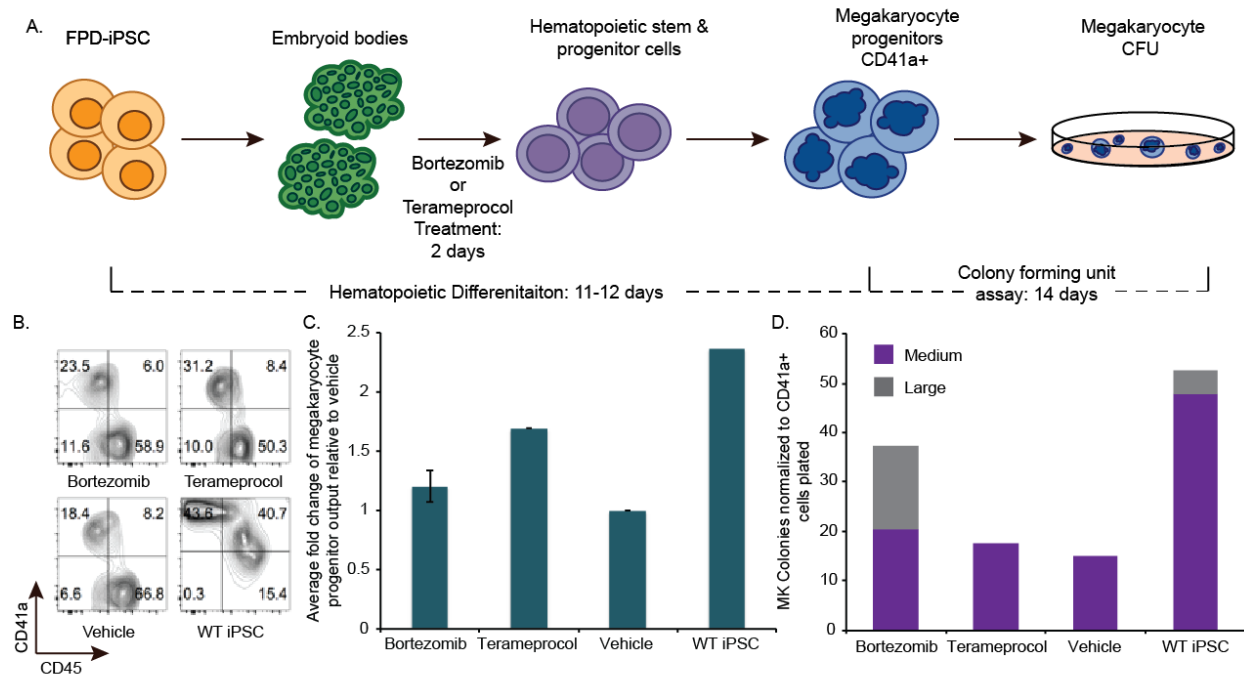


Figure 2.5. Transient inhibition of RUNX1 proteolytic degradation during megakaryocytic differentiation of FPD/AML patient-derived iPSC. A. iPSC differentiation protocol. B. Flow cytometric analysis, representative results, compared to vehicle-treated and wild type (1) iPSC. C. Graphical representation of flow cytometric analysis, as depicted in part B (bortezomib and vehicle, n=3; terameprocol and WT iPSC, n=1). D. Megakaryocyte colony formation (n=1). Confidence interval represents standard deviation.

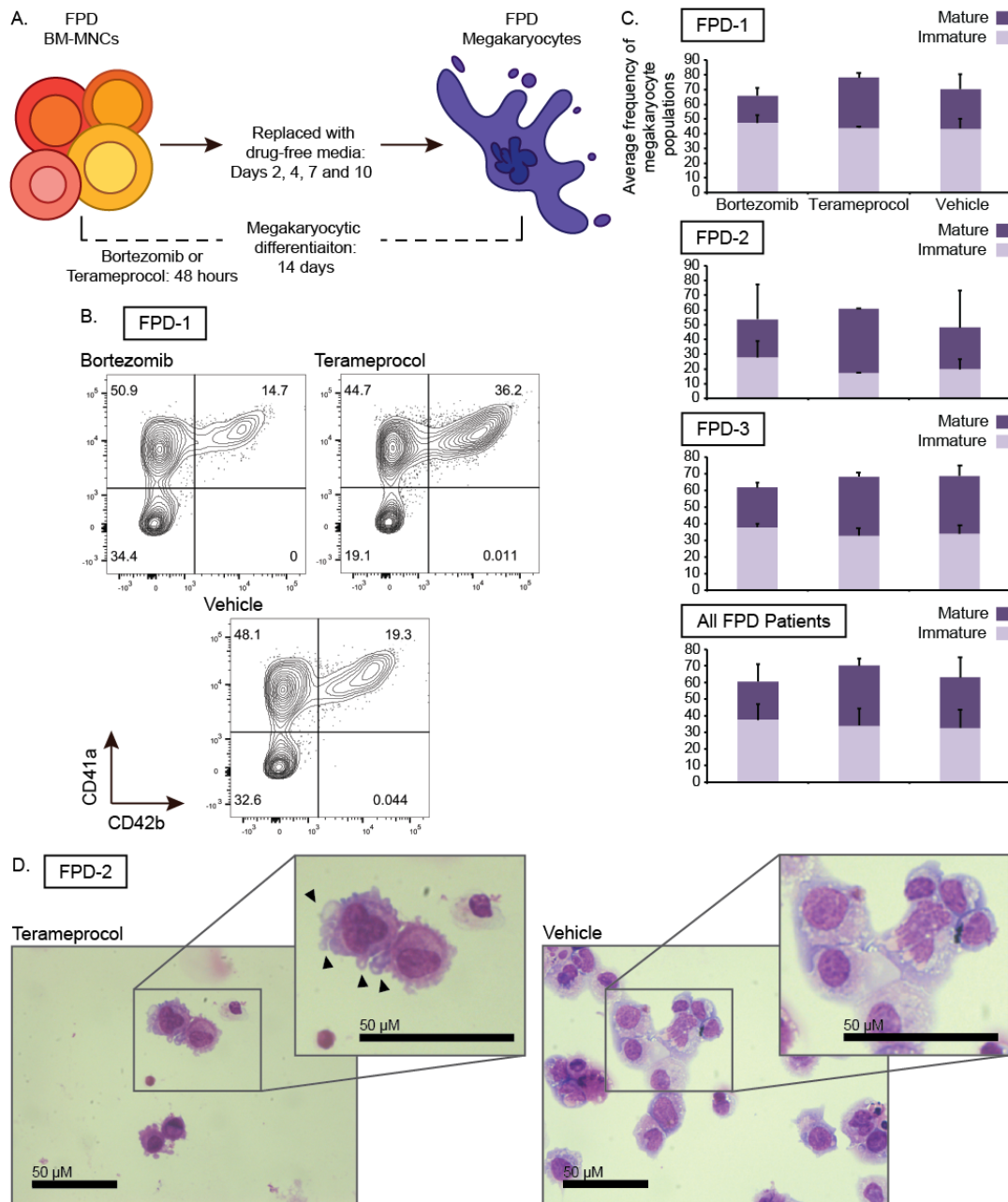


Figure 2.6. Primary FPD/AML mononuclear bone marrow cells treated with inhibitors of RUNX1 proteolytic degradation early during *in vitro* megakaryocyte differentiation. A. Differentiation protocol. B. Representative flow cytometric analysis of megakaryocytes generated from patient FPD-1 at conclusion of differentiation of protocol. C. Graphical representation of flow cytometric analysis, as depicted in part B, relative to vehicle-treated control, for each patient (FPD-1, -2, and -3, or all three analyzed collectively). Immature megakaryocyte populations correspond to CD41a+/CD42b- and mature populations correspond to CD41a+/CD42b+. Confidence interval represents standard deviation of 1-4 repetitions. D. Cytospin preparation of cells (Wright Giemsa stain) harvested at conclusion of differentiation protocol, representative results obtained from FPD-2. Arrows indicate blebs consistent with proplatelet formation.

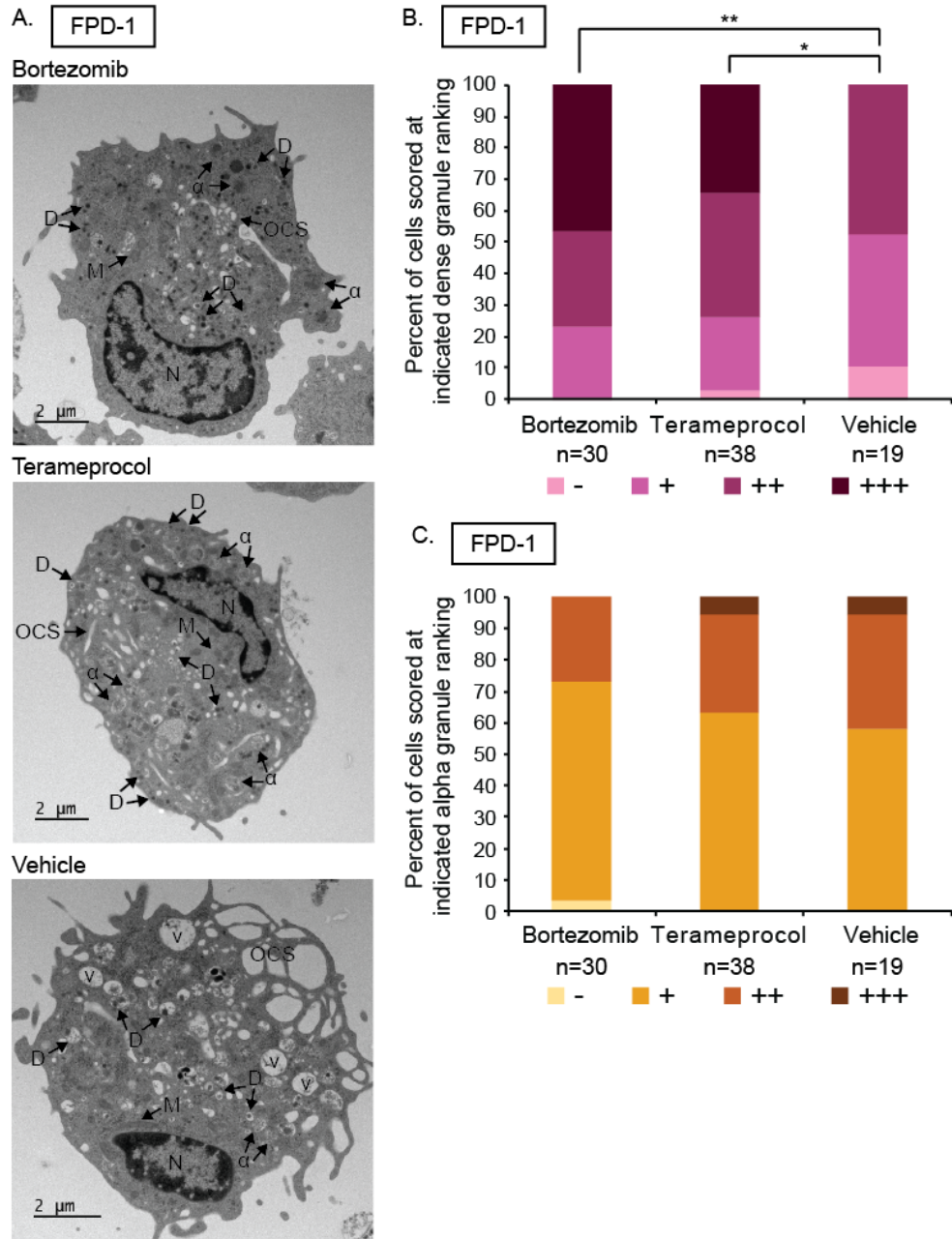


Figure 2.7. Effect of RUNX1 degradation inhibitor treatment on platelet granule formation during *in vitro* megakaryocyte differentiation of primary FPD/AML mononuclear bone marrow cells. Primary cells from an FPD/AML patient were treated and harvested as shown above (Fig 2.6A). A. Thin section transmission electron microscopy images of cells treated either with bortezomib, terameprocol, or vehicle. Arrows indicate ultrastructural components: dense granules (D), alpha granules (α), open canalicular system (OCS), nucleus (N), mitochondria (M), and vacuoles (V). Proportion of total cells scored at given ranking for presence of dense (B) and alpha (C) granules, respectively. Rankings were designated as the following number of granules/cell: - = 0, + = 1-10, ++ = 10-20, +++ = >20. Unidentifiable granules were not included in ranking. P values: * <0.05 , ** <0.01 using a chi-square test of independence.

2.6. Supplementary Tables

Patient ID	Mutation	Age	Patient history	Marrow presentation at time of BM harvest	Treatment	Differentiation 1		Differentiation 2		Differentiation 3	
						Percentage of immature megakaryocytes (n=# of cells)	Percentage of mature megakaryocytes (n=# of cells)	Percentage of immature megakaryocytes (n=# of cells)	Percentage of mature megakaryocytes (n=# of cells)	Percentage of immature megakaryocytes (n=# of cells)	Percentage of mature megakaryocytes (n=# of cells)
FPD-1		14	regular menses since 11yo, bruises easily, no nosebleeds or oral bleeding, mild thrombocytopenia (150)	Normocellular, 50% megakaryocytic changes	Vehicle	39.2% n=1292	33.8% n=1083	48.1% n=2164	18.3% n=868		
					Bortezomib	43.8% n=1375	22.2% n=695	50.9% n=1950	14.7% n=562		
					Terameprocol	43.4% n=2088	31.9% n=1536	44.7% n=3909	36.2% n=3160		
FPD-2	NM_001754 c.1242C>A, p.Y414X	41	thrombocytopenia and life-long history of easy bruising and heavy menses, iron-deficiency anemia secondary to menorrhagia	Mildly hypocellular, virtually absent iron stores (ferritin=4), 2% blasts	Vehicle	24.8% n=758	10.7% n=327	14.9% n=661	45.9% n=2034		
					Bortezomib	35.7% n=1126	8.66% n=273	20.2% n=844	42.6% n=1781		
					Terameprocol			17.4% n=835	43.6% n=2095		
FPD-3		11	premenarchal, bruises easily, no other bleeding symptoms, well child except history of reactive airways	Hypocellular averaging 40%, mild panhypoplasia	Vehicle	29.9% n=1194	40.10% n=1604	32.8% n=935	35.6% n=1015	39.9% n=754	27.5% n=528
					Bortezomib	38.9% n=1156	27.3% n=810	38.9% n=831	22.5% n=480	35.4% n=621	21.8% n=383
					Terameprocol	30.6% n=590	35.7% n=689	37.9% n=828	32.8% n=715	30% n=593	37.3% n=738

Supplementary Table 2.1. FPD patient information and flow cytometry analysis at time of harvest following *in vitro* megakaryocytic differentiation.

Drug Target	Drug Name	Vendor information	Drug concentration used					
			293T	K562	MEG-01	FPD-iPSC	Primary FPD-BM	
Cyclin Dependent Kinase	Roscovitine	Fisher Scientific Catalog #: 50-101-3564	50uM	50uM	25uM			
	Flavopiridol hydrochloride	Tocris Catalog #: 3094	300nM	300nM	150nM			
	Termaprocol	Sigma-Aldrich Catalog #: T3455-10mg	25uM	25uM	12.5uM	25uM	25uM	
	P276-00	Selleckchem Catalog #: S8058	3uM	3uM	750nM			
	R547	Tocris Catalog #: 5494	8nM	8nM	16nM			
	SCH 727965	Selleckchem Catalog #: S2768	2nM	2nM	400pM			
S26 Proteasome	Bortezomib	Fisher Scientific Catalog #: 50-431-40001	6.5uM	6.5uM	500nM for RNAseq	10nM	5nM	3.25nM
	Carfilzomib	Fisher Scientific Catalog #: 50-101-3564	5uM	5uM	156.25nM			
	Ixazomib	UBPBio Catalog #: F1110	500nM	500nM	3.9nM			
	Oprozomib	Selleckchem Catalog #: S7049	80nM	80nM	80nM			
Neddylaton	Pevonedistat	Selleckchem Catalog #: S7109	200nM	200nM	400nM			

Supplementary Table 2.2. Summary of drug information and concentrations used for cell studies.

Antibody	Vendor Information	Antibody Species	Clone	Conjugation	Blocking Conditions	Staining Conditions (Concentration, diluent, incubation)
Anti-Actin	Sigma-Aldrich Catalog #: A1978	Mouse	AC-15 Monoclonal	Unconjugated	3% BSA in TBST, 30min RT	1:1000 1% BSA, 0.02% Sodium Azide in TBST overnight 4°C
Anti-AML1 (RUNX1)	Cell Signaling Technologies Catalog #: 4334S	Rabbit	Polyclonal	Unconjugated	5% milk in TBST, 30min RT	
Anti-FLAG-tag	Biologend Catalog #: 902401 (Poly9024)	Rabbit	Polyclonal	Unconjugated	3% BSA in TBST, 30min RT	
Anti-Rabbit Secondary	ThermoFisher Scientific Catalog #: A16124	Goat	Polyclonal	HRP	N/A	1:10,000 1% BSA in TBST 1hr RT
Anti-Mouse Secondary	ThermoFisher Scientific Catalog #: A16072	Goat	Polyclonal	HRP		

Supplementary Table 2.3. Summary of antibodies used for immunoblotting in cell studies.

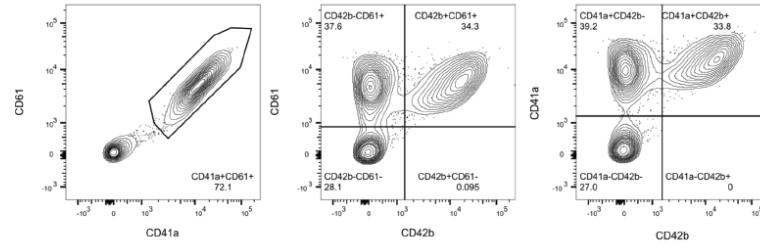
Antibody Target	Vendor Information	Antibody Species	Clone	Conjugation	Concentration used
CD41a	BD Pharmingen Catalog #: 561424	Mouse	HIP8	PE-Cy7	1:50
	BD Horizon Catalog #: 561425		HIP8	V450	1:100
CD42b	BD Pharmingen Catalog #: 551061		HIP1	APC	1:100
CD61	BD Pharmingen Catalog #: 555753		VI-PL2	FITC	1:50
CD45	BD Pharmingen Catalog #: 555485		HI30	APC	1:20

Supplementary Table 2.4. Summary of antibodies used for flow cytometry in cell studies.

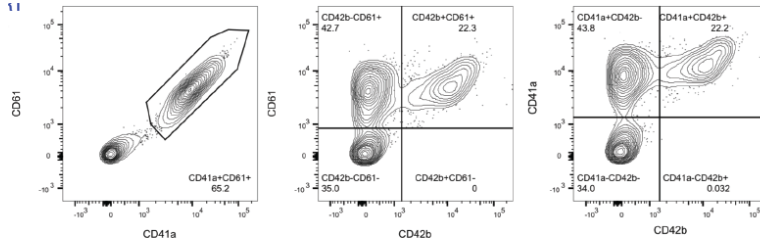
2.7. Supplementary Figures

A. FPD-1

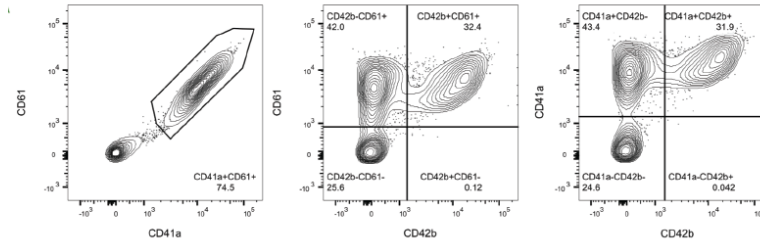
**Differentiation 1
Vehicle**



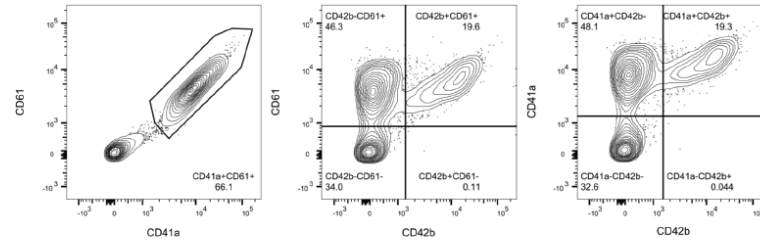
**Differentiation 1
Bortezomib**



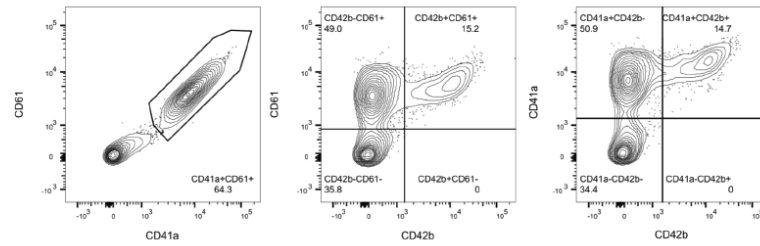
**Differentiation 1
Terameprocol**



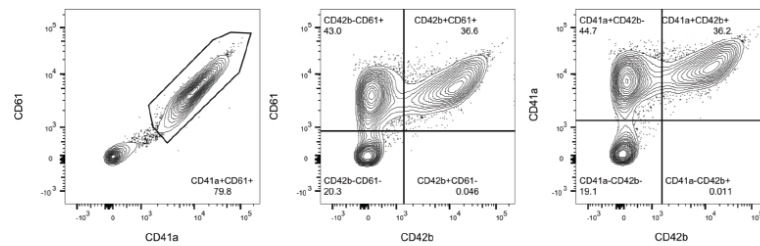
**Differentiation 2
Vehicle**



**Differentiation 2
Bortezomib**

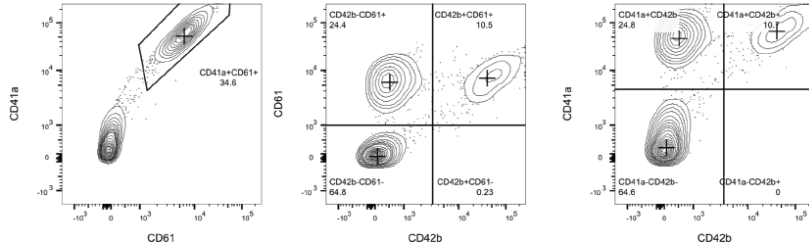


**Differentiation 2
Terameprocol**

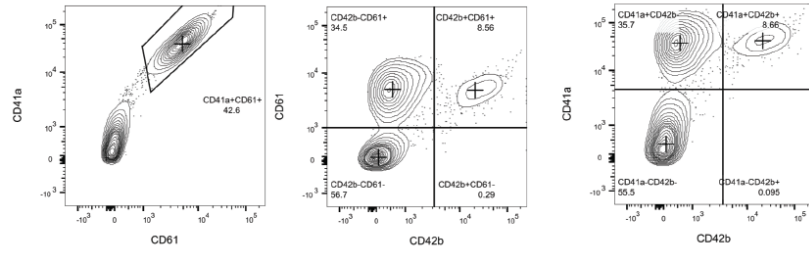


B. **FPD-2**

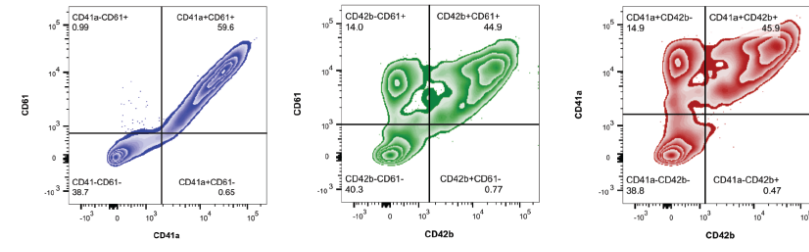
Differentiation 1
Vehicle



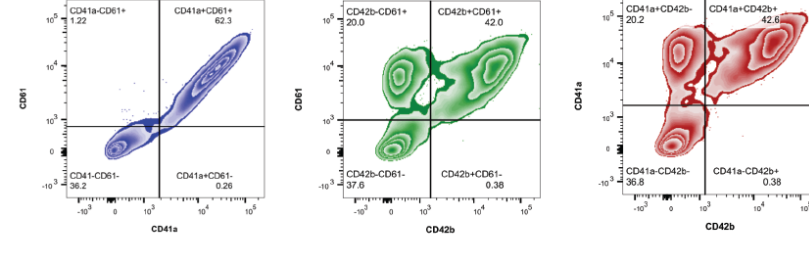
Differentiation 1
Bortezomib



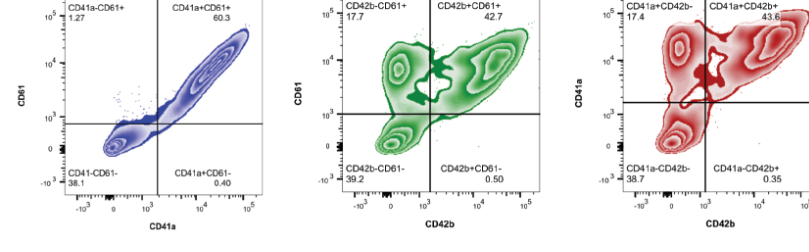
Differentiation 2
Vehicle



Differentiation 2
Bortezomib

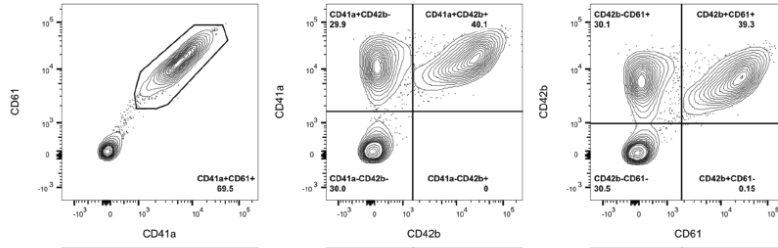


Differentiation 2
Terameprocol

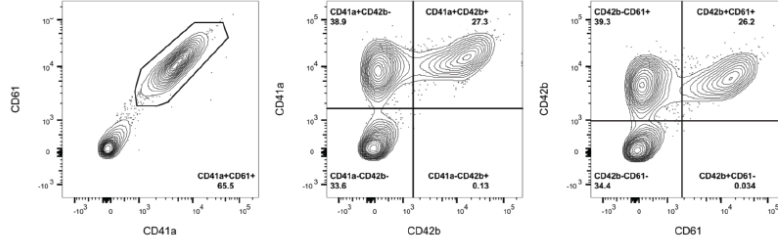


C. **FPD-3**

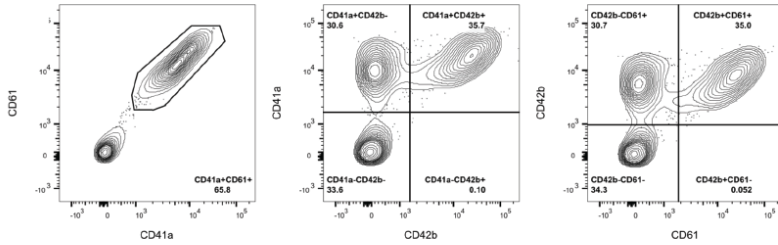
Differentiation 1
Vehicle



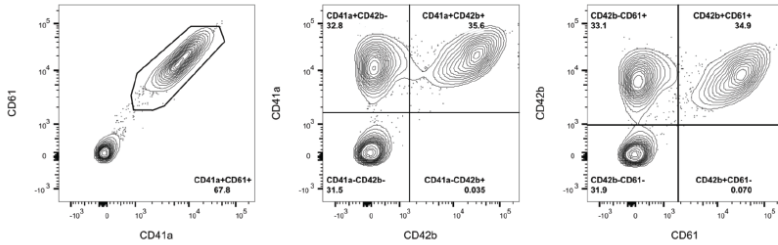
Differentiation 1
Bortezomib



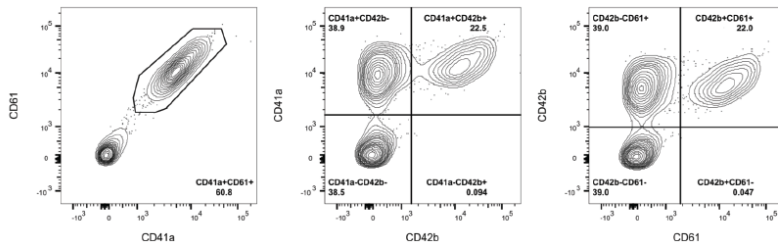
Differentiation 1
Terameprocol



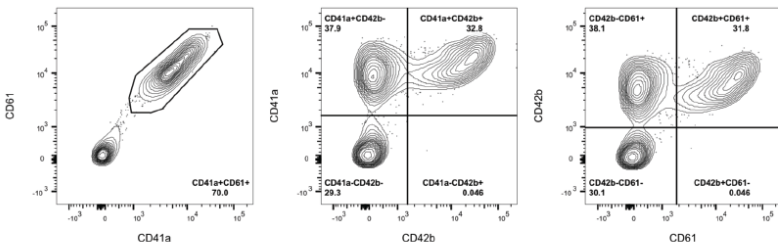
Differentiation 2
Vehicle



Differentiation 2
Bortezomib

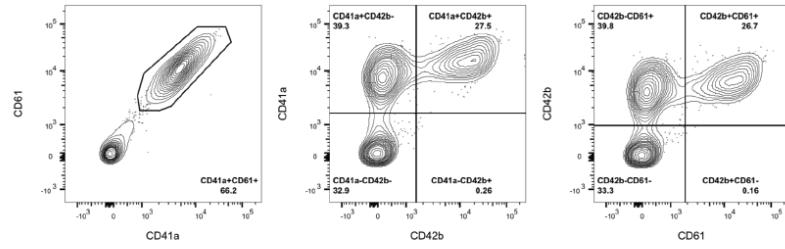


Differentiation 2
Terameprocol

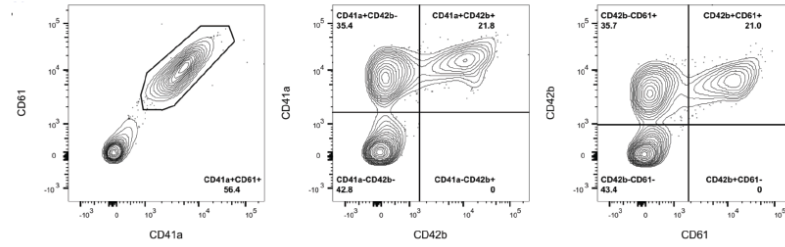


FPD-3

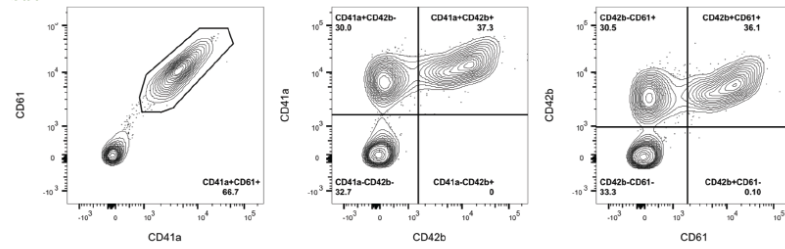
Differentiation 3
Vehicle



Differentiation 3
Bortezomib

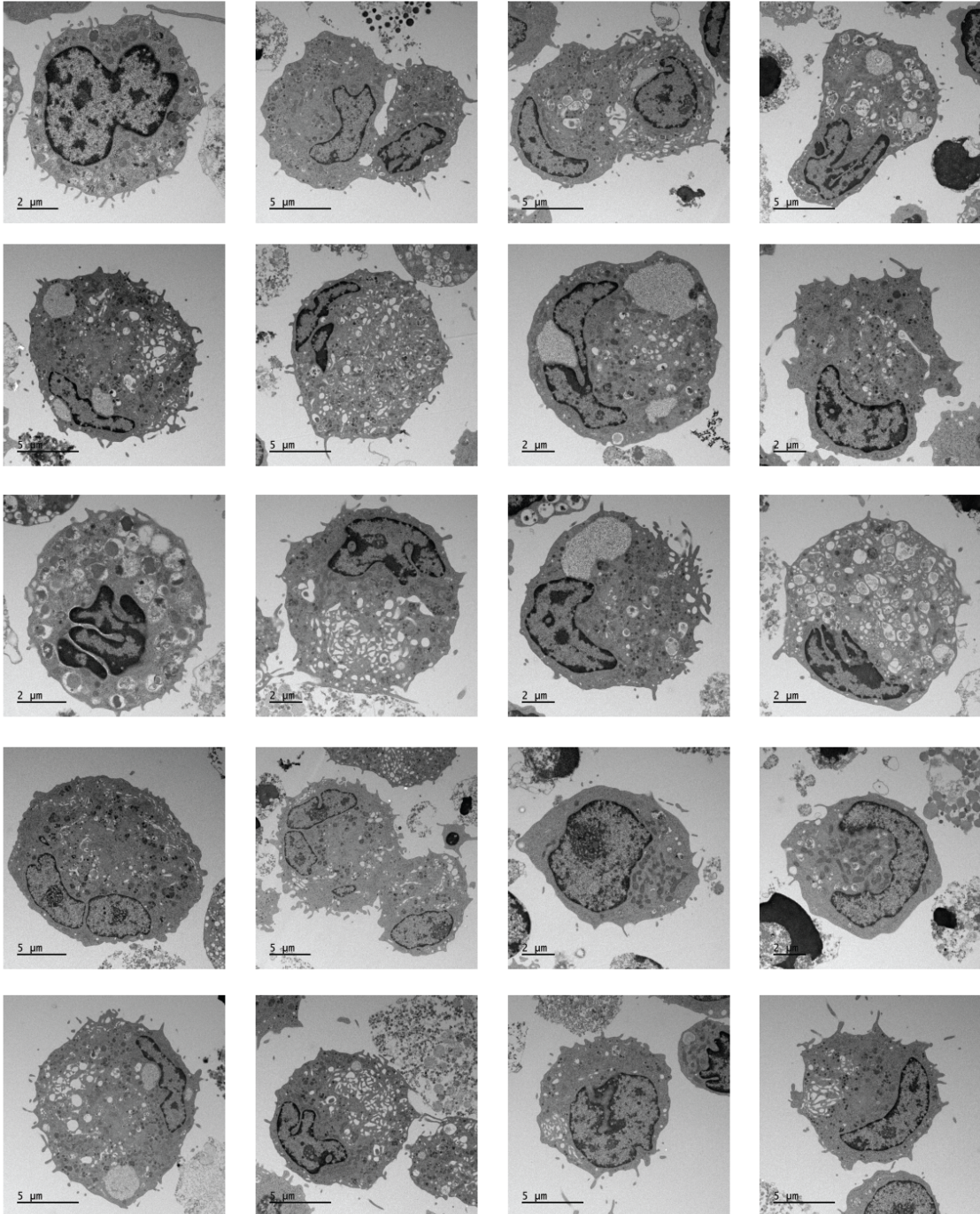


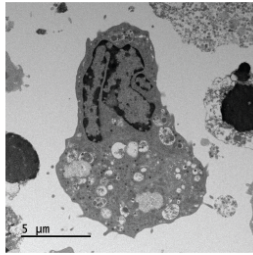
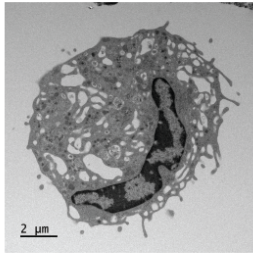
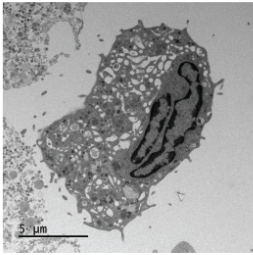
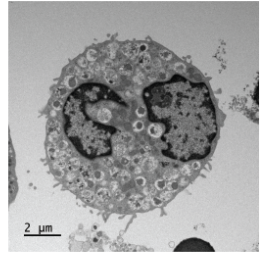
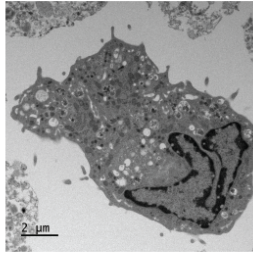
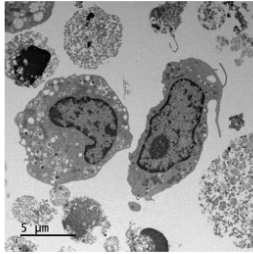
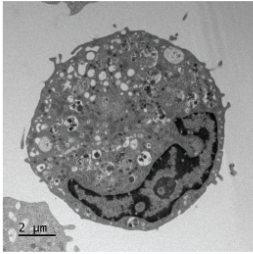
Differentiation 3
Terameprocol



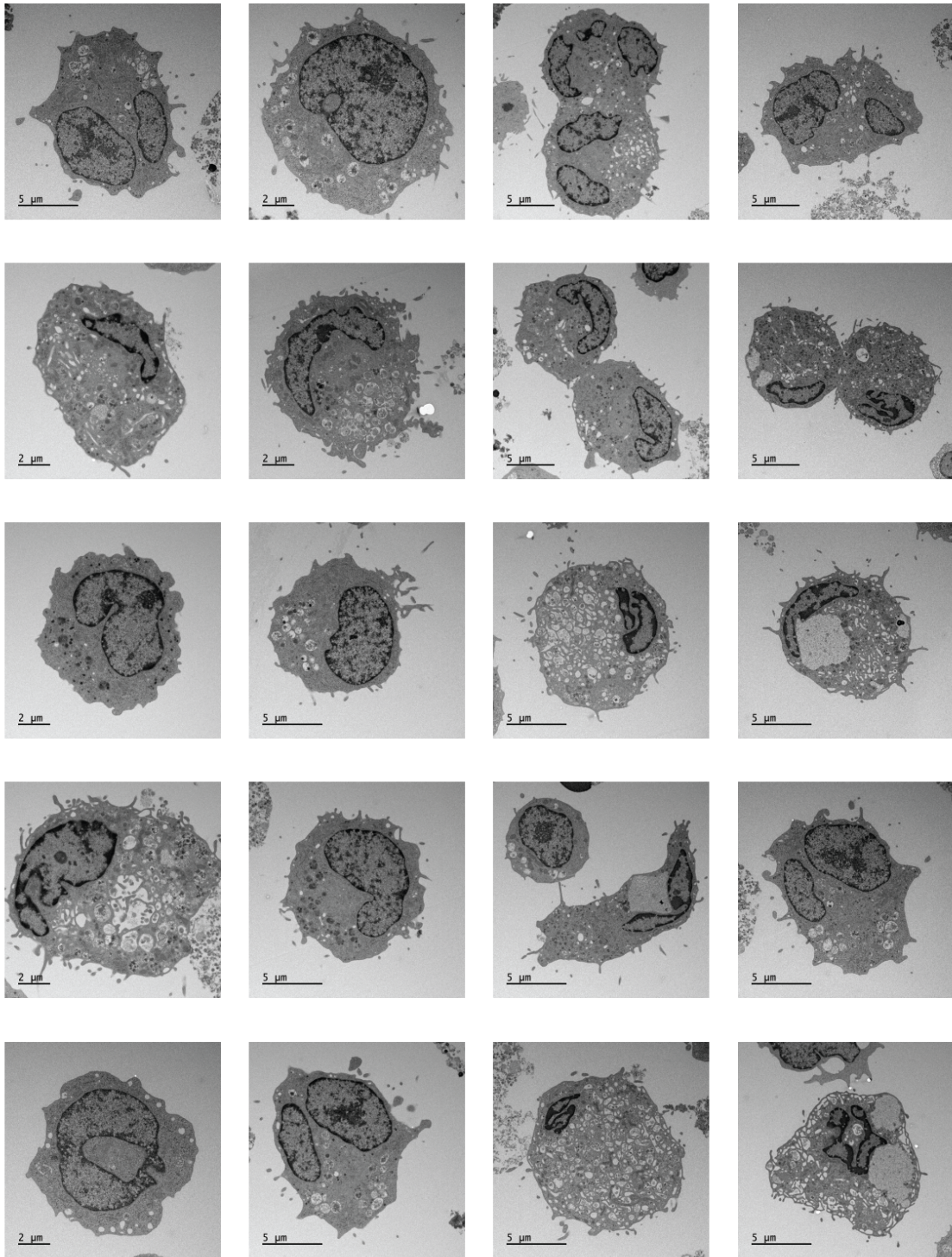
Supplementary Figure 2.1. Flow cytometry analysis of primary FPD patient bone marrow-derived megakaryocytes. A. FPD-1 analysis. FPD-2 analysis. FPD-3 analysis.

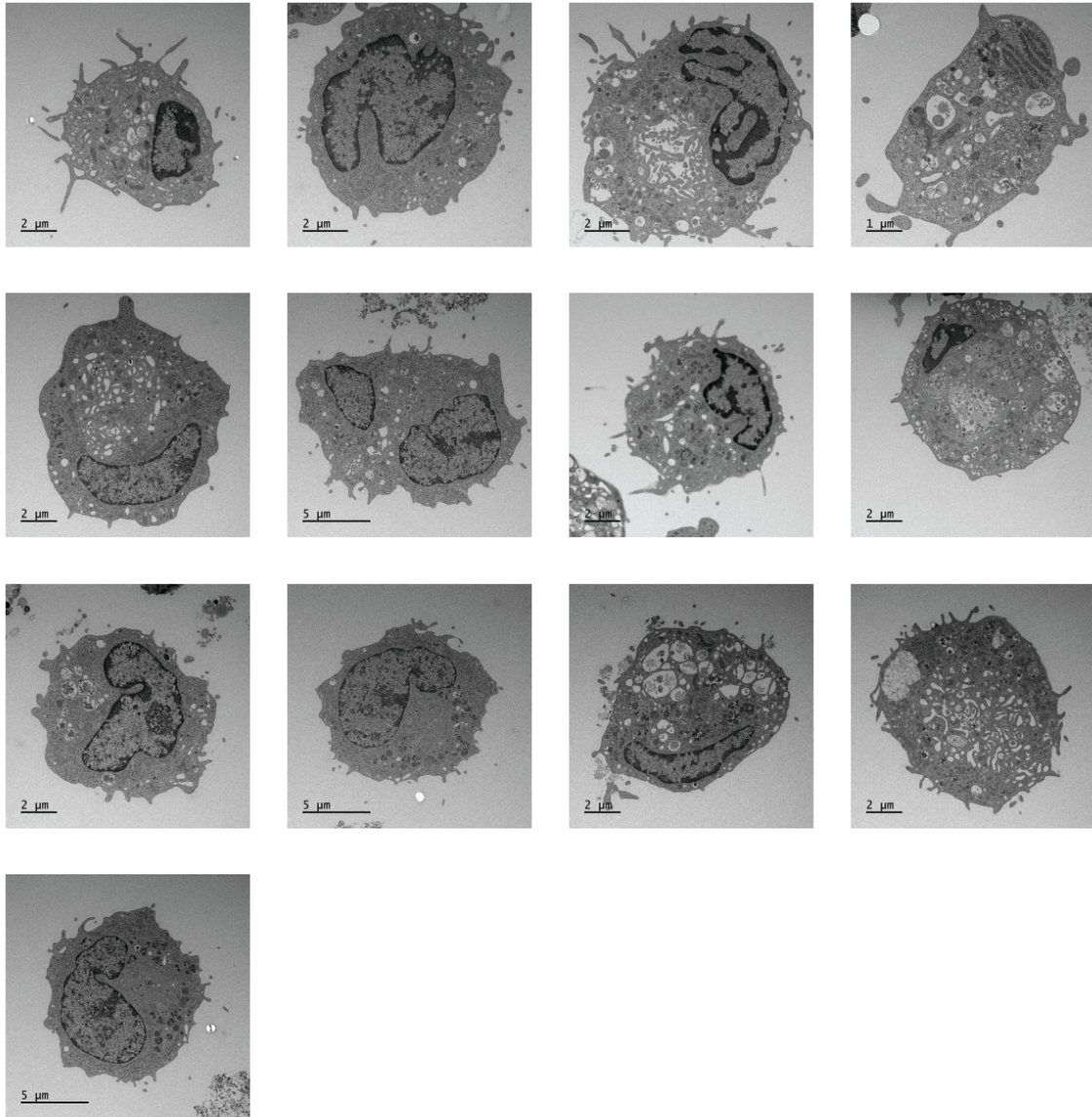
B.





C.





Supplementary Figure 2.2. Transmission electron microscopy images of primary FPD-1 patient bone marrow-derived megakaryocytes. A. Vehicle treated cells (n=19). B. Bortezomib treated cells (n=30). C. Terameprocol treated cells (n=38).

2.8. References

1. Downton SB, Beardsley D, Jamison D, Blattner S, Li FP. Studies of a familial platelet disorder. *Blood*. 1985;65(3):557-63.
2. Latger-Cannard V, Philippe C, Bouquet A, Baccini V, Alessi MC, Ankri A, et al. Haematological spectrum and genotype-phenotype correlations in nine unrelated families with RUNX1 mutations from the French network on inherited platelet disorders. *Orphanet J Rare Dis*. 2016;11:49.
3. Tober J, Maijenburg MW, Speck NA. Taking the Leap: Runx1 in the Formation of Blood from Endothelium. *Curr Top Dev Biol*. 2016;118:113-62.
4. Duployez N, Willekens C, Marceau-Renaut A, Boudry-Labis E, Preudhomme C. Prognosis and monitoring of core-binding factor acute myeloid leukemia: current and emerging factors. *Expert Rev Hematol*. 2015;8(1):43-56.
5. Matheny CJ, Speck ME, Cushing PR, Zhou Y, Corpora T, Regan M, et al. Disease mutations in RUNX1 and RUNX2 create nonfunctional, dominant-negative, or hypomorphic alleles. *EMBO J*. 2007;26(4):1163-75.
6. Churpek JE, Pyrtel K, Kanchi KL, Shao J, Koboldt D, Miller CA, et al. Genomic analysis of germ line and somatic variants in familial myelodysplasia/acute myeloid leukemia. *Blood*. 2015;126(22):2484-90.
7. Song WJ, Sullivan MG, Legare RD, Hutchings S, Tan X, Kufrin D, et al. Haploinsufficiency of CBFA2 causes familial thrombocytopenia with propensity to develop acute myelogenous leukaemia. *Nat Genet*. 1999;23(2):166-75.
8. Owen CJ, Toze CL, Koochin A, Forrest DL, Smith CA, Stevens JM, et al. Five new pedigrees with inherited RUNX1 mutations causing familial platelet disorder with propensity to myeloid malignancy. *Blood*. 2008;112(12):4639-45.
9. Preudhomme C, Renneville A, Bourdon V, Philippe N, Roche-Lestienne C, Boissel N, et al. High frequency of RUNX1 biallelic alteration in acute myeloid leukemia secondary to familial platelet disorder. *Blood*. 2009;113(22):5583-7.
10. Huang G, Shigesada K, Ito K, Wee HJ, Yokomizo T, Ito Y. Dimerization with PEBP2beta protects RUNX1/AML1 from ubiquitin-proteasome-mediated degradation. *EMBO J*. 2001;20(4):723-33.
11. Goyama S, Huang G, Kurokawa M, Mulloy JC. Posttranslational modifications of RUNX1 as potential anticancer targets. *Oncogene*. 2015;34(27):3483-92.
12. Kim JH, Jang JW, Lee YS, Lee JW, Chi XZ, Li YH, et al. RUNX family members are covalently modified and regulated by PIAS1-mediated sumoylation. *Oncogenesis*. 2014;3:e101.
13. Martinez M, Hinojosa M, Trombly D, Morin V, Stein J, Stein G, et al. Transcriptional Auto-Regulation of RUNX1 P1 Promoter. *PloS one*. 2016;11(2):e0149119.
14. Horwitz M. Hypermethylated myoblasts specifically deficient in MyoD autoactivation as a consequence of instability of MyoD. *Exp Cell Res*. 1996;226(1):170-82.
15. Lin YC, Boone M, Meuris L, Lemmens I, Van Roy N, Soete A, et al. Genome dynamics of the human embryonic kidney 293 lineage in response to cell biology manipulations. *Nat Commun*. 2014;5:4767.

16. Ogura M, Morishima Y, Ohno R, Kato Y, Hirabayashi N, Nagura H, et al. Establishment of a novel human megakaryoblastic leukemia cell line, MEG-01, with positive Philadelphia chromosome. *Blood*. 1985;66(6):1384-92.
17. Koefler HP, Golde DW. Human myeloid leukemia cell lines: a review. *Blood*. 1980;56(3):344-50.
18. Yang W, Mills JA, Sullivan S, Liu Y, French DL, Gadue P. iPSC Reprogramming from Human Peripheral Blood Using Sendai Virus Mediated Gene Transfer. *StemBook*. Cambridge (MA)2008.
19. Papapetrou EP, Sadelain M. Derivation of genetically modified human pluripotent stem cells with integrated transgenes at unique mapped genomic sites. *Nat Protoc*. 2011;6(9):1274-89.
20. Kotini AG, Chang CJ, Chow A, Yuan H, Ho TC, Wang T, et al. Stage-Specific Human Induced Pluripotent Stem Cells Map the Progression of Myeloid Transformation to Transplantable Leukemia. *Cell Stem Cell*. 2017;20(3):315-28 e7.
21. Chisholm KM, Denton C, Keel S, Geddis AE, Xu M, Appel BE, et al. Bone Marrow Morphology Associated With Germline RUNX1 Mutations in Patients With Familial Platelet Disorder With Associated Myeloid Malignancy. *Pediatr Dev Pathol*. 2019:1093526618822108.
22. Chen D, Uhl CB, Bryant SC, Krumwiede M, Barness RL, Olson MC, et al. Diagnostic laboratory standardization and validation of platelet transmission electron microscopy. *Platelets*. 2018;29(6):574-82.
23. Goyal S, Suzuki T, Li JR, Maeda S, Kishima M, Nishimura H, et al. RUNX1 induces DNA replication independent active DNA demethylation at SPI1 regulatory regions. *BMC Mol Biol*. 2017;18(1):9.
24. Zhang L, Fried FB, Guo H, Friedman AD. Cyclin-dependent kinase phosphorylation of RUNX1/AML1 on 3 sites increases transactivation potency and stimulates cell proliferation. *Blood*. 2008;111(3):1193-200.
25. Biggs JR, Peterson LF, Zhang Y, Kraft AS, Zhang DE. AML1/RUNX1 phosphorylation by cyclin-dependent kinases regulates the degradation of AML1/RUNX1 by the anaphase-promoting complex. *Mol Cell Biol*. 2006;26(20):7420-9.
26. Wang S, Zhang Y, Soosairajah J, Kraft AS. Regulation of RUNX1/AML1 during the G2/M transition. *Leuk Res*. 2007;31(6):839-51.
27. Lapenna S, Giordano A. Cell cycle kinases as therapeutic targets for cancer. *Nat Rev Drug Discov*. 2009;8(7):547-66.
28. Swords RT, Erba HP, DeAngelo DJ, Bixby DL, Altman JK, Maris M, et al. Pevonedistat (MLN4924), a First-in-Class NEDD8-activating enzyme inhibitor, in patients with acute myeloid leukaemia and myelodysplastic syndromes: a phase 1 study. *Br J Haematol*. 2015;169(4):534-43.
29. Kubickova L, Pour L, Sedlarikova L, Hajek R, Sevcikova S. Proteasome inhibitors - molecular basis and current perspectives in multiple myeloma. *J Cell Mol Med*. 2014;18(6):947-61.
30. Connelly JP, Kwon EM, Gao Y, Trivedi NS, Elkahlon AG, Horwitz MS, et al. Targeted correction of RUNX1 mutation in FPD patient-specific induced pluripotent stem cells rescues megakaryopoietic defects. *Blood*. 2014;124(12):1926-30.

31. Mouthon MA, Freund M, Titeux M, Katz A, Guichard J, Breton-Gorius J, et al. Growth and differentiation of the human megakaryoblastic cell line (ELF-153): a model for early stages of megakaryocytopoiesis. *Blood*. 1994;84(4):1085-97.
32. Flaumenhaft R, Dilks JR, Richardson J, Alden E, Patel-Hett SR, Battinelli E, et al. Megakaryocyte-derived microparticles: direct visualization and distinction from platelet-derived microparticles. *Blood*. 2009;113(5):1112-21.
33. Bluteau D, Glembotsky AC, Raimbault A, Balayn N, Gilles L, Rameau P, et al. Dysmegakaryopoiesis of FPD/AML pedigrees with constitutional RUNX1 mutations is linked to myosin II deregulated expression. *Blood*. 2012;120(13):2708-18.
34. Manasanch EE, Orlowski RZ. Proteasome inhibitors in cancer therapy. *Nat Rev Clin Oncol*. 2017;14(7):417-33.
35. Gribble SM, Roberts I, Grace C, Andrews KM, Green AR, Nacheva EP. Cytogenetics of the Chronic Myeloid Leukemia-Derived Cell Line K562. *Cancer Genetics and Cytogenetics*. 2000;118(1):1-8.
36. Naumann S, Reutzel D, Speicher M, Decker H-J. Complete karyotype characterization of the K562 cell line by combined application of G-banding, multiplex-fluorescence in situ hybridization, fluorescence in situ hybridization, and comparative genomic hybridization. *Leukemia Research*. 2001;25(4):313-22.
37. Raedler L. Velcade (Bortezomib) Receives 2 New FDA Indications: For Retreatment of Patients with Multiple Myeloma and for First-Line Treatment of Patients with Mantle-Cell Lymphoma. *Am Health Drug Benefits*. 2015;8(Spec Feature):135-40.
38. Schwartz R, Davidson T. Pharmacology, pharmacokinetics, and practical applications of bortezomib. *Oncology (Williston Park)*. 2004;18(14 Suppl 11):14-21.
39. Mazepa MA, Raval JS, Moll S, Ma A, Park YA. Bortezomib induces clinical remission and reduction of ADAMTS13 inhibitory antibodies in relapsed refractory idiopathic thrombotic thrombocytopenic purpura. *Br J Haematol*. 2014;164(6):900-2.
40. Beckman JD, Rollins-Raval MA, Raval JS, Park YA, Mazepa M, Ma A. Bortezomib for Refractory Immune-Mediated Thrombocytopenia Purpura. *Am J Ther*. 2018;25(2):e270-e2.
41. Lu JM, Nurko J, Weakley SM, Jiang J, Koungias P, Lin PH, et al. Molecular mechanisms and clinical applications of nordihydroguaiaretic acid (NDGA) and its derivatives: an update. *Med Sci Monit*. 2010;16(5):RA93-100.
42. Tibes R, McDonagh KT, Lekakis L, Bogenberger JM, Kim S, Frazer N, et al. Phase I study of the novel Cdc2/CDK1 and AKT inhibitor terameprocol in patients with advanced leukemias. *Invest New Drugs*. 2015;33(2):389-96.
43. Lopez RA, Goodman AB, Rhodes M, Blomberg JA, Heller J. The anticancer activity of the transcription inhibitor terameprocol (meso-tetra-O-methyl nordihydroguaiaretic acid) formulated for systemic administration. *Anticancer Drugs*. 2007;18(8):933-9.
44. Grossman SA, Ye X, Peereboom D, Rosenfeld MR, Mikkelsen T, Supko JG, et al. Phase I study of terameprocol in patients with recurrent high-grade glioma. *Neuro Oncol*. 2012;14(4):511-7.
45. Chang CC, Heller JD, Kuo J, Huang RC. Tetra-O-methyl nordihydroguaiaretic acid induces growth arrest and cellular apoptosis by inhibiting Cdc2 and survivin expression. *Proc Natl Acad Sci U S A*. 2004;101(36):13239-44.

46. Mak DH, Schober WD, Chen W, Heller J, Andreeff M, Carter BZ. Tetra-O-methyl nordihydroguaiaretic acid inhibits growth and induces death of leukemia cells independent of Cdc2 and survivin. *Leuk Lymphoma*. 2007;48(4):774-85.
47. Bauer J, Nelde A, Bilich T, Walz JS. Antigen Targets for the Development of Immunotherapies in Leukemia. *Int J Mol Sci*. 2019;20(6).
48. Heller JD, Kuo J, Wu TC, Kast WM, Huang RC. Tetra-O-methyl nordihydroguaiaretic acid induces G2 arrest in mammalian cells and exhibits tumoricidal activity in vivo. *Cancer Res*. 2001;61(14):5499-504.
49. Bernardin-Fried F, Kummalue T, Leijen S, Collector MI, Ravid K, Friedman AD. AML1/RUNX1 increases during G1 to S cell cycle progression independent of cytokine-dependent phosphorylation and induces cyclin D3 gene expression. *J Biol Chem*. 2004;279(15):15678-87.
50. Glembotsky AC, Bluteau D, Espasandin YR, Goette NP, Marta RF, Marin Oyarzun CP, et al. Mechanisms underlying platelet function defect in a pedigree with familial platelet disorder with a predisposition to acute myelogenous leukemia: potential role for candidate RUNX1 targets. *J Thromb Haemost*. 2014;12(5):761-72.
51. Michaud J, Wu F, Osato M, Cottles GM, Yanagida M, Asou N, et al. In vitro analyses of known and novel RUNX1/AML1 mutations in dominant familial platelet disorder with predisposition to acute myelogenous leukemia: implications for mechanisms of pathogenesis. *Blood*. 2002;99(4):1364-72.
52. Stockley J, Morgan NV, Bem D, Lowe GC, Lordkipanidze M, Dawood B, et al. Enrichment of FLI1 and RUNX1 mutations in families with excessive bleeding and platelet dense granule secretion defects. *Blood*. 2013;122(25):4090-3.
53. Mullighan CG, Goorha S, Radtke I, Miller CB, Coustan-Smith E, Dalton JD, et al. Genome-wide analysis of genetic alterations in acute lymphoblastic leukaemia. *Nature*. 2007;446(7137):758-64.

Chapter 3

Additional studies of preleukemic diseases

Chapter 3.1: Determining the role of neutrophil elastase proteolysis in *ELANE*-associated severe congenital neutropenia pathogenesis and normal neutrophil development through iPSC modeling.

3.1.1. Introduction

Roughly 20 years ago, our lab determined that heterozygous mutations in *ELANE*, encoding the potent serine protease, neutrophil elastase (NE), cause cyclic neutropenia (CyN) and are the most common cause of severe congenital neutropenia (SCN) (1, 2). Occasionally attributed to the same genetic mutation, SCN and CyN phenotypes are widely different. In CyN, neutrophil counts dramatically oscillate between normal levels down to nearly zero on a 21-day cycle. Interestingly, monocytes are also found to cycle in CyN but do so reciprocally to neutrophils (3). This effect is believed to stem from the fact that monocytes and neutrophils share the GMP progenitor, and commitment sways between the two cell types as a result of compensating feedback loops. This can also potentially explain monocytosis commonly observed in SCN (4). On the other hand, SCN presentation is marked by profoundly low neutrophil counts accompanied by predisposition to myelodysplasia (MDS) and acute myeloid leukemia (AML). Bone marrow from SCN patients exhibits a block in neutrophil maturation at the promyelocyte stage (5). Notably, *ELANE* expression during granulopoiesis is restricted to a very brief window of neutrophil development in promyelocytes. This fact makes it increasingly difficult to isolate mutant NE-producing cells to assess the pathogenic pathways prior to cell death.

As discussed in chapter 1 of this thesis, although there are several well-supported, yet competing hypotheses regarding pathophysiology, there has been no unifying model to describe SCN or CyN pathogenesis. It is first important to consider that nearly 100 mutations recorded in SCN and CyN and none of these mutations have been found to encompass the three catalytic residues necessary for NE proteolysis, which may suggest retention of these residues is important for SCN and CyN pathology. This is even more significant because full length NE is only 268

residues.

The “mislocation” hypothesis is based on the observation that NE trafficking to granules is frequently disrupted and suggests that damage to the cells is caused by inadequate compartmentalization of an otherwise indiscriminate protease (6-9). It has also been found that some NE mutations can activate ER stress and, in turn, the unfolded protein response (UPR). This observation provides evidence for the “misfolding hypothesis;” whereby mutant NE does not fold properly, and UPR promotes apoptosis (8, 10-12). The “ mistranslation” hypothesis recently presented by our lab states that mutations at or adjacent to the translational start site, and potentially UPR-inducing mutations, may utilize downstream in-frame start sites within *ELANE* to produce short NE peptides that escape trafficking and catalytic regulation (7). Different mutations confer different cellular responses, so although these three hypotheses are inclusive, they do not provide a concrete theory in their reasoning for *ELANE*-associated congenital neutropenia pathogenesis.

Currently the field is divided in NE’s developmental role in granulopoiesis. Although we observe an obvious block in neutrophil maturation in SCN, it is unknown if this response is due to the previously mentioned hypotheses, or if two copies of wild type NE is required to reach neutrophil maturity. Recent studies have shown that WT NE has the ability to degrade not only G-CSF, but G-CSFR as well, both of which are key drivers of neutrophil development (13, 14). Although there is some discussion on post-translational modifications on G-CSF being necessary for immediate degradation (14), these findings indicate a clear connection between NE and granulocytic signaling. With this in mind, it is not outside the realm of possibility that degranulation or apoptosis of developing progenitors possessing mutant NE may influence the normal pathways of granulocyte differentiation resulting in some of the pathological aspects observed in SCN and CyN.

There are a number of endogenous NE inhibitors that act to curb the cytotoxic effects seen with mass degranulation, such as α 1-protease inhibitor, secretory leukocyte protease inhibitor

(SLPI), and other members within the serpin family (15). Interestingly, WT NE has been found to drive *SLPI* expression, SLPI in turn regulates G-CSFR signaling in myeloid progenitors, which we know drives proliferation, differentiation and survival. Interestingly, SCN patients have been found to produce significantly decreased levels of SLPI compared to the normal population which may be explained by mutant NE being unable to perform the necessary molecular mechanisms for normal neutrophil development. (16).

Deficiencies in these endogenous NE inhibitors outside of SCN, particularly with hereditary loss of α 1-protease inhibitor, can result in emphysematous lung disease, due to unchecked NE degradation of elastin and other connective tissues in the lung (16). Considering the prevalence of pulmonary diseases, development of synthetic NE inhibitors has been of great clinical interest. Sivelestat is one such inhibitor, is licensed for use in Japan and has been used in multiple clinical trials for acute lung injury (17); however, due to mixed results it has not been widely accepted as a therapy elsewhere, although it was recently proposed as potential therapy for *ELANE*-associated neutropenia (8). Overall, neutrophil elastase-driven damage can be associated with many different diseases outside of neutropenia, therefore research into modulating catalysis of this robust protease is medically valuable. If *ELANE*-associated SCN (EA-SCN) pathogenesis is found to be dependent on proteolysis, NE inhibitors would theoretically abolish the phenotype without targeting or altering survival, replicative, or differentiation signals as seen with G-CSF.

Animal models unfortunately do not faithfully recapitulate the neutropenic phenotypes seen in patients without harsh drug exposure, making them less than ideal models for studying EA-SCN pathology (18, 19). Additionally, this disease is uncommon and patient sampling requires bone marrow aspiration, a high-risk procedure for the immune deficient. Peripheral blood from patients does not contain many neutrophils, and even upon G-CSF mobilization they are fragile, and past the developmental stage of *ELANE* expression. Utilization of cancer cell lines to study NE pathology have proved valuable for foundational studies but can be inconsistent models of

associated SCN or CyN phenotypes. It is therefore very exciting that our laboratory, as well as others, have recently developed patient-derived iPSC models of *ELANE*-associated neutropenia. Upon *in vitro* myeloid differentiation, SCN-iPSCs reproduce pathological aspects of granulopoiesis, including neutropenia and monocytosis. These cell models can also exhibit aspects of mislocalization, misfolding, and/or mistranslation of NE. These iPSC models have allowed us to study potential disease mechanisms of *ELANE*-associated neutropenia and test the various hypotheses proposed for its pathogenesis (7, 8, 20). Importantly, Nayak et al showed that sivelestat, when used in combination with low G-CSF treatment of SCN-iPSCs during *in vitro* granulocytic differentiation was able to successfully overcome developmental blockade and rescue neutrophil maturation equivalent to 20× the amount of G-CSF alone. This result adds support to the need to explore new approaches to treat SCN due to the growing knowledge that G-CSF therapy has been implicated in malignant transformation, especially in high-risk individuals requiring $\geq 8\mu\text{g}/\text{kg}/\text{d}$ of G-CSF (21).

My specific goals for this project are to develop additional SCN-iPSC models to better observe the molecular effects of mutant *ELANE* expression directly, as well as determine how NE catalysis contributes to neutrophil development and SCN pathogenesis.

3.1.2. Methods

In order to address how NE proteolysis contributes to neutrophil differentiation and SCN pathology I designed and produced four non-viral vectors harboring specific changes within exon five of *ELANE* to be incorporated into a wild type iPSC cell (WTC). Each of these integration vectors either harbored: a particularly severe SCN patient mutation (G214R), a single amino acid substitution at the catalytic serine resulting in NE inactivation (S202A), a combination of the two (S202A-&-G214R), or wild type *ELANE* (WT-*ELANE*). Importantly, all of the integrated *ELANE* variants are co-expressed with a GFP reporter under a gene-trap promoter (Fig 3.1.1). This feature was designed with the intention to capture the minority subpopulation actively expressing NE during *in vitro* differentiation and study the pathogenic effects immediately following mutant

NE production. Additional elements were also added to the integration vectors to assist with selection of positively-integrated clones such as puromycin resistance and red fluorescent protein (RFP). With the exception of the WT-*ELANE* vector, plasmids were synthesized by System Biosciences, transformed into chemically competent *E. coli* for endo-free maxi prep (Qiagen).

Each of these integration vectors underwent paired transfection via GeneJuice (Millipore-Sigma) and subsequent spinoculation with an equal amount (1.25ug) of non-commercial, multi-cystronic plasmid vector expressing the cutter variation of Cas9 enzyme and guide RNA complementary to the fifth exon of *ELANE* near the sites of interest. This system initiated double stranded breaks at the *ELANE* locus, promoted non-homologous recombination, and in turn integration of the vector. Notably, the integration vectors all possessed silent changes at the genomic guide sequence complementary to the guide RNA that facilitates Cas9 cutting, so that Cas9 would not continuously cut at the guide site once integrated. These guide changes, although silent on the protein level, were found to be beneficial in screening potential clones as the guide site is in close proximity to the intended amino acid changes. The cell line used for editing was the Wild Type Control iPSCs (WTC), previously derived in the Conklin laboratory (22), distributed from the Coriell Institute, and gifted by the Ruohola-Baker lab at the University of Washington. On the day of transfection, 1×10^6 versene-passaged single cells were plated onto a 10cm culture plate coated with Matrigel growth factor reduced basement membrane matrix (Corning) in mTeSR media (Stem Cell Technologies) containing transfection reagents. CloneR supplement (Stem Cell Technologies) was added to culture media for the first 48 hours following transfection. Two days after transfection, cells were exposed to 300ng/mL puromycin for 72 hours and allowed to rebound from selection under normal culturing conditions for 4 days. Surviving clones were hand-picked, expanded, and characterized for integration by Sanger sequencing and Southern blot, and screened for detrimental chromosomal changes via karyotype (Fig 3.1.1 and 3.1.2). It is important to note that the clones generated were not expanded from single cells, meaning the cell lines generated may represent an oligoclonal or polyclonal population.

Integration status and later, heterozygosity was first determined by performing unbiased PCR amplification of exon 5 in *ELANE* using the primers shown in Fig 3.1.1 from genomic DNA harvested from the entire cell culture. I then cloned these amplicons into CloneJET vector (Thermo-Fisher) via ligation. Subsequent to bacterial transformation I minipreped and sequenced ~20-50 transformants for genotype and calculated the frequency of vector integrated to wild type sequence to infer heterozygosity. Cells were also monitored visually for stable RFP presence via fluorescence microscopy.

3.1.3. Results

Thus far, I have generated iPSC clones possessing the G214R or S202A changes; both variants have clones that have been characterized as heterozygously or homozygously integrated. The cell line found to harbor a heterozygous G214R SCN mutation (G13-het) via Sanger sequencing was found to also be karyotypically normal (Fig 3.1.3A-B). Heterozygosity testing for clone G13-het presented with 30% WT sequence and 70% vector integrated sequence (n=51), possibly suggesting a mosaic culture, yet Southern blot revealed a clonal population with single integration of the vector at the *ELANE* locus (Fig 3.1.3C-D). Homozygous G214R clone (G9-homo) was found to be karyotypically normal yet Southern blot analysis suggests integration of the vector at unintended sites within the genome, or alternatively a non-clonal cell population (Fig 3.1.3D, 3.1.4). Although not ideal, we have an additional candidate G214R-homozygous clone (G6-homo) that has passed sequencing screening and karyotype but still needs to be tested for multiple integration via Southern blot or ddPCR (Fig 3.1.5). If need be, we can culture the G9-homo cell line in puromycin or perform single cell expansion to see if we can resolve a mixed culture.

I also established a WTC-edited cell line bearing a heterozygous mutation at S202A (S9-het) that was confirmed by Sanger sequencing and that passed karyotype analysis (Fig 3.1.6A-C). Upon heterozygosity testing, transformant sequencing reflected 53% WT *ELANE* and 47% vector integrated *ELANE* (n=19) (Fig 3.1.6D). Characterization via Southern blot displayed single

integration at the *ELANE* locus (Fig 3.1.6E). These results indicate a low probability of a mosaic culture. There are two clone candidates for the homozygous S202A genotype (clones S20-homo and S23-homo). Clone S20-homo has been found to be karyotypically normal (Fig 3.1.7) yet Southern blot doesn't indicate single-site integration (Fig 3.1.6E). This issue could be approached as previously described for polyclonal-presenting G214R clones. Alternatively, clone S23-homo has passed initial genomic screening and karyotype analysis but still needs to be tested for off-target integration via Southern blot or ddPCR (Fig 3.1.8).

3.1.4. Discussion

One of the obvious next steps for this project is to perform genome editing again with the two remaining integration vectors S202A-&-G214R and WT-*ELANE*. Additionally, I will perform the necessary characterization of candidate clones and subject all the cell lines generated to *in vitro* granulocytic differentiation. Monitoring the cells during differentiation for GFP positivity will provide us with the power to conduct fluorescent-activated cell sorting (FACS) to isolate mutant *ELANE* expressing cells. We are interested in using these isolates for RNA-seq to determine changes in gene expression brought on by mutant NE. I will also assess clonal capacity via colony forming unit assays (CFU) and evaluate cell population dynamics via flow cytometry for granulocytic surface markers.

These cell lines allow us the opportunity to investigate how catalytic activity of neutrophil elastase influences neutrophil development and SCN pathology, both questions that are unanswered or under scrutiny in the field. It is also critical to mention that our method of genome editing creates models whereby expression of the mutant protein is detectable through a reporter. This characteristic makes our models superior to other existing iPSC models that have not been able to achieve mutant protein reporting due to direct reprogramming of primary SCN samples. The CRISPR guide site we discovered and tested in exon 5 of *ELANE* will also prove very useful to the field as we have shown that it can successfully target and edit an exon frequently associated with more severe cases of SCN and some of the most common mutations found in CyN.

Additionally, these integration vectors can be easily adapted to harbor any desired changes in exon 4 or 5 of *ELANE*. Lastly, although neither homozygous or S202A mutations in *ELANE* have been observed in normal, SCN, or CyN individuals, these novel cell models will provide us with the tools to determine the interaction between NE proteolysis and granulopoiesis in both normal and diseased states.

3.1.5. Figures

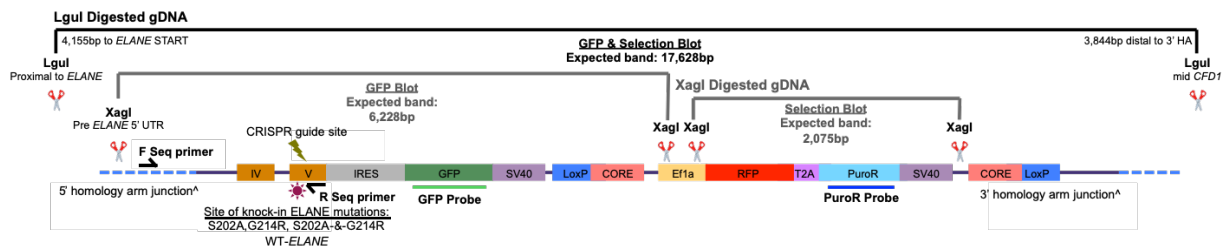


Figure 3.1.1. Schematic of *ELANE* locus after non-viral vector integration and strategies of clone characterization. R seq primer: reverse sequencing primer, F seq primer: forward sequencing primer, PuroR: puromycin resistance.

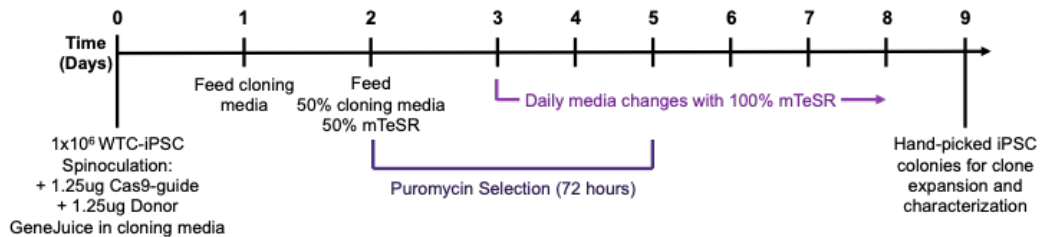


Figure 3.1.2. Transfection protocol and timeline used to generate *ELANE*-edited iPSCs.

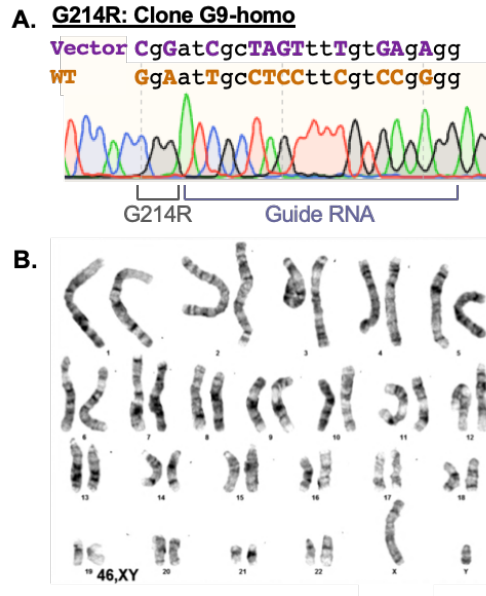


Figure 3.1.4. Characterization of clone G214R-G9-homo. A. Sanger sequencing chromatogram of *ELANE* locus at site of CRISPR editing. B. Karyotype of iPSC clone G9-homo.

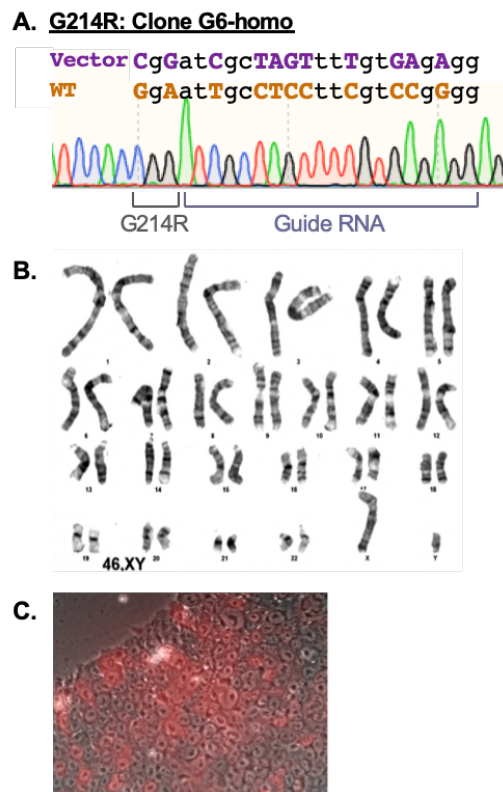
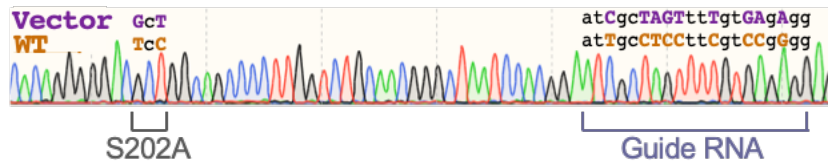
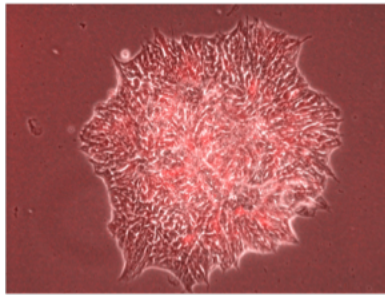


Figure 3.1.5. Characterization of clone G214R-G6-homo. A. Sanger sequencing chromatogram of *ELANE* locus at site of CRISPR editing. B. Karyotype of iPSC clone G6-homo. C. Fluorescence microscopy with Rhodamine merge of clone G6-homo iPSC, magnification 20X.

A. S202A: Clone S23-homo



B.



C.

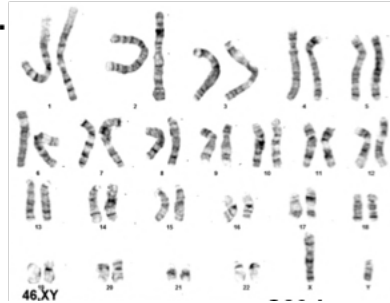


Figure 3.1.8. Characterization of clone S202A-S23-homo. A. Sanger sequencing chromatogram of *ELANE* locus at site of CRISPR editing. B. Karyotype of iPSC clone S23-homo. C. Fluorescence microscopy with Rhodamine merge of clone S23-homo iPSC, magnification 20X.

Chapter 3.2: *SUZ12*: a novel gene implicated in severe congenital neutropenia

3.2.1. Introduction

As discussed in chapter 1.4.4, congenital neutropenia is a genetically heterogeneous disease. Similarly, our lab has contributed to this growing list of genetic factors found causative of neutropenia, the example of *ELANE*-associated neutropenia being the most valuable to the field. In order to expand the current knowledge of neutrophil development and biology it is critical for us to continue the search for novel genes or mutations that produce a neutropenic phenotype. In this chapter I will present evidence that suggests harboring a specific mutation in the gene *SUZ12* can be causative of congenital neutropenia.

Collaborators at Memorial Sloan Kettering Cancer Center (MSKCC) contacted us regarding two unrelated families with neutropenic children bearing the same mutation in the polycomb repressive complex 2 protein *SUZ12*. Kindred 1 (Fig 3.2.1) is a complex case whereby the father (16-6) was asymptomatic, the mother (16-5) presented with intermittent anemia over her lifetime, and the four children presented as either unaffected/unknown presentation (16-1, 16-4) or with severe neutropenia (16-2, 16-3). Proband 16-2, 9 years of age at the time, exhibited with profound neutropenia and reoccurring infections. Upon genetic screening via FoundationOne, a commercial platform for identifying “actional” somatic and germline cancer-associated mutations, the proband was found to harbor a heterozygous variant of unknown significance (VUS) in the gene *SUZ12* (c.2036C>T; p.Thr679Ile; chr17:30325838). This variant exists at a very low allele frequency within the normal population (0.0002059). The amino acid change is located just outside the VES domain, an element involved in the catalytic domain interacting with *EZH2* (23). Interestingly, the patient was also found to be a carrier for Shwachman-Diamond syndrome (SDS), possessing a nonsense mutation in *SBDS* (c.184A>T; p.Lys62*; chr7:66459273). A pancreatic workup and *SBDS* protein analysis via western blot to exclude an occult deletion of one *SBDS* allele resulting in half-normal protein production, helped confirm that the proband was simply a carrier of SDS and this status should

not be causative of her neutropenic state. Significantly, the proband was found to be hyporesponsive to G-CSF therapy. Our curiosity regarding *SUZ12* in SCN was piqued when we were made aware of an additional, unrelated family (kindred 2) whereby monozygotic twins were both found to possess the same *SUZ12* variant of unknown significance. Notably, only one of the twins in kindred 2 presented as neutropenic. These observations by our collaborators laid the groundwork for our studies into how the T679I VUS in *SUZ12* appears to confer congenital neutropenia.

The gene *SUZ12* encodes for a polycomb group protein bearing the same name and is a critical component of polycomb repressive complex 2 (PRC2). Together with its binding partners EZH2, and EED, PRC2 works to repress transcription of genes through di and trimethylation of lysine (K) 27 of histone 3 (H3) to H3K27me2 or 3 (24). These core components of PRC2 are necessary for development, as knockout studies have proved to be embryonic lethal (25, 26). Chromatin remodeling via PRC2 plays an important role in early development as well as lineage commitment. Stem cells specifically rely upon PRC2 to control epigenetic regulation governing differentiation and proliferation, and cells deficient in *SUZ12* display a global loss of H3K27 trimethylation and increased levels of differentiation-specific genes due to lack of silencing machinery (27). Importantly, conditional knockout of *SUZ12* results in failure of hematopoiesis and loss of HSC maintenance (28). These findings highlight the role PRC2 plays in epigenetic-driven development and suggest that altered *SUZ12* function can be associated with hematological pathology.

Although *SUZ12* mutations have not previously been identified as a driver of neutropenia outright, there was a report of an EA-SCN patient that underwent leukemic transformation to AML where their blasts possessed a novel mutation in *SUZ12* among others (29). Myelodysplastic syndromes and myeloproliferative neoplasms have been associated with inactivating-mutations of PRC2 proteins (30-32). Conversely, activating mutations in PRC2 component *EZH2* have been found in multiple cases of B-cell lymphoma (33, 34). Elevated expression of *EZH2* has been found

in cases of hematological malignancies and is associated with a poor prognosis of prostate and breast cancer (35). Overall, there is evidence that revision of polycomb functionality can be oncogenic, yet how these changes can preferentially target specific cell types, in the case of neutrophils for our patients, remains unknown. In order to explore this idea further and gain information of the pathogenesis in the case of our *SUZ12* VUS patients, we acquired primary samples from all members of kindred 1 for genetic analysis and iPSC modeling of the proband.

3.2.2. Methods

Fibroblasts were generated from proband samples at MSKCC through unknown methodology.

Whole blood was obtained from all members of kindred 1. Ficoll separation was performed to isolate peripheral blood mononuclear cells (PBMCs) which were either pelleted and lysed for genomic DNA extraction or frozen in 80% bovine serum albumin (BSA), 20% dimethylsulfoxide (DMSO) and transferred to liquid nitrogen. Genomic DNA was harvested from all family members via DNeasy Blood & Tissue Kit (Qiagen). The proband sample underwent exome sequencing, the hit results of which were used to genotype all other kindred 1 members.

Remaining PBMCs from the proband and her unaffected brother (16-1) were thawed and subjected to the Sendai CytoTune 2.0 reprogramming kit (Life Technologies) under the guidance of the University of Washington Institute for Stem Cell and Regenerative Medicine (ISCRM). This approach of reprogramming uses non-integrating, viral vectors where pluripotency transcription factors *Oct4*, *Sox2*, *Klf4* and *c-Myc* are expressed off of a replicative-deficient strain of Sendai virus, which is eventually diluted out of reprogrammed cells by passaging. Clones were picked, and expanded until the Sendai virus became undetectable via PCR. Established 16-2 clones were then karyotyped, genotyped via Sanger sequencing to confirm exome results, and underwent stem cell characterization via iPSC flow cytometry for stem cell surface markers.

Western blots of undifferentiated 16-2 iPSC clones and 16-2 fibroblasts were performed using *SUZ12* (Cell Signaling Technologies), *EZH2* (Cell Signaling Technologies), *H3K27me3*

(Millipore), and H3 (Cell Signaling Technologies) antibodies at a concentration of 1:1000 for SUZ12 and EZH2 and 1:2,500 for H3K27me3 and H3. All antibodies except SUZ12 were incubated in 5% milk protein in TBST, the later using 5% BSA in the same diluent.

Chromatin immunoprecipitation sequencing (ChIPseq) of undifferentiated iPSCs was performed in the Hawkin's lab at University of Washington using either H3K27me3, H3K4me3 (open, active chromatin), or SUZ12 antibodies for pull down and subsequent sequencing of bound loci and reference alignment. Epigenetic landscape was initially assessed through visual screening of entire chromosomes using the ENCODE-H1-ESC ChIPseq reference track as a control.

Neutrophil differentiation of 16-2 iPSC clones was performed *in vitro* using the protocol described in (8). Viability of cultures was determined by NucleoCounter NC-200 cell counter (chemometec). Colony forming unit assays (Stem Cell Technologies) were seeded after initial flow cytometry assessment for CD34+CD45+ and seeded equally across all clones and control bone marrow isolated CD34+ cells purchased from HemaCare. Cytospin with Wright-Giemsa staining was prepared following colony forming unit assays and analyzed for morphology by a licensed pathologist.

3.2.3. Results

Genotype results of all members in kindred 1 at *SUZ12* and *SBDS* loci are summarized in Fig 3.2.1. Unfortunately, there was no genotype-phenotype correlation with the SDS carrier status or *SUZ12* VUS.

Reprogramming efforts for 16-1 proved unsuccessful. Proband 16-2 reprogramming was found to be successful yielding three clones after expansion and characterization: C-1, C-2, C-3. All three 16-2 clones were found to be karyotypically normal and retain the *SUZ12* variant first evident in exome sequencing (Fig 3.2.2). These clones also presented with bonafide stem cell markers Tra1-81, SSEA-4, and SSEA-3 via flow cytometry after confirmed loss of Sendai reprogramming factors (Fig 3.2.2, 3.2.3). It is important to note that 12 additional proband iPSC

clones were generated during reprogramming. However, these clones were found to retain robust Sendai-specific pluripotency factor expression far past the expected passage of clearance. These results may suggest that the pluripotency of these *SUZ12* variant clones was dependent on transgene expression and could not achieve full reprogramming due to altered *SUZ12* function.

Endogenous protein levels of *SUZ12*, *EZH2*, *H3K27me3* and *H3* in patient-derived fibroblasts were all reduced in comparison to wild type fibroblasts with the exception of *H3*, which was used as an internal control (Fig 3.2.4A). The same protein analysis on 16-2 iPSC clones did not show any change in *SUZ12* levels, yet decreased *EZH2* and global *H3K27me3* was evident (Fig 3.2.4B). The decrease in *EZH2* protein may suggest altered binding potential of the PRC2 complex but requires further study. The remarkable change in global *H3K27me3* was consistent between 16-2 clones which prompted us to evaluate the epigenetic landscape of the undifferentiated iPSC clones via ChIPseq for *SUZ12*, repressive marker *H3K27me3*, and activation marker *H3K4me3*.

Clone C-3 was used for preliminary ChIPseq tests, results from clones C-1 and C-2 are still under review. The overall chromosomal trends observed in C-3 compared to wild type iPSC were: decrease in *H3K27me3* levels, increased amount of *H3K4me3* signal, and minor differences in *SUZ12* binding sites (Fig 3.2.5). This data supports the results observed in western blots and further suggests that the *SUZ12* VUS alters normal epigenetic regulation.

Hematopoietic differentiation studies revealed no significant change in hematopoietic progenitor (HP) viability generated from 16-2 iPSC clones compared to WT iPSCs (n=4) (Fig 3.2.6A). There was however a significant and near-significant decrease in CD34+CD45+ hematopoietic progenitor frequency derived from 16-2 iPSC clones C-3 and C-2 respectively (P=0.02, 0.06 respectively, n=4) (Fig 3.2.6B). Myeloid commitment defined by CD33 surface marker positivity on HPs revealed that although not significant, 16-2 clones tended to produce less myeloid-committed cells (n=2) (Fig 3.2.6C).

At the time of studies, granulocyte differentiation of hematopoietic progenitors was low efficiency and flow cytometry of neutrophil progenitors needed to be optimized, therefore we utilized a colony forming unit (CFU) assay to evaluate 16-2 neutrophil commitment and maturation (Fig 3.2.7). Results indicate *SUZ12-VUS* clone C-1 produced significantly less erythroid colonies (BFU-E) compared to wild type bone marrow (BM) control ($P=0.026$, $n=2$). Additionally, 16-2 clone C-3 generated significantly more monocyte colonies (CFU-M) as well as granulocyte-monocyte mixed colonies (CFU-GM) relative to control BM ($P=0.009$, 0.015 respectively, $n=2$). It is important to note that although *SUZ12-VUS* clones did not present with a difference in granulocytic colony (CFU-G) production compared to BM, there appears to be a decrease of output compared to WT iPSCs ($n=1$). Notably, although I performed four hematopoietic differentiations, the 16-2 clone C-2 never produced enough CD34+CD45+ hematopoietic progenitors to seed for a successful CFU assay. Considering CFU-G represents all granulocytes, I isolated cell plugs from granulocyte CFUs of WT iPSCs and *SUZ12-VUS* clones and identified the cell types present (Fig 3.2.8). Cytospin preparation and Wright-Giemsa staining of cells recovered showed WT iPSCs primarily produced neutrophils at various stages of maturation ($n=2$) while the CFU-G harvested from C-1 was almost entirely basophils. Clone C-3 displayed various granulocytes with neutrophils at multiple stages of maturation ($n=1$). This is an especially interesting observation as it allows us to point to overall differences in lineage commitment where 16-2 clones lean towards monocyte over granulocyte development, as well as how neutrophils specifically may have compromised maturation.

3.2.4. Discussion

This project provides evidence to imply that a T679I residue change in *SUZ12* is causative of SCN. I have established multiple *SUZ12-VUS* iPSC clones from one individual that upon initial studies produce phenotypes suggestive of deficient hematopoiesis and potential granulocytic failure. More studies need to be performed on the 16-2 fibroblast and iPSC lines, as well as other kindred 1 family members to elucidate the molecular mechanisms of how altered *SUZ12* protein

influences hematopoietic commitment. The apparent decrease in global H3K27me3 in undifferentiated iPSCs is also of great interest to us. It is however important to consider that the WT iPSC line used as a control was not reprogrammed with the same methodology. With this in mind we are open to generating or using new, wild type lines that have since been reprogrammed similarly.

A limitation of these studies was the inability to obtain additional clinical information on individuals harboring this genetic variant because they were lost to follow-up. Nevertheless, we believe that the available clinical and experimental data suggest that the *SUZ12* variant may be contributing to neutropenia but remains unproven until additional families with variants in the PRC2 complex are found who demonstrate similar clinical phenotypes. We are especially curious to test the iPSC models for G-CSF hyporesponsiveness seen in the proband. By performing neutrophil differentiations under G-CSF or a lesser potent cytokine driver of granulopoiesis, granulocyte-monocyte colony stimulating factor (GM-CSF), we can determine if clones recapitulate the patient phenotype. The molecular mechanisms of G-CSF hyporesponsiveness may also be revealed through epigenetic mapping via ChIPseq analysis of developing HSC progenitors at the G-CSF locus. Since beginning this project we have successfully established multiple methods of granulocytic differentiation, therefore we aim to conduct neutrophil enrichment subsequent to HSC differentiation and flow cytometry for neutrophil surface markers to see if results complement the CFU plug data already generated.

One aspect that truly highlights the influence of epigenetic remodeling in hematopoiesis for the *SUZ12*-VUS is that the monozygotic twins in kindred 2 presented differently although they both harbor the same variant. For this reason, I worked to establish three 16-2 iPSC clones just in case epigenetic memory or subpopulations within circulation possessed different capacities for proliferation or differentiation. Unfortunately, members of kindred 2 did not consent to research studies, however we believe this observation supports our theory that *SUZ12*-VUS T679I can confer severe congenital neutropenia due to altered epigenetic machinery and/or landscape.

3.2.5. Figures

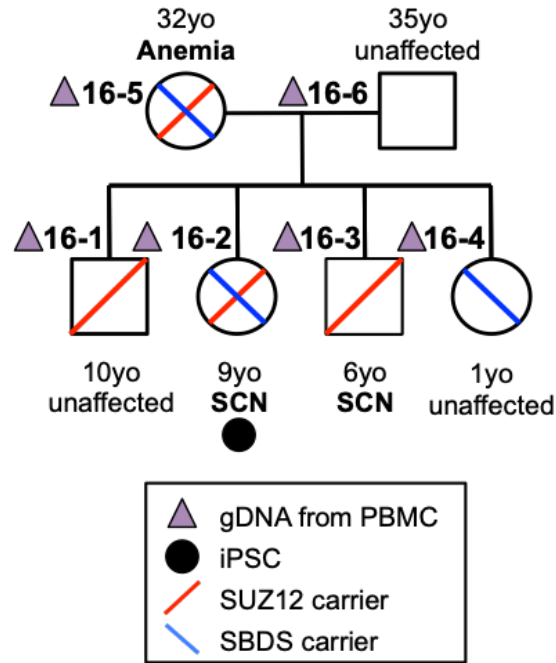


Figure 3.2.1. Kindred 1 pedigree denoting patient presentations and genotype. iPSC: induced pluripotent stem cell, SCN: severe congenital neutropenia, yo: years old.

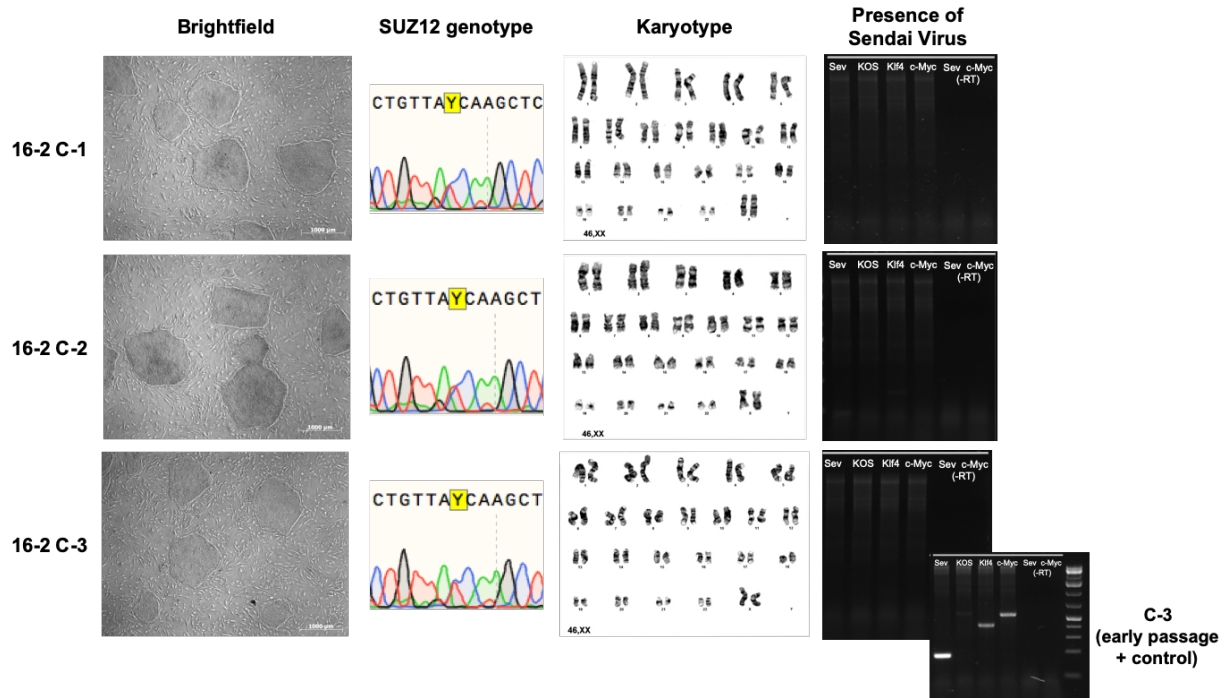


Figure 3.2.2. Patient 16-2 iPSC clone characterization.

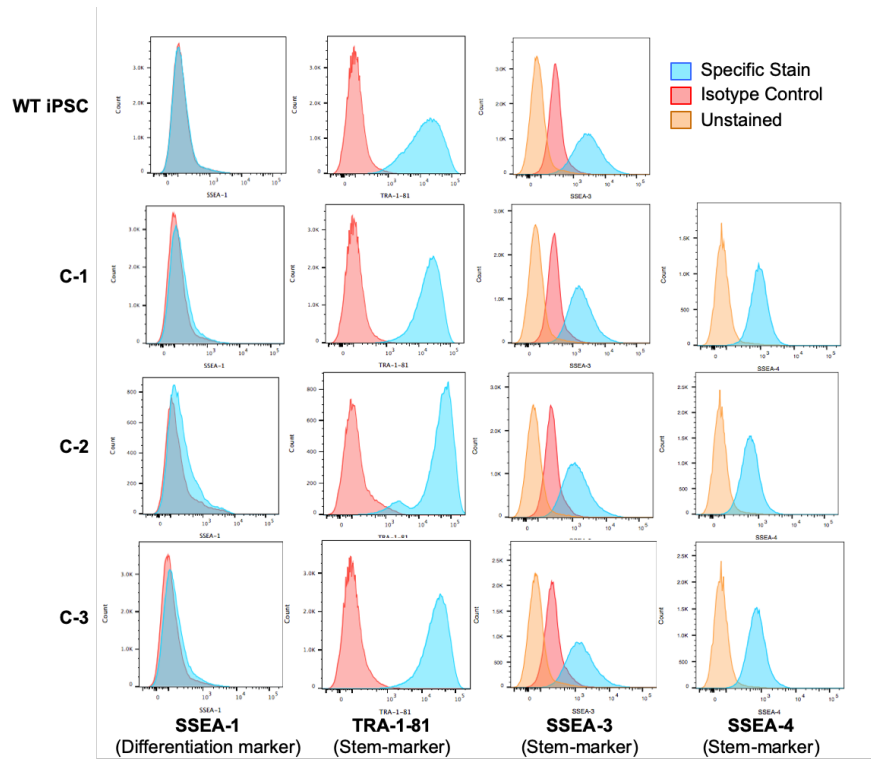


Figure 3.2.3. Flow cytometry results of 16-2 iPSC clones C-1, C-2, C-3 to assess surface markers indicative of stem cell identity and differentiation.

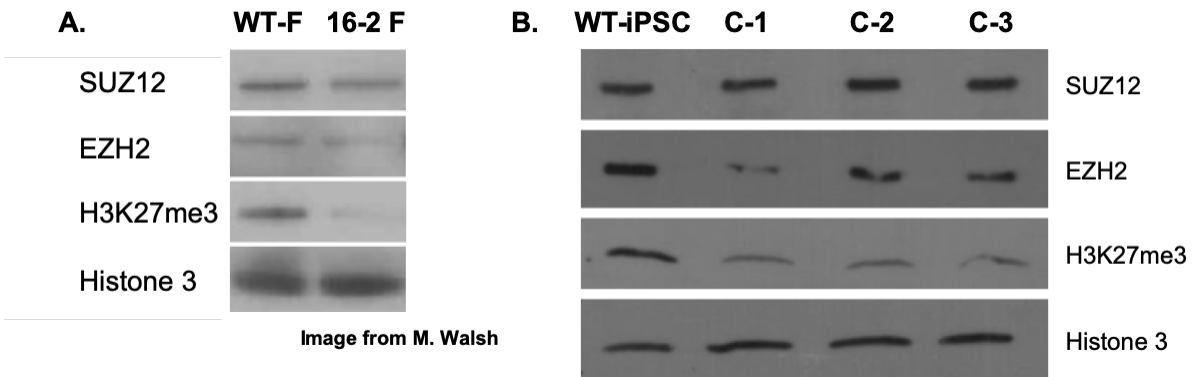


Figure 3.2.4. Western blot of 16-2 PRC2 protein components and epigenetic markers. A. Western blot of wild type control fibroblasts and patient 16-2-derived fibroblasts. **B.** Endogenous levels of SUZ12, EZH2, H3K27me3 and H3K4me3 protein in undifferentiated iPSC clones C-1-3 and wild type iPSC.

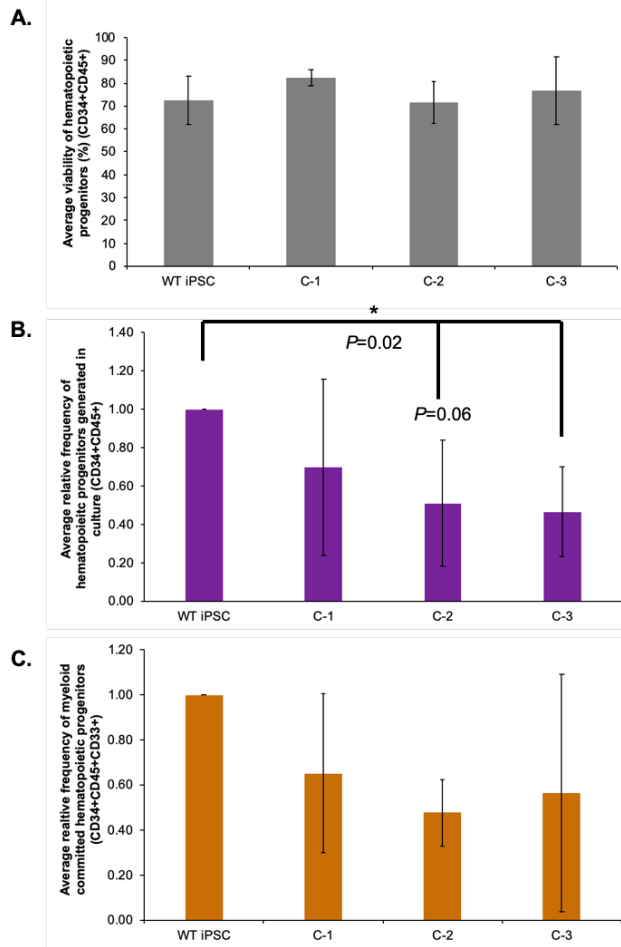


Figure 3.2.6. *In vitro* hematopoietic differentiation of 16-2 iPSC clones. A. Average viability of CD34+CD45+ hematopoietic progenitors derived from WT and 16-2 iPSC clones. B. Average frequency of CD34+CD45+ hematopoietic progenitors generated in differentiation relative to WT iPSC control (n=4). C. Average relative frequency of CD34+CD45+CD33+ myeloid progenitors produced in culture compared to WT iPSC. Error bars represent standard deviation, *=p<0.05.

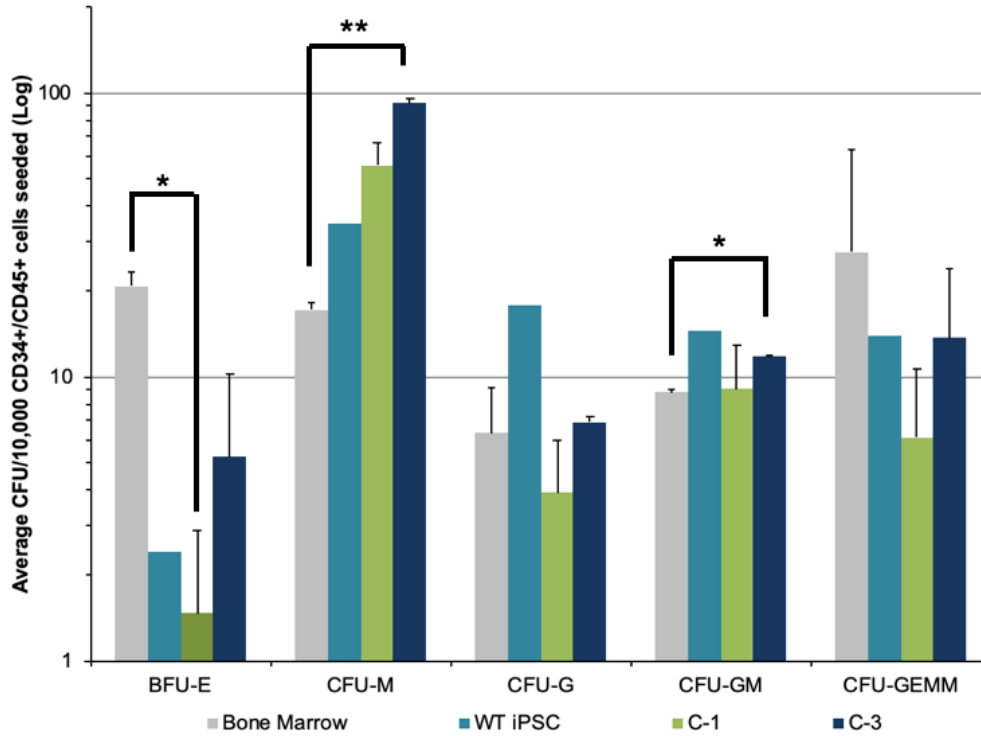


Figure 3.2.7. Colony forming unit assay of 16-2 iPSCs and control samples. BFU-E: blast forming unit-erythrocyte, CFU-M: monocyte colony, CFU-G: granulocyte colony, CFU-GM: granulocyte and monocyte mixed colony, CFU-GEMM: granulocyte, erythroid, monocyte and megakaryocyte mixed colony. Error bars represent standard deviation. *= $p < 0.05$, **= $p < 0.01$.

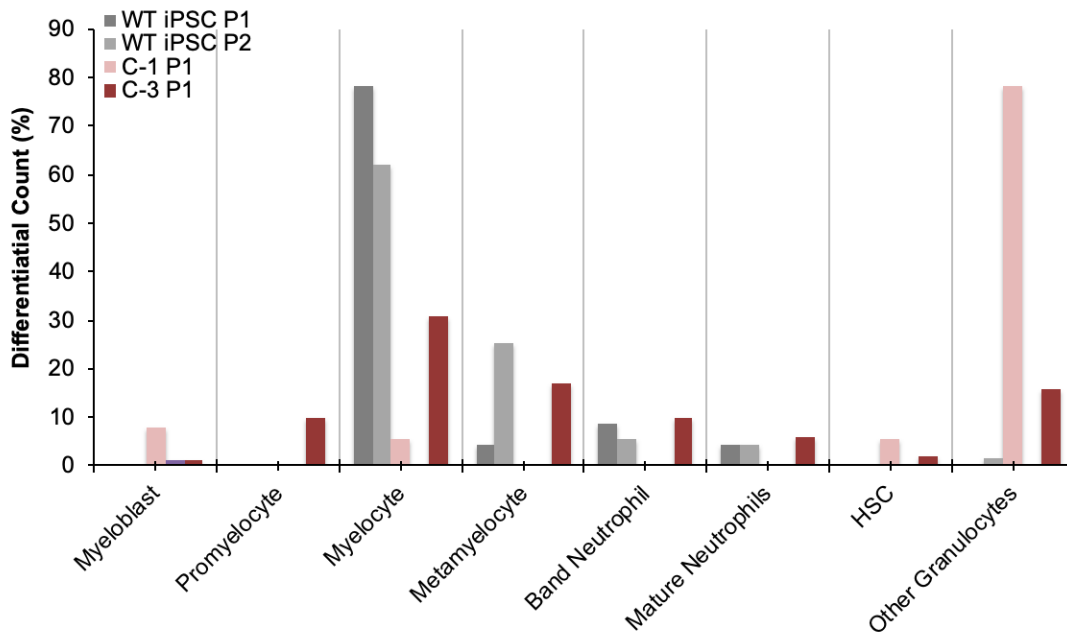


Figure 3.2.8. Quantitative analysis of cell types present in CFU-G plugs. P: plug.

3.3. References

1. Horwitz M, Benson KF, Person RE, Aprikyan AG, Dale DC. Mutations in ELA2, encoding neutrophil elastase, define a 21-day biological clock in cyclic haematopoiesis. *Nat Genet.* 1999;23(4):433-6.
2. Dale DC, Person RE, Bolyard AA, Aprikyan AG, Bos C, Bonilla MA, et al. Mutations in the gene encoding neutrophil elastase in congenital and cyclic neutropenia. *Blood.* 2000;96(7):2317-22.
3. Guerry Dt, Dale DC, Omine M, Perry S, Wolff SM. Periodic hematopoiesis in human cyclic neutropenia. *J Clin Invest.* 1973;52(12):3220-30.
4. Meuret G, Fliedner TM. Neutrophil and monocyte kinetics in a case of cyclic neutropenia. *Blood.* 1974;43(4):565-71.
5. Berliner N. Lessons from congenital neutropenia: 50 years of progress in understanding myelopoiesis. *Blood.* 2008;111(12):5427-32.
6. Salipante SJ, Rojas ME, Korkmaz B, Duan Z, Wechsler J, Benson KF, et al. Contributions to neutropenia from PFAAP5 (N4BP2L2), a novel protein mediating transcriptional repressor cooperation between Gfi1 and neutrophil elastase. *Mol Cell Biol.* 2009;29(16):4394-405.
7. Tidwell T, Wechsler J, Nayak RC, Trump L, Salipante SJ, Cheng JC, et al. Neutropenia-associated ELANE mutations disrupting translation initiation produce novel neutrophil elastase isoforms. *Blood.* 2014;123(4):562-9.
8. Nayak RC, Trump LR, Aronow BJ, Myers K, Mehta P, Kalfa T, et al. Pathogenesis of ELANE-mutant severe neutropenia revealed by induced pluripotent stem cells. *J Clin Invest.* 2015;125(8):3103-16.
9. Massullo P, Druhan LJ, Bunnell BA, Hunter MG, Robinson JM, Marsh CB, et al. Aberrant subcellular targeting of the G185R neutrophil elastase mutant associated with severe congenital neutropenia induces premature apoptosis of differentiating promyelocytes. *Blood.* 2005;105(9):3397-404.
10. Grenda DS, Murakami M, Ghatak J, Xia J, Boxer LA, Dale D, et al. Mutations of the ELA2 gene found in patients with severe congenital neutropenia induce the unfolded protein response and cellular apoptosis. *Blood.* 2007;110(13):4179-87.
11. Xia J, Link DC. Severe congenital neutropenia and the unfolded protein response. *Curr Opin Hematol.* 2008;15(1):1-7.
12. Kollner I, Sodeik B, Schreek S, Heyn H, von Neuhoff N, Germeshausen M, et al. Mutations in neutrophil elastase causing congenital neutropenia lead to cytoplasmic protein accumulation and induction of the unfolded protein response. *Blood.* 2006;108(2):493-500.
13. El Ouriaghli F, Fujiwara H, Melenhorst JJ, Sconocchia G, Hensel N, Barrett AJ. Neutrophil elastase enzymatically antagonizes the in vitro action of G-CSF: implications for the regulation of granulopoiesis. *Blood.* 2003;101(5):1752-8.
14. Piper MG, Massullo PR, Loveland M, Druhan LJ, Kindwall-Keller TL, Ai J, et al. Neutrophil elastase downmodulates native G-CSFR expression and granulocyte-macrophage colony formation. *J Inflamm (Lond).* 2010;7(1):5.
15. Thusberg J, Vihinen M. Bioinformatic analysis of protein structure-function relationships: case study of leukocyte elastase (ELA2) missense mutations. *Hum Mutat.* 2006;27(12):1230-43.

16. Klimenkova O, Ellerbeck W, Klimiankou M, Unalan M, Kandabarau S, Gigina A, et al. A lack of secretory leukocyte protease inhibitor (SLPI) causes defects in granulocytic differentiation. *Blood*. 2014;123(8):1239-49.
17. Aikawa N, Kawasaki Y. Clinical utility of the neutrophil elastase inhibitor sivelestat for the treatment of acute respiratory distress syndrome. *Ther Clin Risk Manag*. 2014;10:621-9.
18. Grenda DS, Johnson SE, Mayer JR, McLemore ML, Benson KF, Horwitz M, et al. Mice expressing a neutrophil elastase mutation derived from patients with severe congenital neutropenia have normal granulopoiesis. *Blood*. 2002;100(9):3221-8.
19. Nanua S, Murakami M, Xia J, Grenda DS, Woloszynek J, Strand M, et al. Activation of the unfolded protein response is associated with impaired granulopoiesis in transgenic mice expressing mutant Elane. *Blood*. 2011;117(13):3539-47.
20. Dannenmann B, Zahabi A, Mir P, Oswald B, Bernhard R, Klimiankou M, et al. Human iPSC-based model of severe congenital neutropenia reveals elevated UPR and DNA damage in CD34(+) cells preceding leukemic transformation. *Exp Hematol*. 2019;71:51-60.
21. Rosenberg PS, Alter BP, Bolyard AA, Bonilla MA, Boxer LA, Cham B, et al. The incidence of leukemia and mortality from sepsis in patients with severe congenital neutropenia receiving long-term G-CSF therapy. *Blood*. 2006;107(12):4628-35.
22. Kreitzer FR, Salomonis N, Sheehan A, Huang M, Park JS, Spindler MJ, et al. A robust method to derive functional neural crest cells from human pluripotent stem cells. *Am J Stem Cells*. 2013;2(2):119-31.
23. Jiao L, Liu X. Structural basis of histone H3K27 trimethylation by an active polycomb repressive complex 2. *Science*. 2015;350(6258):aac4383.
24. Cao R, Zhang Y. SUZ12 is required for both the histone methyltransferase activity and the silencing function of the EED-EZH2 complex. *Mol Cell*. 2004;15(1):57-67.
25. Faust C, Lawson KA, Schork NJ, Thiel B, Magnuson T. The Polycomb-group gene *eed* is required for normal morphogenetic movements during gastrulation in the mouse embryo. *Development*. 1998;125(22):4495-506.
26. O'Carroll D, Erhardt S, Pagani M, Barton SC, Surani MA, Jenuwein T. The polycomb-group gene *Ezh2* is required for early mouse development. *Mol Cell Biol*. 2001;21(13):4330-6.
27. Pasini D, Bracken AP, Jensen MR, Lazzarini Denchi E, Helin K. Suz12 is essential for mouse development and for EZH2 histone methyltransferase activity. *EMBO J*. 2004;23(20):4061-71.
28. Lee SC, Miller S, Hyland C, Kauppi M, Lebois M, Di Rago L, et al. Polycomb repressive complex 2 component Suz12 is required for hematopoietic stem cell function and lymphopoiesis. *Blood*. 2015;126(2):167-75.
29. Beekman R, Valkhof MG, Sanders MA, van Strien PM, Haanstra JR, Broeders L, et al. Sequential gain of mutations in severe congenital neutropenia progressing to acute myeloid leukemia. *Blood*. 2012;119(22):5071-7.
30. Score J, Hidalgo-Curtis C, Jones AV, Winkelmann N, Skinner A, Ward D, et al. Inactivation of polycomb repressive complex 2 components in myeloproliferative and myelodysplastic/myeloproliferative neoplasms. *Blood*. 2012;119(5):1208-13.
31. Ernst T, Chase AJ, Score J, Hidalgo-Curtis CE, Bryant C, Jones AV, et al. Inactivating mutations of the histone methyltransferase gene *EZH2* in myeloid disorders. *Nat Genet*. 2010;42(8):722-6.

32. Nikoloski G, Langemeijer SM, Kuiper RP, Knops R, Massop M, Tonnissen ER, et al. Somatic mutations of the histone methyltransferase gene EZH2 in myelodysplastic syndromes. *Nat Genet.* 2010;42(8):665-7.
33. Morin RD, Johnson NA, Severson TM, Mungall AJ, An J, Goya R, et al. Somatic mutations altering EZH2 (Tyr641) in follicular and diffuse large B-cell lymphomas of germinal-center origin. *Nat Genet.* 2010;42(2):181-5.
34. Sneeringer CJ, Scott MP, Kuntz KW, Knutson SK, Pollock RM, Richon VM, et al. Coordinated activities of wild-type plus mutant EZH2 drive tumor-associated hypertrimethylation of lysine 27 on histone H3 (H3K27) in human B-cell lymphomas. *Proc Natl Acad Sci U S A.* 2010;107(49):20980-5.
35. Sparmann A, van Lohuizen M. Polycomb silencers control cell fate, development and cancer. *Nat Rev Cancer.* 2006;6(11):846-56.

Chapter 4

Conclusions, broader impacts, and future directions

Chapter 4.1. Closing remarks

My graduate work has broadly contributed to the field of preleukemia in multiple aspects. I have worked to evaluate novel therapeutic strategies in the case of FPD/AML. Additionally, I have generated new cell models to study neutrophil development and *ELANE*-associated congenital neutropenia pathogenesis. Lastly, I have begun work to characterize a previously undescribed variant of unknown significance in the *SUZ12* gene, that we believe to be causative of congenital neutropenia. These approaches and findings align with the Department of Pathology at The University of Washington's goals to understand the underpinnings of disease by way of drug discovery, disease modeling, and identification of genetic influences with the overarching aim to advance translational medicine.

By utilizing drugs that target pathways of protein degradation, more specifically the ubiquitin-proteasome pathway, we were able to boost levels of *RUNX1* transcript and protein in both cancer cell models, and primary models of FPD. Due to the auto-activation dynamics of *RUNX1* protein, literature suggests that even a small, brief increase in expression can restore to protein to near steady-state levels (1). Similar effects were observed through transient expression of exogenous *RUNX1*, yet this strategy would require strict observation in the case of gene therapy, as sustained over-expression of *RUNX1* is implicated in cancer (2, 3). Alternatively, targeted repair of the mutated locus *ex vivo* then reinfusion of the patient's edited HSCs is a potential curative approach. In addition, temporary exposure of FPD HSCs to proteasome or CDK inhibitors *ex vivo* prior to reinfusion may be a powerful method to rescue the *RUNX1* auto-feedback loop and subsequent downstream target expression without the cytotoxic effects commonly seen in cancer patients (4). With this in mind, it is critical to consider the other cellular functions dependent on proteasome function such as mitochondrial processes, regulating cell cycle and apoptosis, and importantly, immune regulation by way of NF- κ B prior to frequent dosing

of these drugs (5, 6). Thorough genetic screening must also be performed before structuring a care plan for FPD patients, as a small proportion of individuals harbor dominant-negative mutations in *RUNX1*, that our proposed paradigm would not be beneficial. With these factors in mind, we must appreciate that there are no current therapies available for FPD patients, except for allogeneic hematopoietic stem cell transplant. Our proposed strategy could influence *RUNX1* levels to not only restore megakaryocyte development and platelet production in turn rescuing thrombocytopenia but relieve the pressure for cells to acquire driver mutations in order to compensate for poor survival and proliferation, therefore preventing or forestalling the onset of leukemic transformation.

The lessons learned from our studies of familial platelet disorder with predisposition to myeloid malignancy reach farther than the case of FPD. Other forms of preleukemic diseases may benefit from a similar therapeutic system, specifically in the case of *GATA2* deficiency. As discussed in chapter 1.4.5, *GATA2* deficiency arises from heterozygous mutations in *GATA2*, a short-lived, auto-activating transcription factor required for proper hematopoiesis (7, 8). Also utilizing the ubiquitin-proteasome pathway of protein degradation, haploinsufficiency of *GATA2* would be a clinically translatable model to test or validate our therapeutic potential of these drugs. Proteasome and CDK inhibitors have been approved for use in multiple cancer types, including multiple myeloma; however they have not, to our knowledge, been used in the case of treating haploinsufficiency (4, 5). In fact, a common thread in pathology of hematopoietic cancers is haploinsufficiency of key transcriptional regulators, echoed in the case of B-cell acute leukemia attributed to loss of function mutations in *PAX5* (9, 10). Other non-malignant, hereditary disorders are also caused by haploinsufficiency, such as Marfan syndrome (*FBN1*) and cleidocranial dysostosis (*RUNX2*) (11, 12).

Regarding the work I performed to generate new models to evaluate pathogenic mechanisms of *ELANE*-associated neutropenia, we have established cell lines and protocols which act as the foundation for further studies. Although we are not the first group to suggest a

role of neutrophil elastase catalysis in SCN pathology (13-15), we are the first group to our knowledge to create novel iPSC lines harboring knock-in variants in the *ELANE* locus to assess exactly how NE proteolysis impacts neutrophil development. These models are unique in that they employ a gene-trap strategy to report endogenous *ELANE* variant expression. This is a powerful tool we can use to monitor neutrophil differentiation and development, as well as provide us with the ability to isolate the mutant-expressing promyelocyte population for further studies.

Serine protease inhibitors in general, have been used as therapies for various diseases for many years (16, 17). As described earlier, neutrophil elastase inhibitors are frequently used in the case of inflammatory pulmonary disorders like cystic fibrosis and chronic obstructive pulmonary disease due to mass degranulation of neutrophils at the sites of inflammation and injury (18-20). Recent studies have also highlighted the role of neutrophil elastase catalysis in chronic kidney disease, autoimmunity, and cancer (21, 22). Although there are many endogenous NE inhibitors and rationally designed small molecular inhibitors, one area of developing interest is the use of neutralizing antibodies to mediate proteolysis (23). Based off of the theorized molecular mechanisms of *ELANE*-associated congenital neutropenia, and paired studies employing sivelestat in previous SCN iPSC models, we are confident that our new cell models will allow us the power to fully evaluate how endogenously expressed, inactive NE impacts neutrophil differentiation, development and SCN pathology.

When considering the effects of catalytic neutralization in neutrophil development, we look to the primary granule protein azurocidin. Classified as an inactive paralog of serine proteases, the catalytic serine and histidine residues of this protein have been replaced over time making it a 'sterile enzyme' (24). Localized in the same genomic region as *ELANE*, the gene *AZU1* has undergone substantial changes ablating proteolysis yet still retains antimicrobial activity through unknown mechanisms (25). For these reasons azurocidin provides traction for inactivating neutrophil elastase catalysis without completely losing functional, immune-mediated capabilities.

With the growing knowledge that G-CSF therapy has been implicated in malignant transformation, alternative therapeutic avenues should be considered for SCN. If pathogenesis is found to be dependent upon proteolysis, NE inhibitors would theoretically abolish the SCN phenotype without targeting or altering survival, replicative, or differentiation signals as seen with G-CSF. Additionally, some SCN patients are found to be hyperresponsive or resistant to G-CSF therapy, either overcompensating with rapid expansion of the granulocytic compartment resulting in hypercellular bone marrow, or requiring large doses of G-CSF to restore neutrophil numbers with resulting selective pressure on the marrow to undergo malignant transformation, respectively (26, 27). These patients specifically would benefit the most from alternative therapies and impel the field to consider an inhibitory mechanism to resolve neutrophil elastase pathogenesis.

Lastly, my work characterizing a novel variant of unknown significance (T679I) in *SUZ12* has provided insights into how epigenetic regulation impacts neutrophil development. Although SCN is known to be a genetically heterogenous disease, none of the affected genes cataloged thus far have been associated with epigenetic mechanisms. This is an area of great interest to the field as there have been many new technologies to map epigenetic fate of developing hematopoietic cells as well as how epigenetic alterations can prompt premalignancy (reviewed in (28)). By using previously published reports of epigenetic regulation of stem cells and neutrophils I aim to determine how the *SUZ12* VUS effects not only the stem cell epigenetic landscape, indicated by our preliminary H3K27me3 western blots of undifferentiated 16-2 iPSC clones, but HSCs and neutrophil precursors as well (29, 30). Although iPSCs are obviously a different cell type than post-mitotic neutrophils, it is important to consider the impact of epigenetic memory in these models. The 16-2 iPSC clones generated from reprogramming may harbor residual epigenetic markers that were once present in somatic samples used for reprogramming, which may describe the dramatic reduction of H3K27me3 retained in *SUZ12* VUS clones compared to WT iPSCs (31). Considering our lab has contributed greatly to the list of SCN-associated genes

over the years, I am excited to test these models further to determine the specific mechanisms leading to faulty neutrophil development due to the *SUZ12* VUS.

Overall, my graduate studies yielded outcomes that further expand the wealth of knowledge in the field of molecular genetics in preleukemic diseases. My findings also provide evidence of FPD and SCN disease pathogenesis, which can inform new therapeutic approaches for treatment.

4.2. References

1. Horwitz M. Hypermethylated myoblasts specifically deficient in MyoD autoactivation as a consequence of instability of MyoD. *Exp Cell Res.* 1996;226(1):170-82.
2. Fu L, Fu H, Tian L, Xu K, Hu K, Wang J, et al. High expression of RUNX1 is associated with poorer outcomes in cytogenetically normal acute myeloid leukemia. *Oncotarget.* 2016;7(13):15828-39.
3. Sun CC, Li SJ, Chen ZL, Li G, Zhang Q, Li DJ. Expression and Prognosis Analyses of Runt-Related Transcription Factor Family in Human Leukemia. *Mol Ther Oncolytics.* 2019;12:103-11.
4. Chauhan D, Anderson KC. Proteasome inhibition, the pursuit of new cancer therapeutics, and the adaptor molecule p130Cas. *BMC Biol.* 2011;9:72.
5. Thibaudeau TA, Smith DM. A Practical Review of Proteasome Pharmacology. *Pharmacol Rev.* 2019;71(2):170-97.
6. Lecker SH, Goldberg AL, Mitch WE. Protein degradation by the ubiquitin-proteasome pathway in normal and disease states. *J Am Soc Nephrol.* 2006;17(7):1807-19.
7. Minegishi N, Suzuki N, Kawatani Y, Shimizu R, Yamamoto M. Rapid turnover of GATA-2 via ubiquitin-proteasome protein degradation pathway. *Genes Cells.* 2005;10(7):693-704.
8. Nakajima T, Kitagawa K, Ohhata T, Sakai S, Uchida C, Shibata K, et al. Regulation of GATA-binding protein 2 levels via ubiquitin-dependent degradation by Fbw7: involvement of cyclin B-cyclin-dependent kinase 1-mediated phosphorylation of THR176 in GATA-binding protein 2. *J Biol Chem.* 2015;290(16):10368-81.
9. Mullighan CG, Goorha S, Radtke I, Miller CB, Coustan-Smith E, Dalton JD, et al. Genome-wide analysis of genetic alterations in acute lymphoblastic leukaemia. *Nature.* 2007;446(7137):758-64.
10. Shah S, Schrader KA, Waanders E, Timms AE, Vijai J, Miething C, et al. A recurrent germline PAX5 mutation confers susceptibility to pre-B cell acute lymphoblastic leukemia. *Nat Genet.* 2013;45(10):1226-31.
11. Pepe G, Giusti B, Sticchi E, Abbate R, Gensini GF, Nistri S. Marfan syndrome: current perspectives. *Appl Clin Genet.* 2016;9:55-65.
12. Farrow E, Nicot R, Wiss A, Laborde A, Ferri J. Cleidocranial Dysplasia: A Review of Clinical, Radiological, Genetic Implications and a Guidelines Proposal. *J Craniofac Surg.* 2018;29(2):382-9.

13. Korkmaz B, Horwitz MS, Jenne DE, Gauthier F. Neutrophil elastase, proteinase 3, and cathepsin G as therapeutic targets in human diseases. *Pharmacol Rev.* 2010;62(4):726-59.
14. Nayak RC, Trump LR, Aronow BJ, Myers K, Mehta P, Kalfa T, et al. Pathogenesis of ELANE-mutant severe neutropenia revealed by induced pluripotent stem cells. *J Clin Invest.* 2015;125(8):3103-16.
15. Makaryan V, Kelley ML, Fletcher B, Bolyard AA, Aprikyan AA, Dale DC. Elastase inhibitors as potential therapies for ELANE-associated neutropenia. *J Leukoc Biol.* 2017;102(4):1143-51.
16. Walker B, Lynas JF. Strategies for the inhibition of serine proteases. *Cell Mol Life Sci.* 2001;58(4):596-624.
17. Patel S. A critical review on serine protease: Key immune manipulator and pathology mediator. *Allergol Immunopathol (Madr).* 2017;45(6):579-91.
18. Groutas WC, Dou D, Alliston KR. Neutrophil elastase inhibitors. *Expert Opin Ther Pat.* 2011;21(3):339-54.
19. Polverino E, Rosales-Mayor E, Dale GE, Dembowsky K, Torres A. The Role of Neutrophil Elastase Inhibitors in Lung Diseases. *Chest.* 2017;152(2):249-62.
20. Heutinck KM, ten Berge IJ, Hack CE, Hamann J, Rowshani AT. Serine proteases of the human immune system in health and disease. *Mol Immunol.* 2010;47(11-12):1943-55.
21. Bronze-da-Rocha E, Santos-Silva A. Neutrophil Elastase Inhibitors and Chronic Kidney Disease. *Int J Biol Sci.* 2018;14(10):1343-60.
22. Safavi F, Rostami A. Role of serine proteases in inflammation: Bowman-Birk protease inhibitor (BBI) as a potential therapy for autoimmune diseases. *Exp Mol Pathol.* 2012;93(3):428-33.
23. Wang J, Lozier J, Johnson G, Kirshner S, Verthelyi D, Pariser A, et al. Neutralizing antibodies to therapeutic enzymes: considerations for testing, prevention and treatment. *Nat Biotechnol.* 2008;26(8):901-8.
24. Gabay JE, Scott RW, Campanelli D, Griffith J, Wilde C, Marra MN, et al. Antibiotic proteins of human polymorphonuclear leukocytes. *Proc Natl Acad Sci U S A.* 1989;86(14):5610-4.
25. Watorek W. Azurocidin -- inactive serine proteinase homolog acting as a multifunctional inflammatory mediator. *Acta Biochim Pol.* 2003;50(3):743-52.
26. Mehta HM, Malandra M, Corey SJ. G-CSF and GM-CSF in Neutropenia. *J Immunol.* 2015;195(4):1341-9.
27. Cottle TE, Fier CJ, Donadieu J, Kinsey SE. Risk and benefit of treatment of severe chronic neutropenia with granulocyte colony-stimulating factor. *Seminars in Hematology.* 2002;39(2):134-40.
28. Goodell MA. Epigenetics in hematology: introducing a collection of reviews. *Blood.* 2013;121(16):3059-60.
29. Srinageshwar B, Maiti P, Dunbar GL, Rossignol J. Role of Epigenetics in Stem Cell Proliferation and Differentiation: Implications for Treating Neurodegenerative Diseases. *Int J Mol Sci.* 2016;17(2).
30. Ostuni R, Natoli G, Cassatella MA, Tamassia N. Epigenetic regulation of neutrophil development and function. *Semin Immunol.* 2016;28(2):83-93.
31. Kim K, Doi A, Wen B, Ng K, Zhao R, Cahan P, et al. Epigenetic memory in induced pluripotent stem cells. *Nature.* 2010;467(7313):285-90.